N79-73515

(NASA-CR-157858) SUBLIMING REFRIGERATOR UNIT: SOLID CRYOGEN REFRIGERATOR FOR 75 DEG K INFRARED DETECTOR COOLING AND ONE YEAR LIFETIME Final Report, 14 Jul. 1967 - 15 Dec. 1969 (Lockheed Missiles and Space Co.) 00/31 Unclas 41550

FF No. (NASA CR OR TMX OR AD NUMBER) [redacted] (CATEGORY)

Lockheed

PALO ALTO RESEARCH LABORATORY

LOCKHEED MISSILES & SPACE COMPANY - A GROUP DIVISION OF LOCKHEED AIRCRAFT CORPORATION

PALO ALTO, CALIFORNIA

REPRODUCED BY
NATIONAL TECHNICAL
INFORMATION SERVICE
U. S. DEPARTMENT OF COMMERCE
SPRINGFIELD, VA. 22161

TP-3005

N-76-70-1

N79-73515

FINAL REPORT
FOR
SUBLIMING REFRIGERATOR UNIT
CONTRACT NO. NAS 5-10457

14 JULY 1967 TO 15 DEC. 1969

Prepared by

LOCKHEED MISSILES AND SPACE COMPANY
LOCKHEED RESEARCH LABORATORIES
3251 HANOVER STREET
PALO ALTO, CALIFORNIA 94304

for

GODDARD SPACE FLIGHT CENTER
GLENN DALE ROAD
GREENBELT, MARYLAND
20771

REPRODUCED BY
NATIONAL TECHNICAL
INFORMATION SERVICE
U.S. DEPARTMENT OF COMMERCE
SPRINGFIELD, VA. 22161

LOCKHEED PALO ALTO RESEARCH LABORATORY
LOCKHEED MISSILES & SPACE COMPANY
A GROUP DIVISION OF LOCKHEED AIRCRAFT CORPORATION

122

FINAL REPORT

for

SUBLIMING REFRIGERATOR UNIT
CONTRACT NO. NAS 5-10457

SOLID CRYOGEN REFRIGERATOR FOR 75°K INFRARED DETECTOR
COOLING AND ONE YEAR LIFETIME

1 JULY 1967 TO 15 DEC. 1969

GODDARD SPACE FLIGHT CENTER

Contracting Officer	Newchy Mignone
Technical Monitor	Peter Leone 623

Prepared by

LOCKHEED MISSILES & SPACE COMPANY
LOCKHEED RESEARCH LABORATORIES
325 Hanover Street
Palo Alto, California 94304

PROJECT MANAGER GARY C. VLIET

for

GODDARD SPACE FLIGHT CENTER
Glen Dale Road
Greenbelt, Maryland, 20771

APPROVED: R. E. Rolling
R. E. Rolling
Senior Member
Aerospace Sciences Lab.

Gary C. Vliet
Gary C. Vliet
Member, Thermophysics
Aerospace Sciences Lab.

Preceding page blank

T. C. Nast
T. C. Nast
Member, Thermophysics
Aerospace Sciences Laboratory

LOCKHEED PALO ALTO RESEARCH LABORATORY
LOCKHEED MISSILES & SPACE COMPANY
A GROUP DIVISION OF LOCKHEED AIRCRAFT CORPORATION

TABLE OF CONTENTS

Section		Page
	FOREWORD	v
	LIST OF ILLUSTRATIONS	vi
	LIST OF TABLES	viii
	ABSTRACT	ix
1.0	INTRODUCTION	1
	1.1 Background	1
	1.2 Technical Objectives	2
2.0	SOLID CRYOGEN REFRIGERATOR DESIGN	5
	2.1 Thermal Design Considerations	5
	2.2 Mechanical Design Considerations	22
3.0	SUPPORTING TESTS	32
	3.1 Initial Fill Tests	32
	3.2 Detector Support Tests	33
	3.3 Structural Tests	34
	3.4 Emittance Tests	34
4.0	SOLID CRYOGEN REFRIGERATOR FABRICATION	38
	4.1 Thermal Model	38
	4.2 Structural Model	50
5.0	SOLID CRYOGEN REFRIGERATOR PERFORMANCE	57
	5.1 Thermal Performance with Argon-Carbon Dioxide	57
	(a) Fill and Ground Hold Tests	57
	(b) Lifetime Tests	59
	(c) Temperature Regulation Tests	68
	5.2 Thermal Performance with Methane-Ethylene	74
	5.3 Structural Performance	76
	5.3.1 Introduction	76
	5.3.2 Test Results	77

TABLE OF CONTENTS
(cont'd)

Section		Page
6.0	CONCLUSIONS AND RECOMMENDATIONS	100
7.0	NEW TECHNOLOGY	105
8.0	BIBLIOGRAPHY	111

FOREWORD

The report was prepared by the Thermophysics Group of the Aerospace Sciences Laboratory, Lockheed Missiles and Space Company, for the Experiment Engineering Branch of NASA Goddard Space Flight Center under Contract NAS 5-10457, for the time period July 14, 1967 to December 15, 1969.

The study was carried out under the direction of R. E. Rolling with G. C. Vliet as the Project Manager. T. C. Nast and G. B. Cline were primarily responsible for the thermal and structural analyses respectively, and T. C. Nast also supervised the assembly and testing. R. E. Barrow did the assembly and conducted the thermal testing. G. Bell made the gold emittance measurements and provided support in the development of the detector mount technique.

LIST OF ILLUSTRATIONS

Figure		Page
1-1	Argon/Carbon Dioxide Refrigerator Configuration	3
2-1	Fiberglas Support System	8
2-2	Thermal Conductivity of Reinforced Expoxies	10
2-3	Effective Thermal Conductivity as a Function of Layer Density for Double Aluminized Mylar-Tissuglas	14
2-4	Allowable Stresses for Support Tube Material	25
2-5	Deflection Pattern for Support Tube Configuration	28
3-1	Total Hemispherical Emittance vs. Temperature for Gold Surface	37
4-1	Carbon Dioxide Container	39
4-2	Argon Container	40
4-3	Argon Tank Upper Dome with Internal Heat Exchanger	41
4-4	Carbon Dioxide Container	41
4-5	Argon Container	42
4-6	Fiberglas Support Tube System	42
4-7	Exterior of Refrigerator before Insulation	47
4-8	Top View of Detector Mount in Jig	48
4-9	Side View of Jig and Collar	48
4-10	Support Flange Configuration	54
4-11	Structural Model Showing Argon Tank and Shroud Fairing	55
4-12	Structural Model Showing Radiation Shield in Place	55
4-13	Completed Structural Model after Multilayer Insulation	56
5-1	Temperature Response of Refrigerator Components after Fill	61
5-2	Outgassing Rates for Tissuglas	65
5-3	Outgassing Rates for Double-Aluminized Mylar	66
5-4	Control (Input) for Axially Excited Resonance Search	82
5-5	Argon Axial Response for Axially Excited Resonance Search	83
5-6	CO_2 Axial Response for Axially Excited Resonance Search	84
5-7	Tube Axial Response for Axially Excited Resonance Search	85

LIST OF ILLUSTRATIONS
(cont'd)

Figure		Page
5-8	Argon Lateral Response for Laterally Excited Resonance Search	87
5-9	CO_2 Lateral Response for Laterally Excited Resonance Search	88
5-10	Tube Lateral Response for Laterally Excited Resonance Search	89
5-11	Control (input) for Axially Excited Acceptance Level Sinusoidal Test	90
5-12	Argon Axial Response for Axially Excited Acceptance Level Sinusoidal Test	91
5-13	CO_2 Response for Axially Excited Acceptance Level Sinusoidal Test	92
5-14	Control (Input) for Laterally Excited Acceptance Level Sinusoidal Test	94
5-15	Argon Lateral Response for Laterally Excited Acceptance Level Sinusoidal Test	95
5-16	CO_2 Lateral Response for Laterally Excited Acceptance Level Sinusoidal Test	96
5-17	Argon Axial Response for Axially Excited Qualification Level Sinusoidal Test	97
5-18	CO_2 Axial Response for Axially Excited Qualification Level Sinusoidal Test	98

LIST OF TABLES

TABLE		PAGE
2-1	Summary of Predicted Heat Rates to Refrigerator as Fabricated	6
2-2	Support Tube Stress Distributions	27
3-1	Structural Tests on Fiberglas-Epoxy Tube Samples	35
4-1	Summary of Component Weights for Refrigerator	51
5-1	Summary of Fill Tests	60
5-2	Measured Operating Parameters of Solid Cryogen Refrigerator	63
5-3	Summary of Thermal Tests	69
5-4	Summary of Temperature Regulation Tests	71
5-5	Comparison of Thermal Performance Tests for Two Dual Cryogen Systems	75
5-6	Acceleration and Vibration Test Summary	78
5-7	Sinusoidal Vibration Test	93

ABSTRACT

Lockheed Missiles and Space Company contracted with Goddard Space Flight Center under Contract NAS 5-10457 to design, construct, test, and deliver an engineering model of a dual solid cryogen refrigerator for a 75°K infrared detector. Argon and carbon dioxide were specified as the primary and secondary refrigerants respectively, and among the more important requirements were: one year of space operation, 35 mw of total detector cooling, maximum of 35 lb. weight, 75-80°K detector temperature, 300°K outer boundary temperature, and capability of surviving a TIROS launch. This report describes in detail the solid cryogen refrigerator thermal and mechanical design, as well as the thermal and structural performance of the refrigerator engineering models which were designed, built and tested to the required specifications.

The refrigerator utilizes solid argon and carbon dioxide as the primary and secondary refrigerants respectively, which are contained in toroidal aluminum containers and supported by a folded glass-reinforced epoxy tubular structure. A shroud attached to the CO_2 container surrounds the argon and one floating radiation shield is located between this shroud and the argon container. All surfaces viewing each other (support tubes, tanks, radiation shield and shroud) are gold coated for low radiation transfer. The refrigerator is insulated with 2 inches of double aluminized mylar-Tissuglas multilayer insulation. The solid cryogens are formed by passing LN_2 through a single coolant line attached to the containers. For each cryogen container there is one fill-vent tube which is grounded to a conductive shield in the insulation to provide vapor cooling of the insulation. Considerable effort was made to meet all of the thermal and mechanical requirements of the engineering model. The major structural requirements were met, however, the design did not satisfy all of

the thermal goals. The actual lifetime of the thermal model was three months. This degraded performance was determined to result primarily from increased thermal absorbtance of the gold coated surfaces due to cryodeposition of water vapor. The system weight of the refrigerator was 40 pounds, which included 26.8 pounds of cryogen.

Tests of the thermal model (purged fill, evacuated fill, hold, thermal lifetime, temperature regulation and warmup) were performed. The refrigerator can be filled satisfactorily under either the purged or evacuated condition.

The refrigerator thermal model is also applicable for operation with solid methane and ethylene as primary and secondary refrigerants, respectively. The model was tested with these cryogens and improvements in thermal performance and weight reductions were substantiated.

A structural model of the refrigerator was also built and tested. The structural model was similar to the thermal model except that it was tested at room temperature using a wax to simulate the solid cryogens, and certain features (i.e. gold coated surfaces) pertinent only to the thermal model were eliminated. The structural testing included acceleration tests in three axes at 10 and 17.6 g's, low level resonant survey tests (5 to 2000 cps) in three axes, sinusoidal vibration tests (5 to 2000 cps) in two axes (lateral and axial) at 5 and 8 g zero to peak; and random vibration tests (20 to 2000 cps) in two axes (lateral and axial) at 10 g rms (0.05 g^2/cps) and 16 rms (0.13 g^2/cps). The model survived all of these structural tests which are equivalent to "TIROS"/M/Improved TOS" flight and prototype level acceleration and vibration specifications.

SOLID CRYOGEN REFRIGERATOR FOR 75°K
INFRARED DETECTOR COOLING AND ONE
YEAR LIFETIME

1.0 INTRODUCTION

This is the final report for Contract No. NAS 5-10457, "Subliming Refrigerator Unit." It describes the design, construction and testing of an engineering model of a solid cryogen refrigerator for 75°K infrared detector cooling and one year lifetime.

1.1 Background

To efficiently detect long wavelength infrared radiation, cooled impurity semiconductors rather than intrinsic semiconductors are required. In an intrinsic semiconductor the band gaps between valence and conduction electrons correspond to maximum detectable wavelengths in the 5 to 7 micron range. Doped or impurity semiconductors, on the other hand, have energy peaks associated with the impurity atoms between the valence and conduction bands of the parent material. Thus certain doped semiconductors have much longer wavelength detector limits than intrinsic semiconductors and are applicable to long wavelength infrared. However, extrinsic semiconductors require cooling to prevent the thermal excitation of the impurity electrons. For extrinsic semiconductors having long wavelength limits in the 8 to 14 micron range, the detector should be operated at or below 80°K to prevent thermal saturation.

For infrared detectors requiring operation at or below 80°K aboard a spacecraft, the problem of supplying the refrigeration is very difficult in view of the requirements of low system weight, volume, power, and high system lifetime and reliability. Conventional means (active refrigeration) are currently inapplicable except for short term missions; although important improvements are being made in this area. However, systems using solid cryogens are presently capable of providing the required infrared detector cooling for long periods in space and with high reliability.

An engineering model of an argon-carbon dioxide dual cryogen cooler for $50^{\circ}K$ operation was designed, built and tested by LMSC under NAS 5-9549 (March 1967) to prove the feasibility of the dual cryogen concept for efficient long term operation. The resulting system weighed 34.1 lb, and had a thermal lifetime of 1 year for 17.6 mw allowable detector heat load, compared to design goals of 30 lb, 1 year and 25 mw, respectively. The detector and carbon dioxide operating temperatures were $52^{\circ}K$ and $129^{\circ}K$, respectively. This model did not undergo extensive structural testing and no attempt was made to couple the argon to a detector mount similar to that required of an operational system. The engineering model described herein goes beyond the feasibility model developed under NAS 5-9549 and includes extensive thermal and structural testing, and a detector mount concept is part of the system. The model which was developed is shown in Fig. 1-1.

1.2 Technical Objectives

The general objectives of this program were to design, build and test both thermally and structurally an engineering model of a solid cryogen refrigerator capable of withstanding launch environment and thereafter providing long term infrared detector cooling in space.

The refrigerator should be capable of providing 35 mw of infrared detector cooling at 75 to $80^{\circ}K$ for one year in space, with a total system weight, excluding the outer vacuum container, of approximately 35 lb, a minimum physical size and a nominal environmental temperature of $300^{\circ}K$. A detector mounting surface not less than 6 mm diam. and 10 mm long; two electrical leads to the sensor of not more than 15 ohms, and an infrared window transparent in the 8-14 micron range with a 60° acceptance angle were to be provided. A dual cryogen refrigerator concept using solid argon and solid carbon dioxide as the primary and secondary refrigerants respectively were specified, and liquid nitrogen could be used for the initial solid cryogen formation and for standby. The refrigerator should be capable of being filled and held at temperature low enough to prevent loss of CO_2 or argon for 24 hours, with external pressure of one atmosphere and external temperature of $300^{\circ}K$. Liquid nitrogen may be used

(A) CO_2 Tank
(B) Argon Tank
(C) Support Tubes
(D) Radiation Shield
(E) CO_2 Cooled Shroud
(F) Insulation (MLI)
(G) Vapor Cooled Shield
(H) Thermal Link
(I) CO_2 Vent-Fill
(J) Argon Vent-Fill
(K) Detector Holder, Taut Wires and Flexible Link
(L) LN_2 Coolant Lines
(M) CO_2 Coolant Coils
(N) Argon Coolant Coil and Heat Exchanger
(O) Manifolds
(P) CO_2 Cooled Shields
(Q) Mylar Radiation Shield
(R) Radiation Disc Shields
(S) Dexiglas
(T) LN_2 Coolant Inlet
(U) LN_2 Coolant Outlet

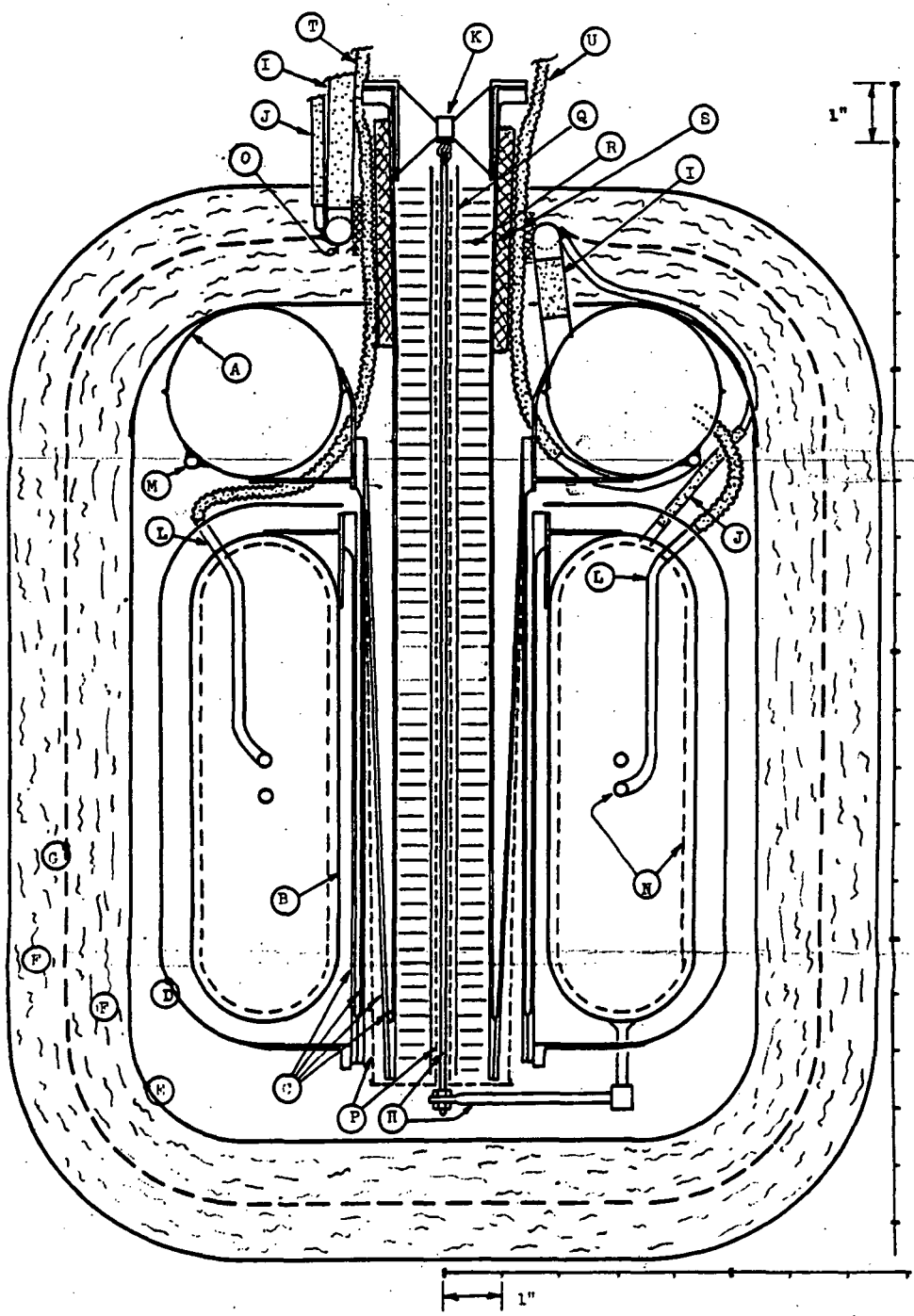

Figure 1-1 Argon/Carbon Dioxide Refrigerator Configuration

in the cooling coils during this time, and a vacuum in the insulation space is not required, but there is to be no condensation or freezing of gases in the insulation. The system must be capable of being warmed to 300°K in 4 hours without impairing the insulation. Each cryogen container shall have one fill-vent line to the outside of the vacuum container. Only one insulation penetration is permitted. The vacuum container in which the thermal testing is performed should be capable of attaining 10^{-5} Torr, and should include two vacuum gages, one in the range 1 atm to 10^{-3} torr and the other 10^{-3} to 10^{-7} torr.

The thermal model was to undergo fill, lifetime, temperature regulation and warmup tests, to determine its thermal performance.

The contract originally did not require that the model be tested to the complete launch environment outlined in "GSFC Specification TIROS M/Improved TOS" dated January 31, 1967; however, the design was to meet the specified acceleration and vibrational environments. The contract was subsequently amended to include testing of a structural model to the equivalent qualification and acceptance levels of acceleration and vibration described in the above "specification." The structural model was to be similar to the thermal model except for features not affecting the structural performance. Testing would be performed in the warm (room temperature) condition with the model loaded with solid ballast to simulate the respective solid cryogens.

2.0 SOLID CRYOGEN REFRIGERATOR DESIGN

As part of the contract a detailed design report, "Thermal and Mechanical Design of Solid Cryogen Refrigerator for 75°K Infrared Detector Cooling," dated Sept. 22, 1967, was submitted for approval to NASA GODDARD SPACE FLIGHT CENTER prior to construction of the refrigerator. The important design information in the above report relevant to the eventual model, as well as additional design changes made during the construction and testing of the refrigerator are presented below.

2.1 Thermal Design Considerations

The thermal design of the refrigerator was extremely critical as a result of the 35 lb weight goal. The design point of 30 g's side loading established the structural criteria for the cryogen tank supports, and this requirement led to substantially greater support member requirements than the refrigerator developed under the prior contract (NAS 5-9549), for which the design side loads were 10 g's. The resulting relatively thick wall support tubing leads to potentially high support heat leaks. A concentrated design effort was focused on various support configurations for both argon and carbon-dioxide containers. Other major efforts were directed at the geometrical arrangement of the CO_2 and argon containers in combination with the various support configurations. Special emphasis was placed on ease of fabrication, simplicity and vacuum integrity of the cryogen containers and ease of access in the event of vacuum leakage.

The basic requirements and assumptions which relate to the thermal design are outlined in Section 1.2.

A summary of the various heat leaks that were included in the calculations and their magnitude is presented in Table 2-1. A consistent set of design parameters was obtained only after several iterations. For example, the required tank volume is affected by the heat leak which in turn is coupled to the

TABLE 2-1

SUMMARY OF PREDICTED HEAT RATES
TO REFRIGERATOR AS FABRICATED

Heat Leak (mW)	Argon (Primary)	CO_2(Secondary)
Supports (including gold conduction)	4.1	28
Radiation to Container	19.5	--
Insulation (2 in.)	-	113
Plumbing Lines	2.0	16.5
Conduction and Radiation to Detector	8.1	--
I^2R Heat Dissipation	10	--
Vent Gas Cooling	-	- 18
Heat Loss to Argon	-	- 24
NET HEAT LOAD	43.7	115

tank dimensions. Additional items are also coupled, so that iteration is necessary to obtain consistent parameters. The techniques and methods used to obtain the various heat rates to the refrigerator are discussed in the following sections.

Support Analysis

Argon Support - The investigation of argon support configurations included the following:

- Dacron or Titanium taut filaments
- Foam support pads
- Stacked washers, including foam, phenolic, and stainless steel.
- An annular space filled with solid argon which would sublimate after boost and leave the argon container suspended on minimum supports.
- Fiberglas tubes and cones, both concentric and re-entrant.

These design studies indicated the latter concept to be preferable. Studies of various fiberglas tube supports included various geometrical configurations. Tube supports which supported the argon can directly from the carbon dioxide container led to prohibitive heat leaks and these were immediately discarded. Re-entrant configurations, which allowed the support tube to pass through a hole in the argon container before attachment was made (similar to the previous refrigerator design), were substantially better although they still fell short of their design goal.

The design which was finally selected is shown in Fig. 2-1 (which also shows the carbon dioxide support) and consists of two concentric fiberglas tubes which result in a long path length and a resultant minimum heat leak. The solid conduction heat leak is given by the following expression.

$$Q = \frac{\bar{k}(T_{CO_2} - T_A)}{\left(\frac{L}{2\pi\delta r}\right)_3 + \left(\frac{L}{2\pi\delta r}\right)_4}$$

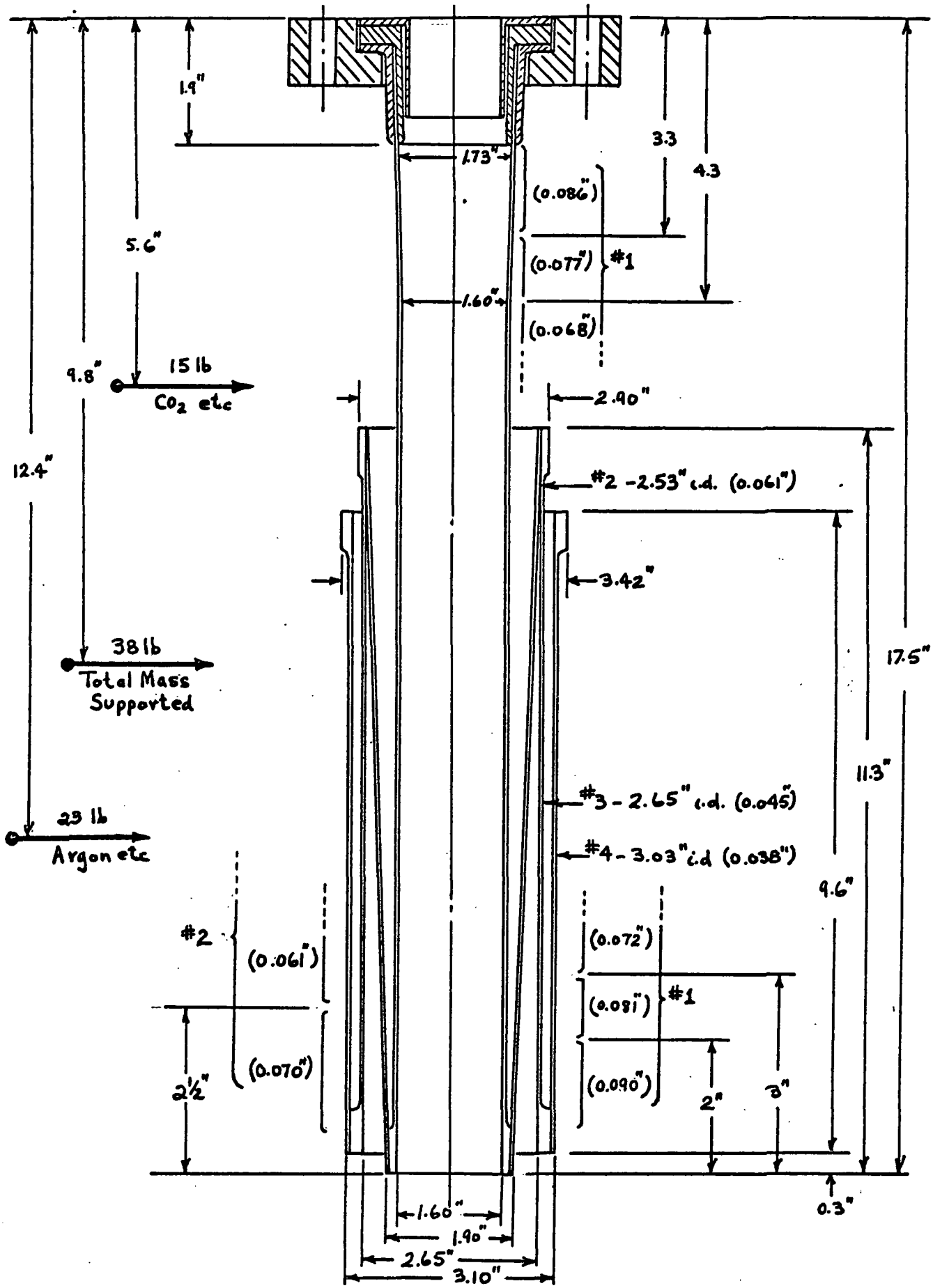

Figure 2-1 Fiberglas Support System

The parameters of the support tubes which determine the heat flow are:

$r_3 = 1.35$ in. $\qquad r_4 = 1.55$ in.

$\delta_s = 0.042$ in. $\qquad \delta_4 = 0.035$ in.

$L_3 = 9.1$ in. $\qquad L_4 = 7.7$ in.

$$(T_{CO_2} - T_A) = 225^oR - 135^oR = 90^oR$$

$$\bar{k} = 0.06 \text{ Btu/Ft Hr}^oR$$

The data on thermal conductivity was obtained from Ref. 1 and is presented in Fig. 2-2. The average value for the various materials was used. The resulting heat leak with this configuration is 3.2 mw. In addition, the gold coating resulted in 0.8 mw due to conduction.

Main CO_2 Support

Investigations of the main support system for the refrigerator were essentially concentrated on fiberglas epoxy reinforced material. Various configurations both with and without re-entrant systems were analyzed. Again, it was found that to withstand the specified loading conditions, it was necessary to utilize a concentric tube design to increase heat conduction path length. This configuration is also shown in Fig. 2-1. In determining the support configuration, the variation in mechanical properties along the tube length due to increased strength with reduced temperature and reduced moments away from the attachment point were included. In this manner, the cross sectional area for heat flow was minimized. Both the wall thickness and diameter of the two support tubes were partially tailored to local stress. The resulting support consisted of a cone-cylinder support within a second conical support.

The heat leak for the CO_2 support system was calculated from the following equation:

$$Q = \frac{\bar{k}(T_4 - T_1)}{\frac{1}{2\pi}\left[\sum \frac{L}{\delta r}\right]}$$

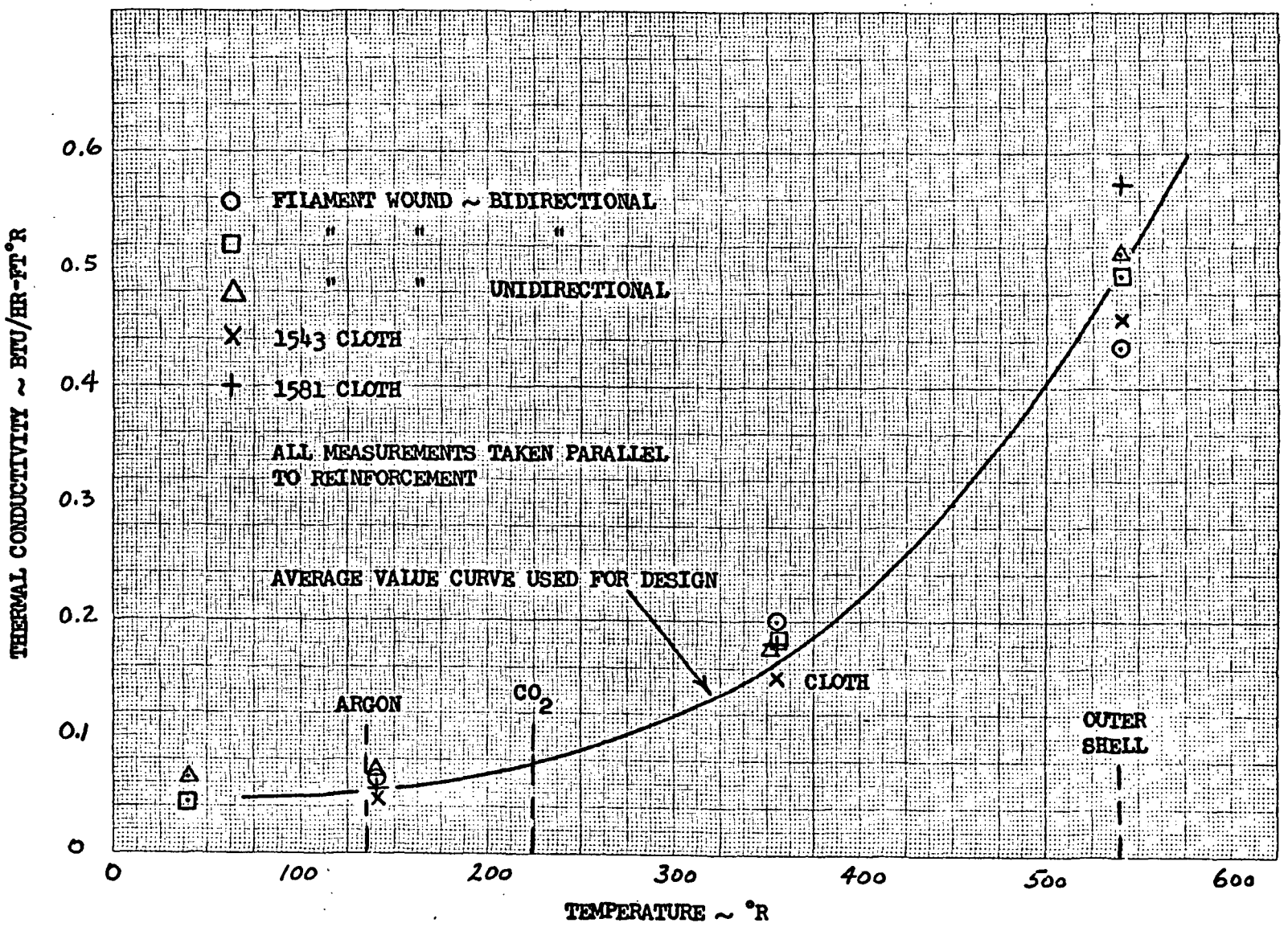

Fig. 2-2. Thermal Conductivity of Glass Reinforced Epoxies

The following parameters were used for the heat leak determination. The data on thermal conductivity was obtained from Figure 2-2 and the average value of conductivity for the various materials was used.

Parameters for CO_2 support heat leak.

$$T_4 - T_1 = 540^\circ R - 225^\circ R = 315^\circ R$$

$$\bar{k} = 0.25 \text{ Btu/hr Ft}^\circ R$$

For the top cone of tube No. 1

$$\frac{L}{\delta \bar{r}} = \frac{3.4 \times 12}{0.077 \times 0.83} = 638.0$$

Cylindrical section of tube No. 1

$$\frac{L}{\delta r} = \frac{12.4 \times 12}{0.068 \times 0.80} = 2{,}740$$

Tube No. 2 (conical)

$$\frac{L}{\delta \bar{r}} = \frac{9.8 \times 12}{0.060 \times 1.10} = 1{,}780$$

The resulting heat leak due to solid conduction was .096 Btu/hr or 28 mW.

Radiation down the central support tube was retarded by placing annular disks of multilayer insulation inside the tube, with the central hole for passage of the thermal link. Without such insulation radiation transfer would be excessive.

Radiation to Argon

The argon is partially protected by the CO_2 cooled gold coated shroud and is further protected from radiative transfer by a gold coated radiation shield between the argon and the CO_2 shroud. The heat transferred by radiation from

the CO_2 container and the CO_2 cooled shield is given by the following expression which is applicable for concentric cylinders or spheres:

$$Q_r = \sigma \mathcal{F}_{12} A_1 (T_2^4 - T_1^4)$$

$$\mathcal{F}_{12} = \frac{1}{\frac{1}{e_1} + \frac{A_1}{A_2}(\frac{1}{e_2} - 1)}$$

where the subscript 2 denotes the outer surface and 1 denotes the inner surface.

Calculations were performed using this expression for the gold surfaces with one radiation shield separating the argon tank from the CO_2 temperature environment.

The following values were utilized for the calculations:

A_2(CO_2 boundary temperature) = 4.7 Ft^2

A_1(Argon area exposed to CO_2) = 2.7 Ft^2

Radiation shield area: 3.17 Ft^2

The emittance as a function of temperature for "Lockspray" and of an electrodeposited gold as measured in the Lockheed Research Laboratory are given in Figure 3-1. The "Lockspray" was selected because of its lower emittance and its utility in coating fiberglas parts. The emittance value used in the calculation were $e_1(75^oK) = 0.011$; and $e_2\ (125^oK) = 0.015$.

It was also assumed that 1% of the surface area of the argon tank was black resulting in an effective emittance of 0.021 for the argon tank.

Solution of the equation assuming these parameters yielded the following heat flux value from the CO_2 boundary to the argon container:

$$Q_r = 19 \text{ mW (gold coated)}$$

The assumption of no black areas would reduce this value to 11 mW. The shield was supported at the junction of the No. 3 and 4 support tubes which approximates the ideal temperature of the radiation shield, 112°K (201°R). Heat transfer between the shield and the connecting support was minimized by constructing the shield from a low conductivity material (fiberglas-epoxy).

Insulation Configuration and Heat Leak

The insulation system used for the refrigerator was similar to that used on the previous refrigerator developed under Contract NAS 5-9549. Extensive testing of various insulation systems has shown the selected system of double aluminized mylar-Tissuglas to have the best thermal performance.

The insulation support shell (CO_2 tank and shroud) was constructed so that the top and bottom ends were rounded to avoid local compressions of the insulation which will seriously degrade insulation performance. At the junction of the insulation and the support tube a layer of Dexiglas was provided to uncouple the insulation from the support tube. A numerical computer analysis was made of the optimum Dexiglas thickness to minimize the net heat transfer to the CO_2. The optimum was approximately 5/8 inch, but was quite flat, and a Dexiglas thickness of approximately 1/2 inches was used.

An effective thermal conductivity of 3×10^{-5} Btu/hr Ft°R (5.2×10^{-7} W/cm °K) was assumed for the insulation system. This value was obtained with the insulation system used on the previous refrigerator. Recent data on this insulation type has been obtained at the Lockheed Research Laboratory and is presented in Fig. 2-3. It should be pointed out that the boundary temperatures of 300°K and 125°K appropriate to the refrigerator design would yield somewhat higher values than shown on the figure.

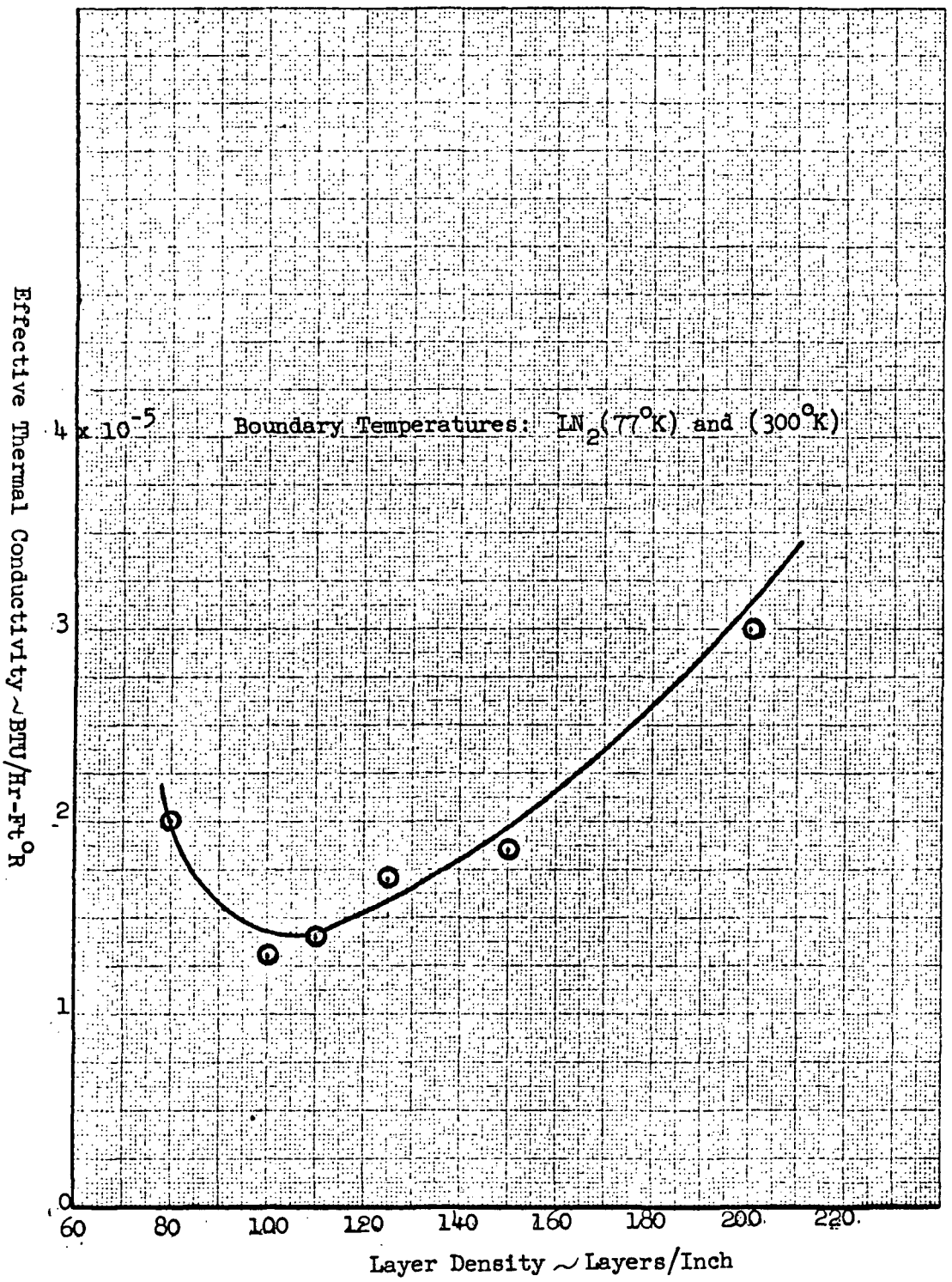

Figure 2-3 Effective Thermal Conductivity as a Function of Layer Density for Double Aluminized Mylar-Tissuglas

The insulation thickness which led to the minimum weight system was obtained from a typical optimization. The optimum insulation thickness was found by summing the cryogen and insulation weights, taking the derivative of total weight with respect to insulation thickness and setting it equal to zero. Solving for $\delta_{opt.}$

$$\delta_{opt.} = \sqrt{\frac{k\Delta T\theta}{H_{subl.}\rho}}$$

Solution for $\delta_{opt.}$ resulted in a value of 4.0 inches, however, the weight savings becomes quite small when insulation thicknesses greater than about 3 inches are exceeded. Consideration of the weight trade-off and the practical problems involving fabricating large insulation thicknesses together with the available envelope of the existing vacuum chamber of the service console led to selection of 3 inches as the design thickness. In wrapping the refrigerator the insulation layer density was approximately 115 layers/inch which was somewhat higher than the anticipated 100 layers/inch. The final insulation blanket contained 230 layers and had a thickness of 2.05 inches, which was used in these calculations. The average insulation area was 7 ft^2 and the temperature difference is 175°K (315°R). The resulting heat leak was 113 mW.

Instrumentation, Service Line and Vent Tube Heat Leak

The heat conduction down the service tubes such as the fill lines, and vent lines was included in the calculations. These lines were constructed from either Mylar or convoluted Teflon and the computed heat rates due to conduction are included in the table below:

Tube	Diameter in.	Length in.	Heat Leak mW
CO_2 vent line	0.5	1	15.8
CO_2 LN_2 service line	0.25	8	0.7
Argon vent line	0.1	4	1.0
Argon LN_2 service line	0.25	10	1.0

These heat leaks could be reduced by providing longer path lengths. The thermocouple instrumentation wires consisted of 5 mil Chromel-Constantan and the calculated conduction due to this source was negligible.

Heat Transfer to Thermal Link and Detector Mount

The configuration of the detector and detector mount is shown below with the assumed emissivity values and temperature distribution. The configuration consisted of the detector mount supported by six taut wires and connected to the argon by a flexible length of gold wires and the gold thermal link. The detector mount and taut wires were "Lockspray" coated.

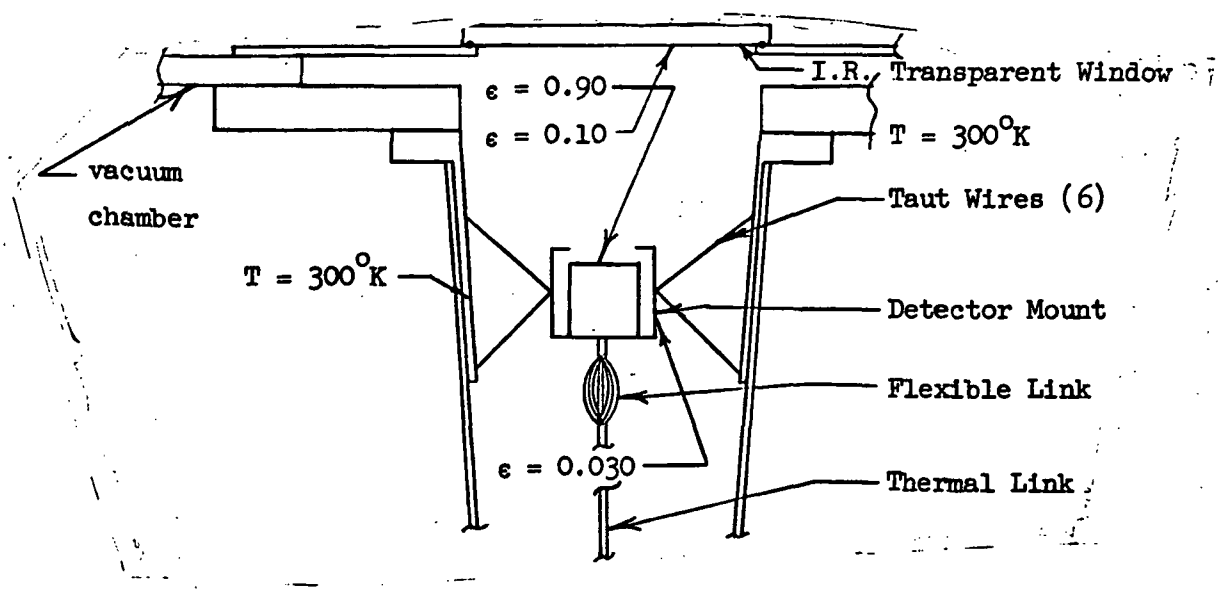

The detector mount dimensions were: 8 mm diameter by 12 mm long.

The radiation flux to the top and sides of the detector mount was based on the assumption that the surrounding surfaces formed a 300°K "Hohlraum" so that

$$Q_v = \sigma e A(T_2^4 - T_1^4)$$

$$A = 4.0 \text{ cm}^2 \text{ , e (for } 300^\circ\text{K radiation)} = 0.03$$

The resulting radiation flux was 5.4 mW. The top aperture which provided access to the interior of the mount provided a black body heat rate of 1.7 mW.

The support system for the detector mount consisted of 6 stainless steel wires* which supported the mount in tension. The wires had a diameter of approximately 3.1 mil and a length of 0.7 in. In determining the heat leak due to the detector support wires, it is necessary to consider the effect of coupled radiation and conduction loads. A simple expression which gives the heat loads to the mount assuming combined radiation and conduction is

$$Q = \pi \left[\frac{k\sigma \bar{\epsilon} D^3 \quad (T_c^5 - 5T_h^4 T_c + 4T_h^5}{10} \right]^{1/2}$$

The assumptions in this equation are: (a) the rod is infinite in length, (b) the wire has constant thermal conductivity and surface emissivity, and (c) mount temperature is T_c and surroundings are at T_h.

Utilizing this expression to calculate the coupled radiation and conduction heat leak to the detector results in a value of 1 mW.

In addition to the above heat leaks there is a required cooling load of 10 mW which was assumed to originate by I^2R heat generation within the detector.

Thermal Link between Detector Mount and Argon:

It is desirable to minimize the temperature gradient between the detector mount and the argon. Calculations of the required size of a thermal link to give a temperature gradient of 1°K resulted in a diameter of approximately 1/3 inch. This diameter led to a large surface area for radiation, and

---

*The original design called for Ti: 6Al, 4V wires for the taut wire supports. This material was used in the first thermal model constructed which was later damaged during testing. Stainless steel wire was used in the second thermal model as none of the Ti alloy was available. The stainless wire is only slightly less efficient than the Ti alloy.

resulted in excessive radiant flux to the link. A permissible temperature gradient of $10^{\circ}K$ was assumed resulting in a diameter of approximately 0.10 inch. The final link design consisted of a 0.110 inch gold link approximately 16 inches long, with a bundle of 20, 10 mil diameter gold wires connecting the link to the detector holder. The gold link passed down the center of the main support tube where it was connected near the bottom of the tube to a horizontal length of 1/4 inch diameter copper rod which was attached to the bottom of the argon container.

In the final design a carbon dioxide cooled shield was placed around the link to provide a CO_2 temperature shield, and this shield was in turn surrounded by a gold coated mylar radiation shield. The radiation to the link from the $125^{\circ}K$ source is calculated to be approximately 1 mW. The heat leak corresponding to an unshielded link is 20 mW.

Vent Tube Design

Each cryogen container had a single entry line used for both filling and venting, and the line was sized according to the venting requirements. The sizing was such that with the normal heat load Q on the solid, a pressure drop corresponding to the desired solid cryogen operating temperature permits the proper vapor mass venting rate $\dot{m} = Q/H_s$. Both the CO_2 and argon vent lines were grounded to the insulation mid-plane shield.

For the venting system considered, the vapor flow is normally laminar because of the low Reynolds number, and $\dot{m}$ to good approximation is given by Poiseulles' equation as

$$\dot{m} = \frac{\pi \bar{\rho} D^4}{128 \bar{\eta} L} (P - P_o)$$

where D and L are the vent line diameter and length respectively.

Since the venting is to vacuum, $P_o = 0$, and the effective average vapor density $\bar{\rho}$ in the venting line is approximated by

$$\bar{\rho} = \frac{\bar{P}M}{R_g\bar{T}} = \frac{1}{2}\ \frac{PM}{R_g\bar{T}}$$

where $\bar{P}$ and $\bar{T}$ are the effective mean pressure and temperature of the vapor along the line. Therefore to good approximation:

$$Q = H_s\dot{m} = H_s\ \frac{\pi M D^4}{256\ R_g\bar{T}\ \bar{\eta}\ L}\ P^2$$

In reality, the available pressure drop $\Delta P = P - P_o$ is less than P since sonic flow will exist near the exit, and the effective mean pressure $\bar{P}$ is greater than P/2 for the same reason. These effects are thus partially compensating. If the venting is adiabatic, the mean temperature drops along the line due to the vapor expansion. However, adiabatic conditions do not normally exist, and in particular, when the thermal capacity of the vapor is used for insulation vapor cooling, the effective mean vapor temperature lies between the insulation warm and cold boundary temperatures.

For the argon

$$\dot{m} = 2.46 \times 10^{-4}\ \text{gms/sec}$$

$$M \doteq 39.9$$

$$\bar{\mu} = 142 \times 10^{-6}\ \text{gm/cm sec (estimated)}$$

$$\bar{T} = 188^{o}K$$

$$R = 8.314 \times 10^{7}\ \text{ergs/gm-mole}\ ^{o}K$$

and the vapor-pressure temperature ralation is

$$P = 6 \times 10^{7} e^{-969/T}$$

Substitution of these figures gives

$$\frac{D^4}{L_s} = \frac{6.2 \times 10^{-4}}{P_1^2}$$

where P_1 is in Torr. For $P_1 = 30$ Torr $(T = 67^{o}K)$

$$\frac{D^4}{L_s} = 70 \times 10^{-7}$$

For $L_s = 10$ cm $\qquad D = 0.029$ cms.

For the carbon dioxide container

$$\dot{m} = 1.27 \times 10^{-4} \text{ gm/sec}$$

$$M = 44$$

$$\bar{\mu} = 177 \times 10^{-6} \text{ gm/cm sec (estimated)}$$

$$\bar{T} = 212^{\circ}K$$

and the vapor pressure temperature relation is

$$P = 9.5 \times 10^{9} e^{-3180/T}$$

Substitution of these figures gives

$$\frac{D^4}{L_s} = \frac{4.07 \times 10^{-4}}{P_1^2}$$

For $P_1 = 0.09$ Torr ($125^{\circ}K$)

$$\frac{D^4}{L_s} = 5.0 \times 10^{-2}$$

For $L_s = 10$ cm

$$D = 0.84 \text{ cm}$$

Previous experience showed that the carbon dioxide can ran at $129^{\circ}K$ rather than at $125^{\circ}K$ with a vent tube sized according to the above equations. This temperature variation implies a pressure of twice the design value. Since pressure is inversely proportioned to diameter squared for a given system, it is desirable that the vent tubes be sized at least $\sqrt{2}$ times larger, since the conductance can be reduced externally, if necessary.

The design vent line diameters were therefore

Argon can	0.38 cm. (0.15 in.)
Carbon dioxide can	1.4 cm. (0.552 in.)

The carbon dioxide vent line was dictated soleby by vent conductance considerations. The argon line was dictated in part by fill time considerations, i.e. the line was significantly oversized. To provide the correct vent conductance during operation a needle throttling valve was installed in the argon vent line external to the chamber.

Temperature Regulation

The detector temperature regulation is a function of the variation in the heat loads on the primary cryogen and the primary cryogen and thermal link properties. The detector temperature regulation is a result of two factors: (a) The variation in primary cryogen temperature as a function of primary cryogen heat load and (b) the variation in thermal link temperature drop as a function of thermal link heat load. The desired control equation is of the form

$$\frac{\Delta T_D}{T_p} \cong \frac{\Delta T_p}{T_p} + \frac{\Delta T_L}{T_p} = f_1 \frac{\Delta Q_p}{Q_p} + f_2 \frac{\Delta Q_L}{Q_L}$$

where the subscripts P, L and D refer to primary cryogen, thermal link and detector, respectively.

Using the solid cryogen vapor-pressure versus temperature relation and Poiseulles' equation describing vent line flow, a relation for the cryogen temperature regulation of the following form is obtained:

$$\frac{\Delta T_p}{T_p} = \frac{T_p}{\beta} \frac{\Delta Q_p}{Q_p}$$

where β is the coefficient in the vapor pressure — temperature relation : $P = \alpha e^{-\beta/T}$.

Similarly, the detector temperature regulation based only on thermal link temperature variation is derived:

$$\frac{\Delta T_L}{T_p} = \frac{L}{KA} \frac{\Delta Q_L}{T_p}$$

Therefore:

$$\frac{\Delta T_D}{T_p} = \frac{T_p}{\beta} \frac{\Delta Q_p}{Q_p} + \frac{L}{KA} \frac{\Delta Q_L}{T_p} .$$

For argon and carbon dioxide the respective β coefficients are 969°K and 3180°K and the respective nominal operating temperatures are 65 and 125°K; thus, for heat load variations of 100 percent the respective cryogen temperature variations are about 3 and 2.5°K, respectively. For the detector, assuming a 100 percent variation in primary cryogen load from 43.7 mW to 87.4 mW, assumed to all result from increased heat load borne by the gold thermal link, the detector temperature variation is 17°K (3°K increase for the cryogen and 14°K increase for the link).

2.2 Mechanical Design Considerations

2.2.1 Support Tube Design

The critical portions of the refrigerator design from the stress/deflection viewpoint are the thin walled support tubes. These tubes must transmit the inertia loads arising from the launch acceleration-vibration environment acting on the refrigerator masses.

The launch environment which is critical to the structural design of the support tubes is the "transverse acceleration" resulting from the vibration, both random and sinusoidal. The random vibration environment specified for the flight model is an essentially flat spectral density distribution over the 20 to 2000 cps frequency range, at 10 grms acceleration in both the thrust and transverse axes. Taking a normal distribution of accelerations

and a "three standard deviation" acceleration level as the peak acceleration to be experienced in service, then the design level of input acceleration is 30 g.

The support tubes are constructed from one of the glass fiber/epoxy laminate materials which are considered to be superior for optimization of high strength-low thermal conductivity. The mechanical properties (allowable compressive and shear stress) for S-glass-1581 cloth/E-787 epoxy from Ref. (1). is shown in Fig. 2-4. These mechanical properties of the fiberglas/epoxy laminate have been taken as conservative values (reported value less 10% from the data of Ref. 1 and Ref. 2). Since the wall of the support tube will undergo both tension and compression the smaller of the ultimate strengths in tension or compression (normally compression) is chosen as the allowable stress σ_{all}.

The average of the tensile and compressive moduli for the S glass-1581 cloth/E 787 epoxy is only weakly temperature dependent, and a constant value of $E = 3.6 \times 10^6$ psi is assumed for design purposes. Also

$$G = \frac{E}{2(1+\gamma)} \quad \frac{3}{8} E$$

Each support tube is a cantilevered thin walled beam subject to a shear load Q, axial load P, and moment $M_o = Qd$ at the free end, due to the inertial load Q acting at a distance d from the free end, as in the sketch below, where the loads Q and P are the products of the supported masses and the accelerations.

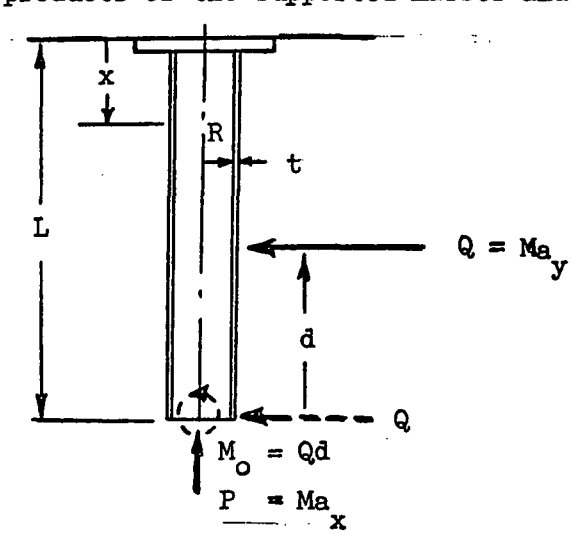

The stress $\sigma_B(x)$ at distance x from the free end due to the bending moment M_o is

$$\sigma_B(x) = \frac{M_o + Q(L-x)}{\pi R^2(x)\ t(x)}$$

where L is the tube length, R(x) the tube radius and t(x) is the tube wall thickness. The axial stress due to the load P is:

$$\sigma_D(x) = \frac{P}{2\pi R(x)t(x)}$$

and the maximum shear stress τ due to the transverse shear load Q is:

$$\tau(x) = \frac{Q}{\pi R(x)t(x)}$$

The local buckling stress σ_{cr} is taken from Ref (9) as

$$\sigma_{cr} = kE\,\frac{t(x)}{R(x)}\ \frac{1}{\sqrt{3\ (1-\nu^2)}} = 0.306\,\frac{Et(x)}{R(x)}$$

where $\nu = 1/3$ is the Poisson's ratio, and k is an empirically determined factor which for the $\frac{R(x)}{t(x)}$ range and material used is taken as 0.5. For homogeneous materials the value of k is approximately 2/3; however, the value is reduced for laminates, and the tests reported in Ref. (10) indicate that the value of 0.5 is more realistic.

The deflections for these cantilevered tubes are calculated, including deflection due to shear strains, from the momentum-curvature and shear-slope relations as given in Ref. (10). The transverse deflection δ_t in the direction of the transverse load Q is

$$\delta_t(x) = \int_0^x \int_0^\eta \frac{M_o + Q(L-\theta)}{\pi E R^3(\theta)\ t(\theta)}\, d\theta\, d\eta + \int_0^x \frac{Q}{\pi G R(\eta)\ t(\eta)}\, d\eta$$

and the axial deflection is:

$$\delta_a(x) = \int_0^x \frac{P}{2\pi E R(\eta)\ t(\eta)}\, d\eta$$

The overall assembly of the support tubes, including dimensions and location and magnitudes of the transverse loads is shown in Figure 2-1. In the support tube stress results which follow, the first and second tubes support essentially

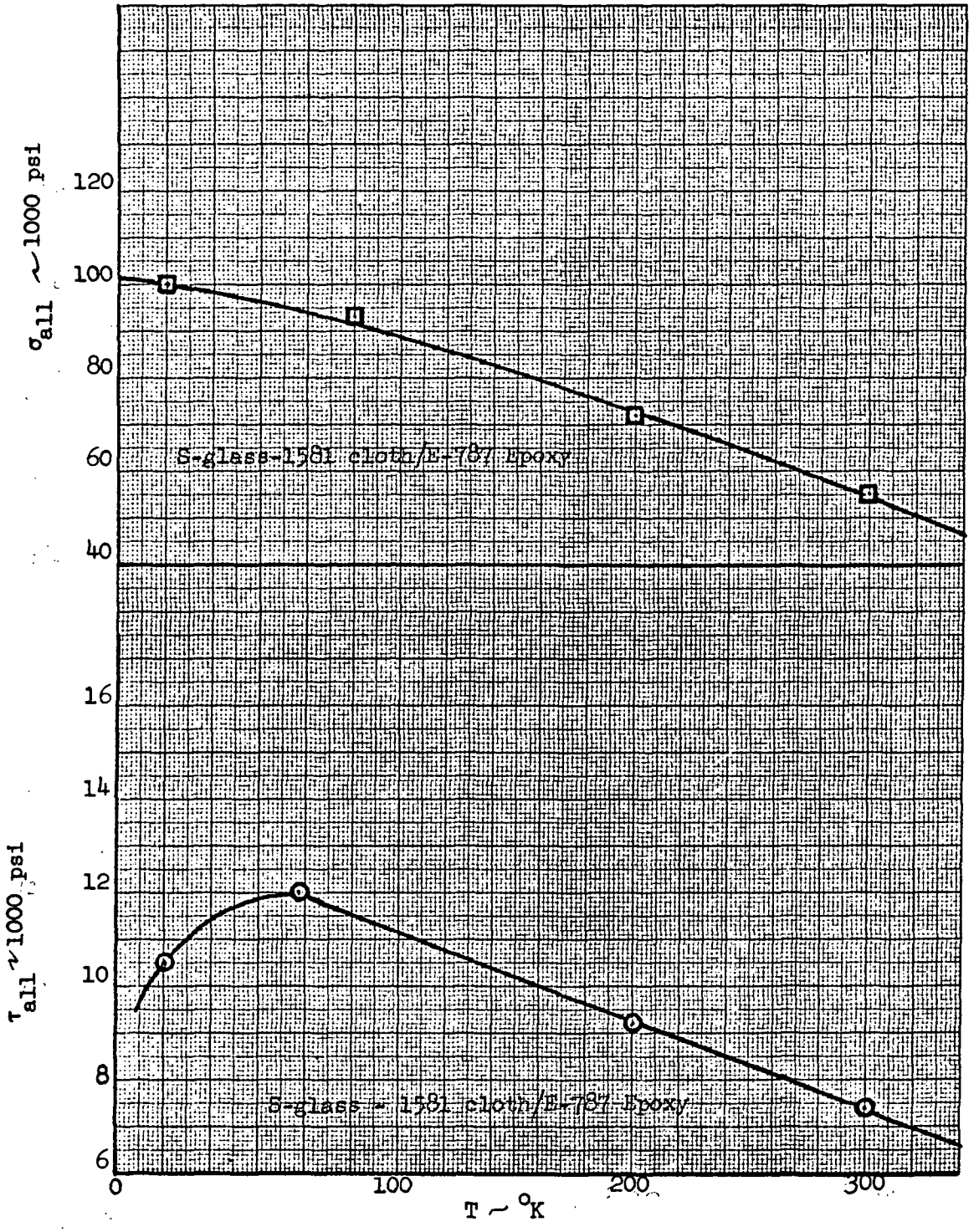

Figure 2-4. Allowable Stresses for Support Tube Material

the entire system mass (38 lb) and the third and fourth tubes support only the argon and its associated tankage ($\sim$23 lb). The first and second tubes are partially tailored to optimize the stress distribution. The computed maximum existing compressive stress is considered to be the sum of $\sigma_B + \sigma_D$ acting simultaneously. The computed compressive (σ) and shear (τ) stresses in each of the support tubes are shown in Table 2-2 and also included are the allowable compressive (σ_{all}) and shear (τ_{all}) stresses, as well as the critical buckling stress (σ_{cr}). It is seen that for the assumed 30 g loading all stresses are well below the allowables.

Using the beam deflection expressions, the deflection of the support tube system resulting from a transverse acceleration of 30 g was computed, to observe the nature of the interference. The deflection calculations were made assuming the tubes were free to deflect (i.e. no interference). The deflection pattern for the series of tubes is shown in Figure 2-5. The displacements are mainly a result of the large deflections of the main support tube. There is considerably less deflection of the other tubes, the deflections of the third and fourth tubes being sufficiently small to result in no possibility of interference between them. This shows that the carbon dioxide and argon masses act essentially at a single rigid mass. However, there is interference of the second tube with the main support tube, as indicated in the figure. The lateral displacement of the junction of the first and second tubes (lower end) is approximately 0.95 inches. Interference between the top of the second support tube and the main support tube would occur approximately 0.1 inch before maximum deflection. Calculations of the stresses developed in the tube wall as a result of interference, indicate that they would not cause failure of the material.

2.2.2 Support Flange

Modifications to the support flange area were required as a result of two test failures during qualification level acceleration and random vibration tests. The resulting modified support flange is shown in Figure 4-10. Eight 3/8 inch NAS bolts on 4 inch centers are used to mount the flange, and the main support tube is epoxy bonded to both inner and outer aluminum collars, each 1-1/2 inches long.

TABLE 2-2

SUPPORT TUBE STRESS DISTRIBUTIONS

		No. 1 (Central)						No. 2			No. 3		No. 4 (outer)	
Location (in) (inches from support)		1.9 (top)	3.3	4.3	14.5	15.5	16.8 (bot)	0 (bot)	1.8	9.9 (top)	0 (top)	9.6 (bot)	0 (bot)	8.2 (top)
Tube Diam (in.) (inside)		1.73	1.66	1.60	1.60	1.60	1.60	1.76	1.90	2.41	2.65	2.65	3.03	3.03
Tube Thickness (in.) (minimum)		0.086	0.077	0.068	0.072	0.081	0.090	0.070	0.061	0.061	0.045	0.045	0.038	0.038
Temperature (^{o}K) (approx)		300	290	280	220	210	200	200	180	130	130	100	100	65
(psi x 10^{-3})	σ_{all}	54	56	58	68	70	72	72	75	84	84	89	89	94
	σ	47	47.5	49.4	40.2	42.8	46.7	49.9	37.4	14.3	17.1	13.2	12.2	12.2
	σ_{cr}	110	102.	94.	99.	111.	124.	87.5	71.0	56.0	37.4	37.4	27.6	27.6
	τ_{all}	7.2	7.5	7.7	9.0	9.2	9.3	9.3	9.8	10.8	10.8	11.4	11.4	11.7
	τ	4.9	5.7	6.7	6.3	5.6	5.0	5.9	6.3	4.9	3.7	3.7	3.7	3.7

Notes:

- o 30 g assumed loading
- o #1 and #2 tubes support 38 lb.
- o #3 and #4 tubes support 23 lb.
- o $\sigma = \sigma_B + \sigma_D$

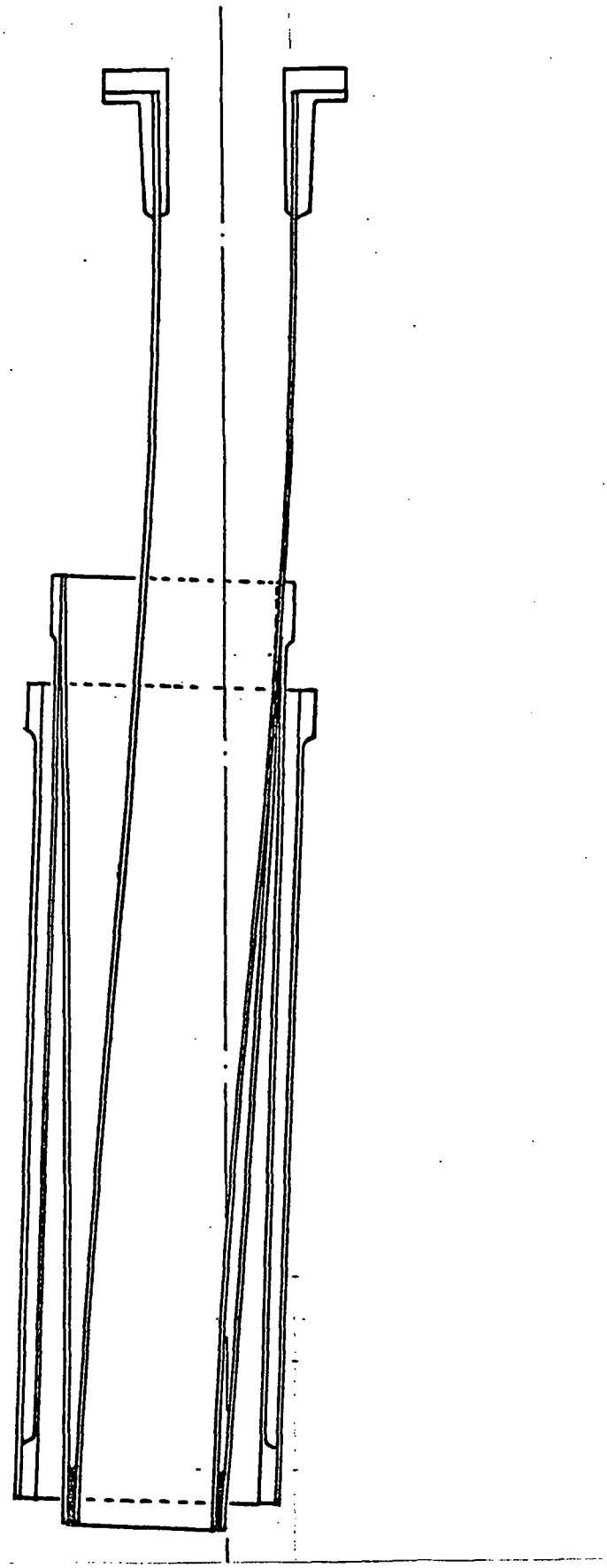

Figure 2-5 Deflection Pattern for Support Tube Configuration

Assuming only two of the support bolts provide the restoring moment for a 30 g transverse acceleration at any instant, the stress in the bolts is 12,7000 psi which is well below minimum tensile strength.

For the modified support with the restoring moment transmitted from the support flange to the main support tube through epoxy bonds on both inside and outside of the tubes, the maximum shear stress in the bond due to a 30 g transverse acceleration is approximately 1200 psi. This is well below allowable shear stresses for epoxy materials.

2.2.3 Detector Mount Analysis

Although there were no specifications regarding the detector alignment to be maintained, a support concept was selected which would result in a minimum misalignment due to vibration or thermal expansion effects, yet result in a small thermal load on the argon. The concept consists of a system of three pairs of taut wires aligned at 45°. This arrangement provides optimum axial and lateral stiffness, and the symmetry reduces the possibility of misalignment due to thermal expansion effects.

For this configuration the tension in each wire of an "n" wire system subject to a vertical load P is:

$$T \cong T_o \pm \frac{P}{n} \sec \alpha$$

where α is the wire angle to the horizontal and T_o is the no load tension in each wire. If the force P is horizontal and aligned with one set of wires, the tension in those wires would be:

$$T = T_o \pm \frac{2P}{n} \sec \alpha$$

Thus, the change in tension due to the horizontal loading is twice that for the vertical loading. The horizontal displacement is:

$$\delta_h = \frac{2PL}{nEA \cos^2 \alpha}$$

where E is the wire elastic modulus, A is the wire cross-sectional area and L the wire length. The lowest natural frequency of vibration, ω, of this system is in the horizontal mode and is

$$\omega = \left[\frac{nEA}{2LM} \cos^2 \alpha \right]^{1/2}$$

where M is the mass of the detector and mount. (In the vertical mode the natural frequency is $\sqrt{2}$ higher.)

The material used for the support wires was Ti:4Al, 6V for which $E = 16 \times 10^6$ psi, and $\sigma_{yield} = 110{,}000$ psi. The mass of the detector-detector mount combination is taken as 1.6 gms or approx. 0.004 lb (assumes solid aluminum plug 0.8 cm long), the maximum acceleration is 30 g, and the wire lengths are 1.0 in.

To maintain a natural frequency well above the 2000 cps upper limit (i.e. $\omega = 4000$ cps) the required wire cross-sectional area is $A \geq 0.87 \times 10^{-5}$ in^2 (i.e. $d \geq 3.4$ mils). The increased stress in the wire due to a horizontal load of

$$P = 0.004 \times 30 = 0.12 \text{ lb is}$$
$$\Delta\sigma = \frac{2P}{nA} \sec \alpha = 6500 \text{ psi}$$

Therefore, since this is well below the yield stress, the wires can be placed in static tension corresponding to a large fraction of the yield stress.

The system* consisted of six Ti: 4Al, 6V wires of 4.3 mil diam. and 1.0 in. long, arranged as shown in Figures 4-8 and 4-9. For this system the lowest natural frequency (horizontal mode) is 5800 cps, and the stress resulting from the load P = 0.12 lb is $\Delta\sigma = 3900$ psi. The wires were placed in static tension of approximately 20,000 psi.

*The Ti alloy was used in the structural mode; however, in the final thermal model 3.1 mil stainless steel wire was used because the Ti alloy was not available. The resultant performance is only slightly degraded in terms of heat flow.

2.2.4 Cryogen Tank Design

In order to be compatible with the re-entrant tubular support concept, toroidal cryogen containers were used. The tanks were constructed of 6061-T6 aluminum to permit them to be spun formed, and to take advantage of the high thermal conductivity of aluminum so as to minimize thermal gradients across each tank. The tanks were designed for a collapse pressure of at least 20.5 psi (1.4 factor of safety over atmospheres). The tank brackets were designed to withstand 30 g's in any direction and were fabricated from 6061-T6 aluminum.

The configurations of each of the CO_2 and argon tanks as well as other pertinent information are shown in Figures 4-1 and 4-2.

3.0 SUPPORTING TESTS

During the design and construction phases of the refrigerator, testing was done on certain components in support of the proposed refrigerator design. These supporting tests are described below.

3.1 Initial Fill Tests

In the initially proposed solidification technique the cooling is provided by LN_2 passing through cooling coils welded to the outside of the toroidal container walls. Energy released during direct solidification (for CO_2) and direct solidification or first condensation (for argon) depending on the pressure, is transferred through the solid (or liquid) to the aluminum container walls where it is conducted to the cooling coils. To determine if the solidification process for carbon dioxide could be achieved in a reasonable time, preliminary fill tests were performed using a configuration similar to that proposed for the thermal model. The tests were conducted in a horizontal 4 inch diameter by 12 inches long cylindrical aluminum container with the LN_2 coolant line soldered (low temperature aluminum) along the lower side of the cylinder and with the fill port at the upper mid-point of the cylinder. Plexiglas windows epoxied to the ends of the cylinder permitted visual observation of the solidification process and the density of the solid. The cylinder was mounted in an evacuated bell jar and surrounded except for the ends by a LN_2 cooled shield.

The preliminary tests using this apparatus for CO_2 solidification were very successful and fill times of 4 to 5 hours were achieved. The tank fill pressure was found to be of minor importance. Direct solidification of the CO_2 from the vapor resulted in an effective density which appeared to approach 100 percent of theoretical solid density. The rapidity of the fill process indicated that internal heat exchangers were unnecessary. Plugging of the fill line by solid CO_2 near the tank entrance due to the high conductivity of the aluminum tank

walls was not found to be a problem, apparently as a result of the warm CO_2 vapor at that point. However, it was felt advisable to locate the LN_2 coolant line remote from the inlet.

Observation of the filling process through the plexiglas window revealed the solid CO_2 formed was extremely clear and transparent indicating a high solid density. The formation of relatively low density frosty or porous solid was not seen at any time or under any condition of testing. Observation of the build-up of the solid indicated that initial solid began forming on the wall nearest the LN_2 coolant tube, then grew to cover the walls, except near the inlet tube, and then gradually built-up until only a "bubble" remained around the inlet tube. The warm gas entering through the inlet prevents freezing of the inlet region until last, and prevents plugging in that area.

3.2 Detector Support Tests

To maintain a low heat load on the argon an efficient detector support concept is required and the one proposed was a taut wire suspension system. The proposed method of attaching the wires to the detector mount and the support ring was epoxy bonding. Tests were conducted in which a small diameter chromel wire was epoxy bonded to a 70 mil thick aluminum plate and loaded to failure. Five mil wires were used and Epon 123 and Hysol epoxies were evaluated. Tests were conducted at both room temperature and LN_2 temperature. The results were as follows:

Epoxy Type	Temperature ^{o}K	Lap Shear at Failure psi
Hysol	300	1320
Hysol	300	1320
Hysol	300	1100
Epon 123	300	1860 (no failure)
Epon 123	300	3160 (wire failed)
Epon 123	77	3160 (no failure)

The tests indicated that the Epon 123 is superior to the Hysol and that shear stresses of 3160 psi can be sustained without bond failure. Calculated shear stresses on the bond for the configuration used in the refrigerator were of the order of 500 psia. The Epon 123 epoxy was used in construction of the refrigerator detector mount.

3.3 Structural Tests

The concentric tube bundle which makes up the low heat leak support system for the refrigerator is the critical structural component of the system. In order to gain further information about the mechanical properties of the material and to evaluate the manufacturers lay up technique, some small cylinders were made up for testing. These cylinders were made from S glass-1581 cloth by U. S. Polymeric Chemicals, Inc. and E-787 epoxy. The diameter was nominally 1.6 inches and various lengths were utilized. The tests consisted of subjecting these samples to various loading conditions at room temperature until failure occurred. The results of the tests are presented in Table 3-1. The results of the tests were quite encouraging, the stress at failure being approximately the design values. The failure stresses exceeded those found for similar cylindrical models tested in Ref. 1. The buckling stress at failure did not reach the predicted value; however, a review of the structural model used for refrigerator design showed that sufficient margin was available to withstand the structural tests to which the refrigerator was subjected.

3.4 Emittance Tests

Prior to the selection of the gold coating which was to be used to control the thermal absorbtance of critical surfaces, representative samples were evaluated. Three basic types of coatings were evaluated over a range of temperature down to 60°K. These were "Lock-sprayed" gold, a sprayed on process (Ref. 3), electrodeposited gold and a vacuum deposited gold. These coatings were applied to 2" disks of varying materials and evaluated in an emittance calorimeter at the Lockheed Research Laboratory. The calorimeter and its

TABLE 3-1

STRUCTURAL TESTS ON FIBERGLAS-EPOXY TUBE SAMPLES

	LMSC Cylinder Test Load at Failure	LMSC Cylinder Test Stress at Failure	Refrigerator Design Values	Ref 1 Cylinder Test Stress at Failure	Ref 1 Coupon Tests Stresses at Failure
Compression Tests	6,250 lbs.(1) 6,050	44,300 psi 5 ,600	53,000 psi	34,820 psi	62,587 psi
Tension Tests	11,650(2) 10,850(1)	> 71,000 > 77,000	not critical to design	66,633	92,506
Buckling Tests(3)	4,050 4,040	27,800 28,000	Predicted Buckling 48,000 32,800	- -	- -

(1) Tube samples consisted of nominal 1.6 inch diameter, and nominal 1/2 inch length. The first sample had a 0.0278 inch mean thickness while the second had a 0.0256 inch mean thickness.

(2) Tube samples consisted of nominal 1.6 inch diameter and nominal 4 inch length. The first sample had a 0.0322 in. mean wall thickness and the second a 0.028 in. mean thickness. In both tests the epoxy bond in the end fixture failed before the ultimate tensile strength of the tube was reached.

(3) Tube samples consisted of nominal 1.6 inch diameter and nominal 4 inch length. The first sample had a 0.0287 in. mean wall thickness and a 0.026 in. minimum wall thickness while the second smple had a 0.0284 in. mean wall thickness and a 0.018 in. minimum wall thickness.

operation are described in Ref. 4. The results of these measurements are presented in Figure 3-1. The total hemispherical emittance for Locksprayed gold was determined for both aluminum and fiberglas substrates and for 200 Å and 1000 Å for the fiberglas sample. The tests with fiberglas were required to determine the suitability of the gold coating on the fiberglas support tubes and the radiation shield. The results show the "Lockspray" technique to be comparable to the vacuum deposited coating at low temperature and somewhat better than the electrodeposited coating at room temperature. The Locksprayed technique was selected for gold coating because of its good performance and its adaptability to the fiberglas components.

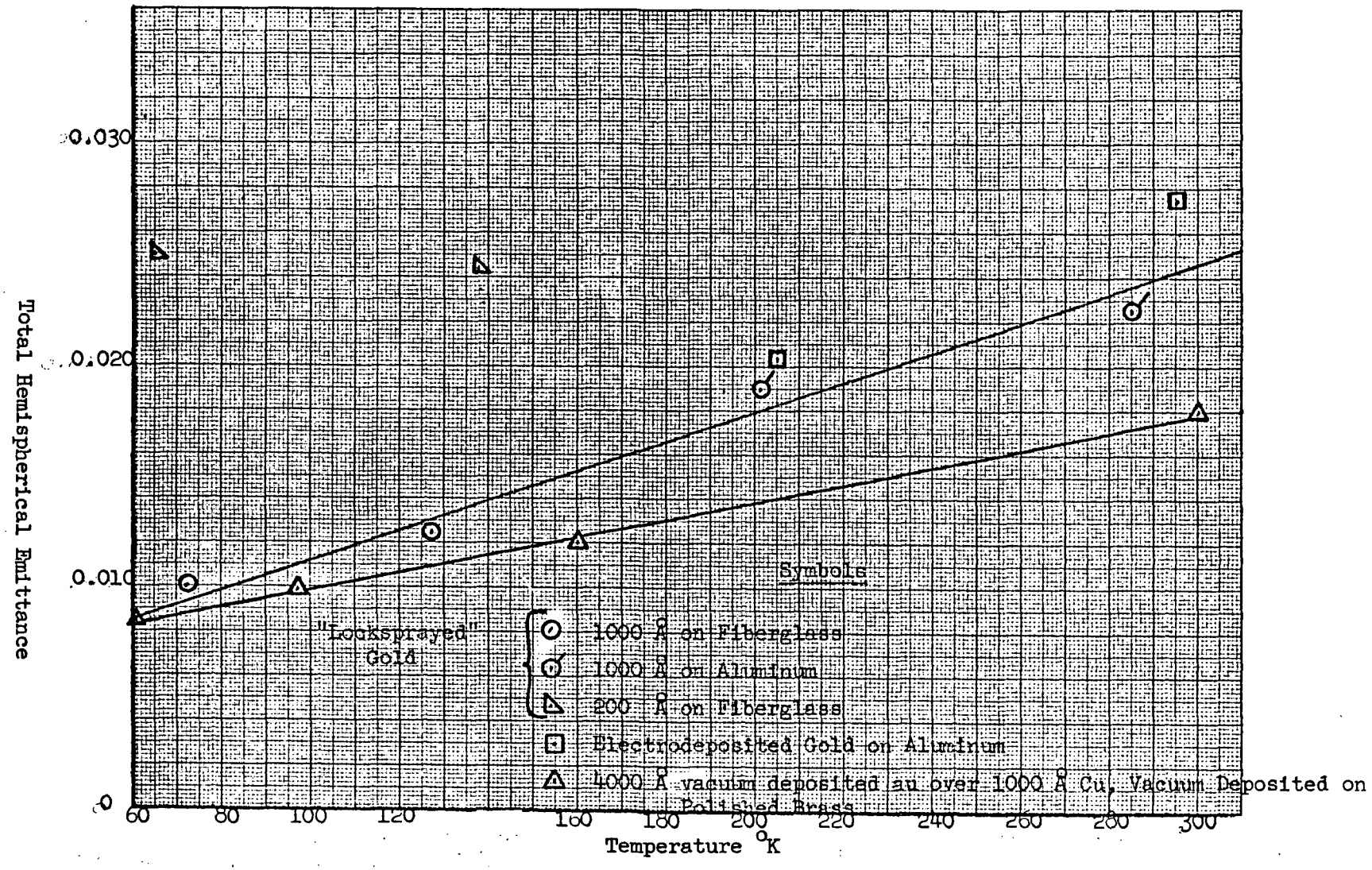

Figure 3-1. Total Hemispherical Emittance vs. Temperature for Gold Surfaces

4.0 SOLID CRYOGEN REFRIGERATOR FABRICATION

4.1 Thermal Model

The refrigerator was constructed primarily of aluminum and epoxy reinforced fiberglas. Aluminum was chosen in preference to steel for construction of the cryogen tanks because of the lighter resultant weight and the high thermal conductivity, which results in more uniform temperature throughout the cryogen, and improves the fill efficiency. Fiberglas was the obvious choice for the support tubes because of its high strength and low thermal conductivity.

The cryogen tanks were constructed from 6061 aluminum, and were toroidal in shape. The tank configurations are shown in Figures 4-1 and 4-2. The carbon dioxide and argon tanks had an external diameter of 9 3/4" and 8 3/4", respectively. The spun domes used in the construction were formed from 0.050" thick 6061-0 aluminum, which resulted in minimum wall thickness at any point of 0.040". The inner and outer cylinders of the argon tank were roll formed from 0.040" stock and butt welded at the joint. The argon tank also had an internal heat exchanger (Figure 4-3) constructed of eighteen 0.010" thick aluminum fins which were soldered to the internal LN_2 cooling coils. The vent/fill connections to the tank were made by welding a length of 1/2" diameter aluminum tubing into a hole in the CO_2 tank, and by welding a 0.15 in. diameter tube into the argon tank. These short sections provided the attachment for the non-metallic vent line.

Various configurations of the weld joint design of the tanks were tried, in order to get the best structural and vacuum tight joint. The final configuration utilized a rolled lip design for the CO_2 tank and a lap joint for the argon tank. The tank components were tungsten inert gas welded together to form the toroidal tanks shown in Figures 4-4 and 4-5. The CO_2 tank had an external LN_2 coolant line added by epoxy bonding a 1/4" 6061 aluminum tube around the tank circumference near the bottom. The LN_2 inlet was located the maximum distance away from the fill inlet to minimize the possibility of forming solid CO_2 near the inlet.

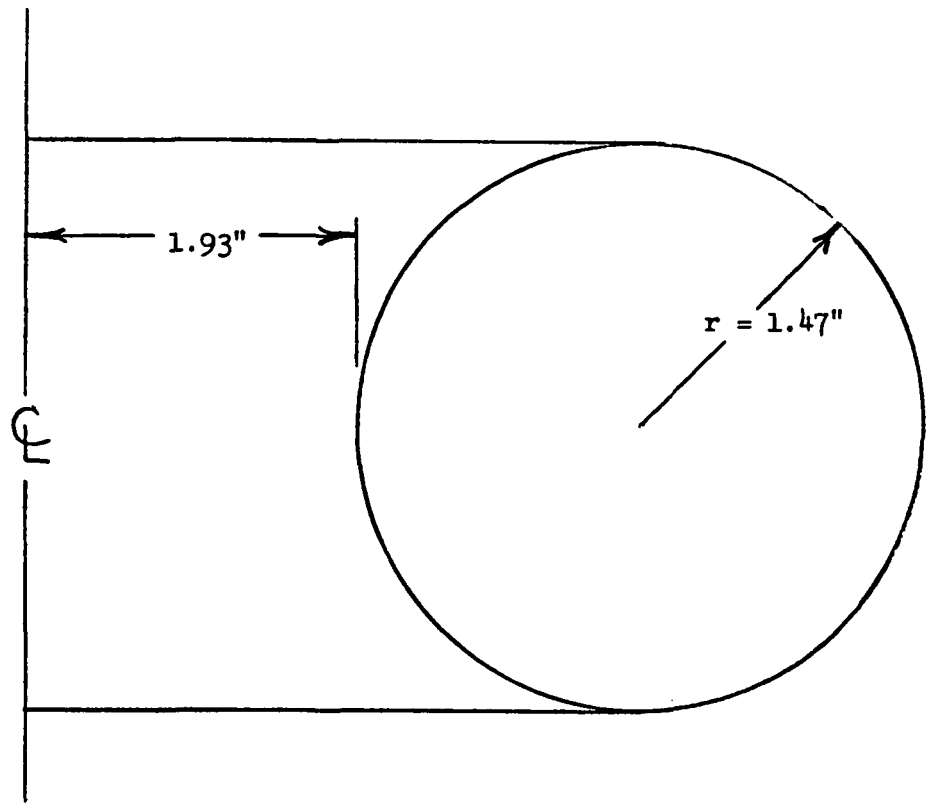

Volume	145 in^3
Capacity	7.6 lbs
Material	6061-T6 Aluminum
Min. Wall Thickness	0.030 in.
W ight	0.86 lbs.
Max. Burst Pressure	475 psi
Collapse Pressure	132 psi
Configuration	torus (above)

Figure 4-1 Carbon Dioxide Container

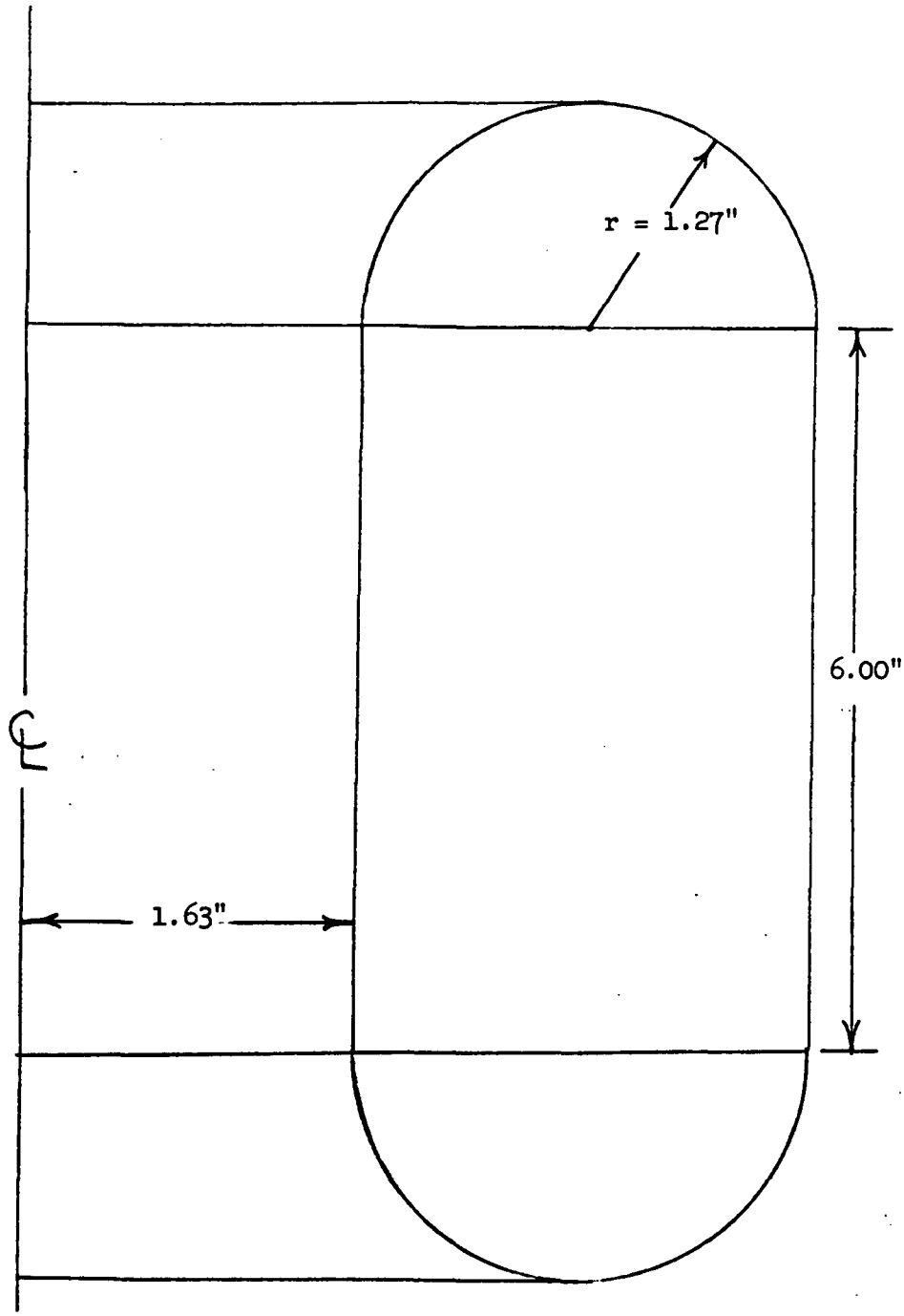

Volume	380 in^3
Capacity	19.9 lbs
Material	6061-T6 Aluminum
Min. Wall Thickness	0.030 in.
Weight (δ = 0.035")	2.1 lb.
Max. Burst (Avg. Pressure)	64 psi
Collapse Pressure (max.)	26 psi
Configuration	Toroid (above)

Figure 4-2 Argon Container

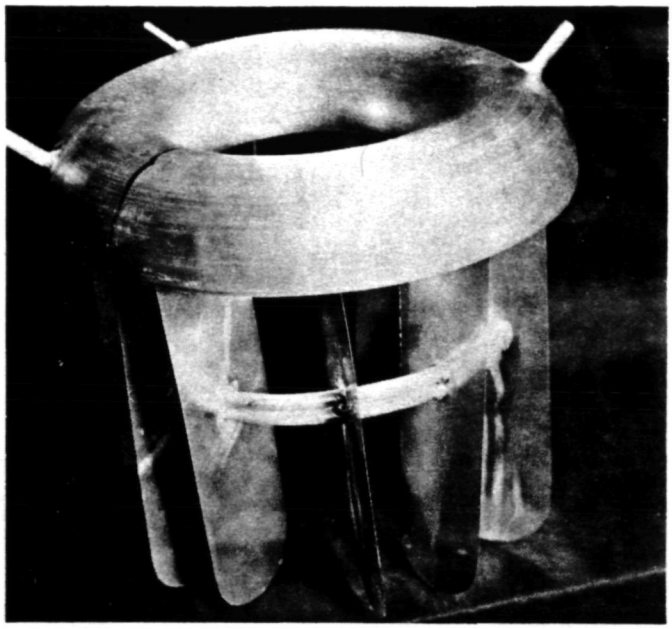

Fig. 4-3 Argon Tank Upper Dome With Internal Heat Exchanger

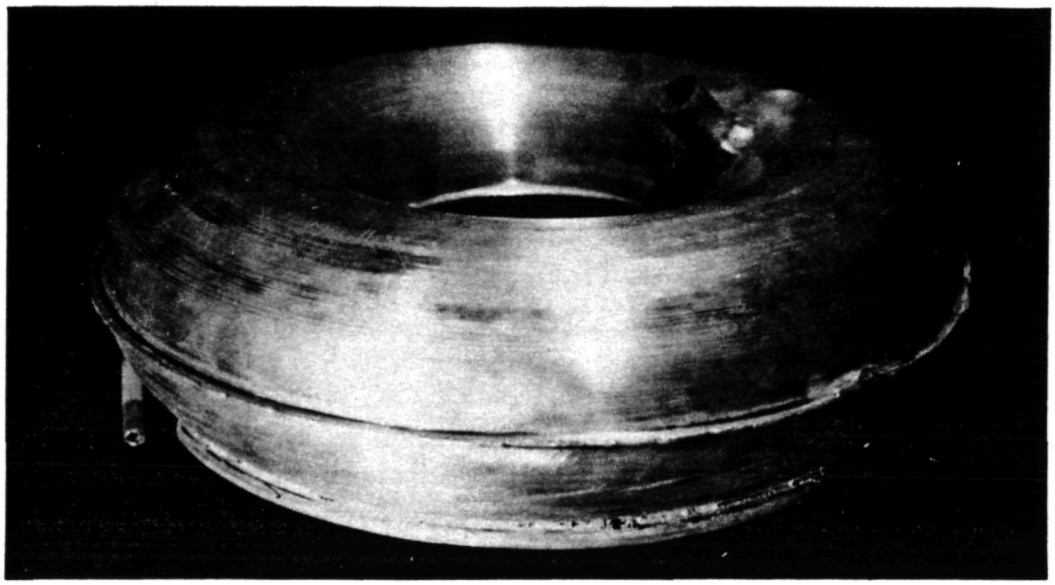

Fig. 4-4 Carbon Dioxide Container

Fig. 4-5 Argon Container

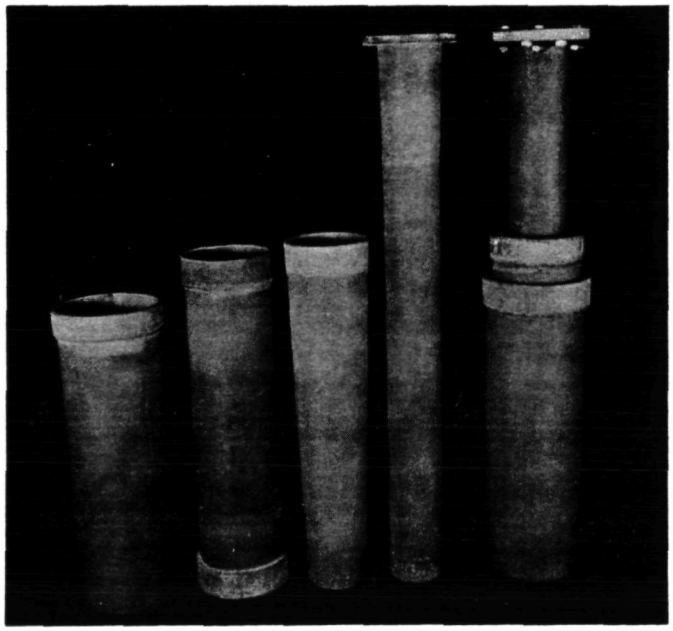

Fig. 4-6 Fiberglas Support Tube System

A mounting bracket was epoxy bonded to the CO_2 tank to provide a means of attaching the tank to the fiberglas support tubes. This mounting bracket was constructed of 0.060" 6061 aluminum. In addition, an aluminum fairing was epoxy bonded to the top of the CO_2 tank to provide an attachment for the CO_2 cooled shroud and to provide a smooth contour for the multilayer insulation which is added to the exterior of the CO_2 cooled shroud. The fairing was constructed of 0.050" thick 6061 aluminum and was spun formed into a 10.9 inch diameter by 2.75 inch deep shape.

The completion of the argon tank required a similar mounting bracket to be epoxy bonded in place. In addition, an aluminum rod 1/4" in diameter was welded to the tank bottom to provide a means for attaching the thermal link to the argon tank.

The completed tanks were subjected to leak checking and several small leaks were detected in the weld regions. Subsequent attempts to obtain vacuum tight tanks by re-welding were only partially successful. The tanks were eventually made vacuum tight by coating the weld regions with epoxy adhesive. Once the epoxy coating was applied, no further leaks were encountered during the program.

The cryogen tanks were then gold coated to provide a low emissivity. The tanks as well as the other gold plated parts were coated with a Lockheed developed spray deposition technique. Emittance versus temperature data for the coating is presented in Section 3.4. The "Lockspray" technique consists of first coating the structure with epoxy paint, then plating with gold by a spray chemical reduction method at ambient temperature. Two aqueous solutions are sprayed simultaneously; one contains complex gold salts and the other contains chemical reducing agents. The resulting metal deposit is high purity gold and requires no curing or post treatment. Further descriptions of this process are contained in Ref. 3. After completion of the tanks, they were again subjected to vacuum leakage testing both at room temperature and at LN_2 temperature and found to be vacuum tight. The LN_2 test was also used to verify that no peeling or deterioration of the gold coating would occur at reduced temperature.

The structural support system for the cryogen tanks required extensive design and development to meet the severe combined requirement of high strength and minimum heat leak. The selected support system consisted of four concentric fiberglas tubes which were epoxy bonded together into a single support structure. The material used in the construction of these tubes was S glass-1581 cloth by U.S. Polymeric Chemicals, Inc., and E-787 epoxy resin. This material selection was based upon a study of the literature, primarily Ref. 1, which contains extensive structural and thermal test data at cryogenic temperature. The fiberglas reinforced tubes were supplied by an outside vendor.* In order to evaluate the fabrication technique and the resulting structural integrity of the tubes, some small size sample tubes were constructed and tested prior to the manufacture of the actual support tubes. The results of these tests are described in Section 3.3. The results of the sample structural tests were excellent and fabrication of the main support tubes was initiated. The dimensions and configuration of the four tubes are shown in Figure 2-1. In order to reduce the radiant transmission between the adjoining tubes, which were at different temperatures, the tubes were coated with gold using the "Lockspray" technique. The tubes were coated on both inner and outer surfaces (except in the regions to be bonded which were masked off). The deposition of the gold coating had to be carefully controlled so that the thickness was sufficiently thick to obtain the low emissivity desired, but thin enough to minimize the solid conduction down the high conductivity gold film. Various spray times and reactant concentrations were tried on sample fiberglas tubes to achieve the desired thickness of approximately 500 Å. The main support tubes were then gold-coated using the optimum procedure for the Lock-Spraying. The resulting thickness measurements as determined by electrical conductivity values ranged from 345 to 530 Å on all surfaces except the outer surface of Tube No. 3 which had 245 Å. After being gold coated the tubes were epoxy bonded together using Epibond 123 epoxy. After some experimentation on samples, it was found that the strongest bond was obtained by a procedure utilizing a combination of MEK cleaning and sand-blasting. Since a silicone release agent was used in making the tubes, the cleaning procedure was found to be quite important. Figure 4-6 shows the four individual tubes used to make up the support system and

---

*Thunderbird Plastics, A Division of Aquanautics, Sunnyvale, Calif.

the resulting assembled support system. The assembled support was the one used for the structural tests and as such does not have the gold coating applied. The integral mounting flange at the top of Tube No. 1 was utilized for mounting the thermal model to the vacuum chamber flange, however, this was found to be unsatisfactory for the structural tests and a different configuration was used. The resulting concentric tube support system was found to be highly satisfactory during the fabrication and testing. The next operation was the assembly of the cryogen tanks to the support tube which was accomplished again by epoxy bonding.

The radiation shield between the argon tank and CO_2 shroud is designed to be attached at the junction of the number 3 and 4 tubes. The temperature at this junction is near the equilibrium temperature of the radiation shield. The efficiency of the radiation shield is improved by minimizing the temperature gradient along the radiation shield to the support point. To further reduce conduction between the radiation shield and the support point the radiation shield was constructed from fiberglas. This shield was formed on a mandrel using three layers of fiberglas cloth laminate. The shield was formed in two halves, separated in the axial direction. The resulting shield was flow coated with several coats of epoxy to provide a smooth surface and was then Locksprayed on both surfaces to a gold thickness of approximately 800Å. Holes were cut in the shield to provide access for the required plumbing and the thermal link. The finished shield was then attached to the 3-4 tube junction with screws,and the two halves were held together with aluminized mylar tape. In this manner the radiation shield could be removed for access to the tank and plumbing, if necessary.

The final plumbing configuration utilized sections of mylar tubing and stainless steel for the two vent/fill lines and convoluted teflon for the coolant lines which transferred the LN_2. Initial thermal testing was conducted using convoluted teflon for both the vent lines and the LN_2 coolant lines. During the thermal testing the teflon lines were replaced with the present Mylar-stainless steel assembly in order to determine if the vent lines might be leaking gas into the interior of the refrigerator. No leakage was found in the teflon vent lines and both materials have been found suitable for low heat leak

vent tubes. Both the carbon dioxide and the argon vent lines were constructed to utilize the refrigeration capacity of the vent gas. This was done by passing the vent lines around the outside of support tube No. 1 below the flange to form a manifold which was thermally shorted to a copper shield placed approximately at the mid-plane of the insulation. The arrangement of this manifold-cooled shield arrangement is shown in Figure 1-1.

The carbon dioxide cooled shroud was constructed of 6061 aluminum. The cylindrical portion was made from 6 mil material and the bottom of the shroud was spun formed from 0.020 mil aluminum. The bottom of the shroud was attached to the cylindrical section with silver epoxy. This assembly was bolted to the upper fairing which had been previously welded to the carbon dioxide tank. The inside surface of this shroud was gold coated (Lock-sprayed) to provide the required low emittance surface. The temperature of this shroud ran within 1 to 2 degrees of the CO_2 tank temperature. This shroud is shown in Figure 4-7 which shows a stage of construction of the structural model.

The detector mount was constructed of aluminum and was supported by a taut wire suspension system utilizing six 3.1 mil diameter stainless steel wires, which were attached to an aluminum collar. A jig was made to assure proper alignment of the detector holder in the collar and to control the tension on the support wires. The detector holder assembly (Fig. 4-8 and 4-9) is shown in the jig during the construction. Epibond 123 epoxy was utilized for the bonding of the wires to the components, and the results of tests to determine the strength of the bond are described in Section 3.2. After assembly, the detector holder/collar assembly was gold coated (Lockspray).

The thermal link between the holder and the argon tank was made from 99.99% pure gold, to achieve a lower emissivity and minimize the temperature drop along the length of the link. The link diameter was 0.11 inches. A flexible attachment was made between the detector support and the link by utilizing 20, 10 mil diameter gold wires. In this manner loads which could be introduced into the link itself were uncoupled from the detector holders. The bottom of the thermal link was attached to the argon tank boss by threading the gold rod into a copper

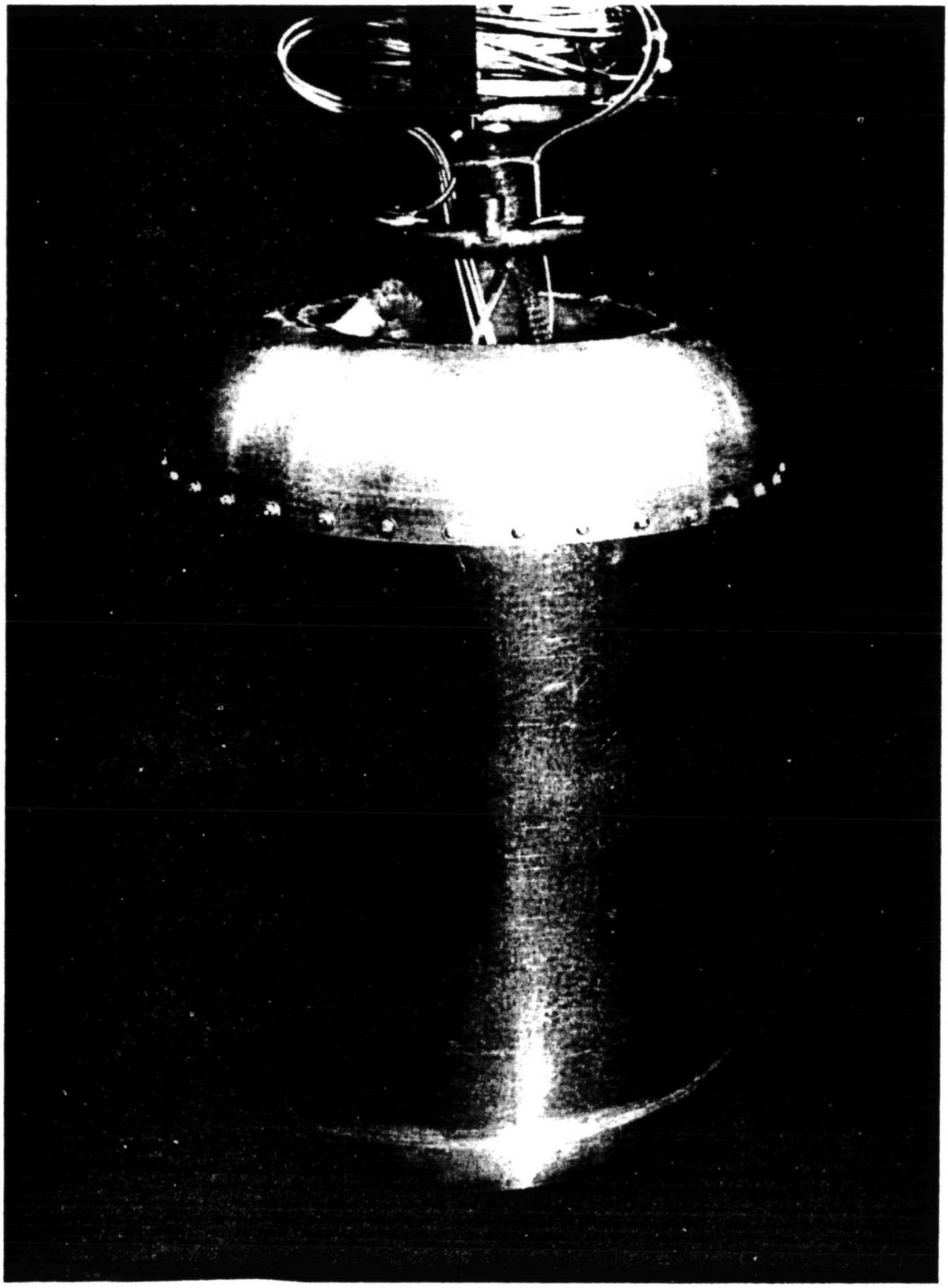

Fig. 4-7 Exterior of Refrigerator Before Insulation (Structural Model)

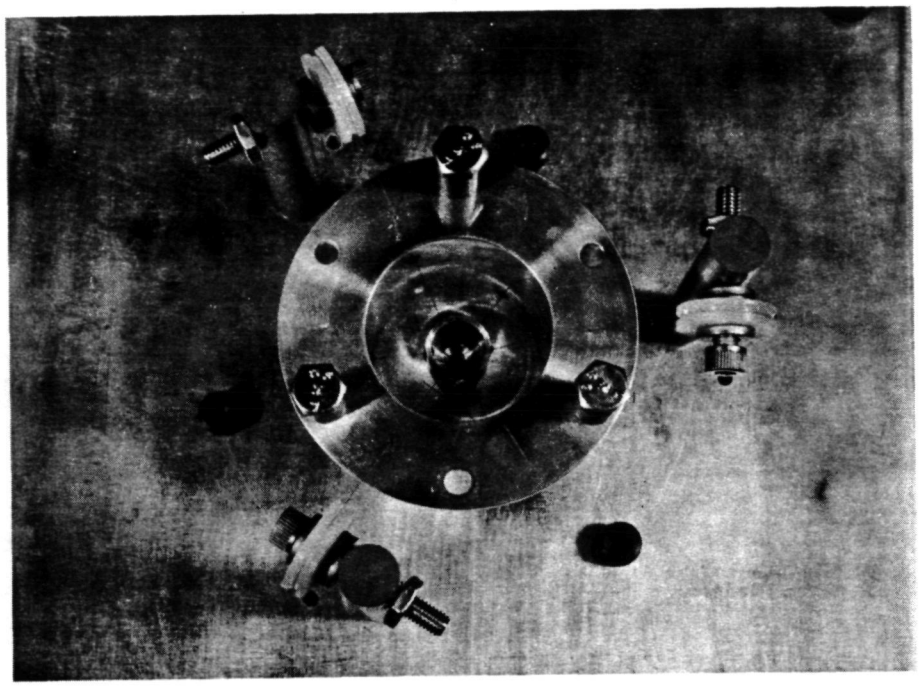

Fig. 4-8 Top View of Detector Mount in Jig

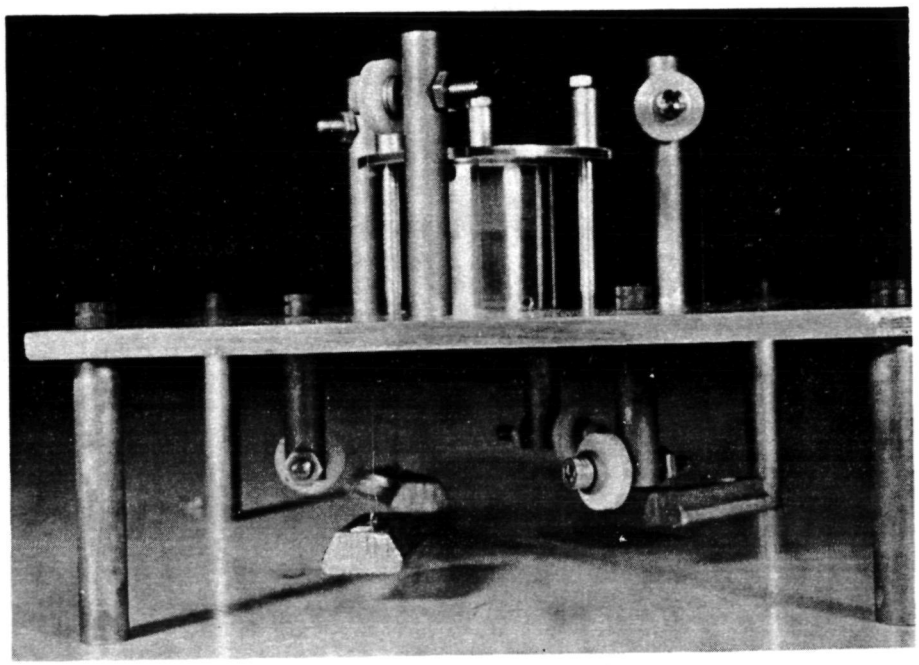

Fig. 4-9 Side View of Jig and Collar

rod which was flattened on the end and tapped to receive the gold link. This copper rod provided the connection between the aluminum boss on the tank and the gold link. Vacuum grease loaded with aluminum powder was used at the joints to insure good thermal contact in the vacuum environment.

Several techniques were tried in order to minimize the radiant and conductive heat load to the link. Initial testing utilized gold coated mylar tubes around the link to act as radiation shields. The final configuration utilized a polished aluminum tube placed around the gold link which was thermally grounded to the carbon dioxide tank at the bottom. This device was used in an attempt to provide a CO_2 temperature environment for radiation to the link. Around this aluminum tube was placed a gold coated mylar tube which served to prevent contact between the aluminum tube and the insulation inside the number one support tube which would have resulted in high conductive heat transfer. The tubes were centered with respect to each other by supporting them with 2 mil nylon thread, tied between the tubes. Rings of "Dimplar"* were used as insulation inside the number one support tube, and essentially filled the space between the fiberglas support tube and the mylar shield tube for the entire length of the support tube. The arrangement of these tubes is shown in Figure 1-1. An aluminum tube was also placed between support tubes No. 2 and 3, so that it was grounded to the CO_2 temperature by contact at the junction of tubes 2 and 3 where the CO_2 tank is attached. The bottom of this tube was closed off by attaching an aluminum disk to its bottom so that the argon tank and its radiation shield were not exposed to temperatures in excess of the CO_2 tank temperature. The bottom plate of this tube provided the CO_2 temperature support point for the aluminum tube that surrounded the thermal link. This arrangement is also shown in Figure 1-1.

The outside of the CO_2 shroud was insulated with 2 inches of double-aluminized mylar-Tissuglas which resulted in a layer density of 115 layers/inch. The outer region of the No. 1 support tube was insulated with 1/2 inch of dexiglas to provide the intermediary between the multilayer insulation and the

*"Dimplar" is a trade name for aluminized mylar which has permanent "dimples" formed in it to reduce contact between layers.

fiberglas support tube. A computer study indicated this to be the optimum thickness of intermediary.

The multilayer insulation was applied by spiral wrapping 10 layers of insulation around the cylinder, and then goring the ends and fastening the gores together with aluminized mylar tape. The procedure was then repeated with another 10 layers. The gores were displaced so that there was not a direct path or opening through the seams, which could increase the radiation load.

A vapor cooled shield was located mid-way through the insulation thickness. The shield was grounded to the vent gas manifold with silver loaded epoxy cement. The shield was constructed from 5 mil copper shim and was made in four sections each of which was six inches wide. Each section was attached to the manifold at the top and was joined at the bottom by overlapping and taping.

During the refrigeration construction temperature instrumentation was placed at key locations. Platinum resistance thermometers (PRT) were placed on the argon tank at the bottom near the attachment point of the thermal link, on the upper half of the CO_2 tank and inside the detector mount. These PRT's were applied with epoxy and covered over with aluminized mylar to provide a low emittance surface. In addition to these, chromel constantan thermocouples were utilized at the bottom of the junction of support tubes 1 and 2, the bottom junction of tubes 3 and 4, the bottom of the CO_2 shroud, and at three locations on the radiation shield.

The resulting empty weight of the system is 13.2 pounds and component weights which made up this total are listed in Table 4-1.

4.2 Structural Model

The structural model was similar to the thermal test model except that certain features of the thermal model which would not compromise its structural performance were omitted or simulated to reduce time and cost.

TABLE 4-1

SUMMARY OF COMPONENT WEIGHTS FOR REFRIGERATOR

Item	Weight (lbs)
Argon Tank	2.1
CO_2 Tank	0.6
Fiberglas Radiation Shield	0.6
Fiberglas Support Tube Assembly	1.7
CO_2 Shroud	1.3
Top Flange Support	1.3
Insulation	4.4
Miscellaneous	1.2
TOTAL EMPTY WEIGHT	13.2
Argon Weight (Design Value)	19.9
CO_2 Weight (Design Value)	7.0
TOTAL LOADED WEIGHT	40.0

The structural model was tested in the warm (room temperature) condition and the containers were loaded with a solid ballast to simulate the masses of solid argon and carbon dioxide. A wax-like tooling compound (Rigidax) was used to simulate solid argon and carbon dioxide which have densities of approximately 1.65 and 1.69 gm/cm^3, respectively. Although the tooling compound is slightly more dense (i.e., 1.80 gm/cm^3) the containers were loaded to the correct masses, which resulted in approximately the correct mass distribution. Tests at temperature with the tanks loaded with their respective cryogen would have made the costs prohibitively high for the scope of the contract.

The aluminum containers, folded fiberglas-epoxy tubular supports, radiation shield, CO_2 shroud, thermal link and coolant and fill-vent lines were similar to the thermal model. However, the portions of these components which were gold plated in the thermal model were not gold plated in the structural model. A mock-up of the detector and holder supported by a taut wire (Ti:4Al-6V) suspension system was included. The multilayer insulation used on the structural model was double aluminized Mylar-Dexiglas rather than double aluminized Mylar-Tissuglas because of the expense of Tissuglas, and a copper foil vapor cooled shield at the insulation mid-plane connected to the argon and CO_2 vent lines was also included. The structural model was tested with both the insulation and the interior at atmospheric pressure (i.e., no vacuum chamber).

The structural model was instrumented with piezoelectric transducers (Endevco, Model 2213) at each of three locations: lower end of central support tube, carbon dioxide container and bottom of argon container. Three of the piezoelectric transducers were located at each location to monitor three axis vibration. The electrical wires for the support tube and argon transducers were led out around the radiation shield where all electrical wires then left the system along the outside of the main support tube so as not to interfere with the mounting fixture. In addition, the mounting fixture was instrumented with three transducers to monitor vibration in three axes. The nine transducers on the refrigerator itself and their wiring were installed prior to wrapping the model with multilayer insulation.

The results of the structural tests are discussed subsequently; however, it is appropriate at this point to describe modifications made to the model as a result of two structural test failures. During the acceleration qualification tests under lateral loading the bolts supporting the model to the test fixture failed, and subsequent calculations indicated the support bolts were overstressed under the lateral loading condition. The support structure (support bolts as well as support tube flange) was modified; however, a subsequent failure in the support flange area occurred during the transverse random vibration qualification test. A further modification to the support flange was made resulting in the final configuration shown in Figure 4-10. The final modified configuration included:

- eight 3/8 inch diameter NAS bolts in place of the original six 1/4 inch standard steel bolts.
- an aluminum adapter ring to hold the support flange to the test fixture
- 1-1/2 inch long aluminum collars epoxied to both the inner and outer diameters of the support tube.
- addition of two layers of fiberglas (4 and 3 inches long) to the upper end of the support tube.*

These structural modifications have a minor affect on the support tube thermal conductance. This final configuration is not the optimum for a flight configuration since it was adapted to the original support flange configuration. In particular, for a flight model the aluminum adapter ring would be combined with the outer aluminum collar resulting in a slightly smaller overall mass. Otherwise the support flange configuration for a flight model would be as shown in Figure 4-10. Various stages of the construction of the structural model are shown in Figures 4-11 through 4-13.

---

*In addition, since the entire structural model had to be rebuilt following the first failure, two layers of fiberglas (approximately 4 inches long) were added to the bottom of the central support tube and one layer was added at the bottom of the second support tube.

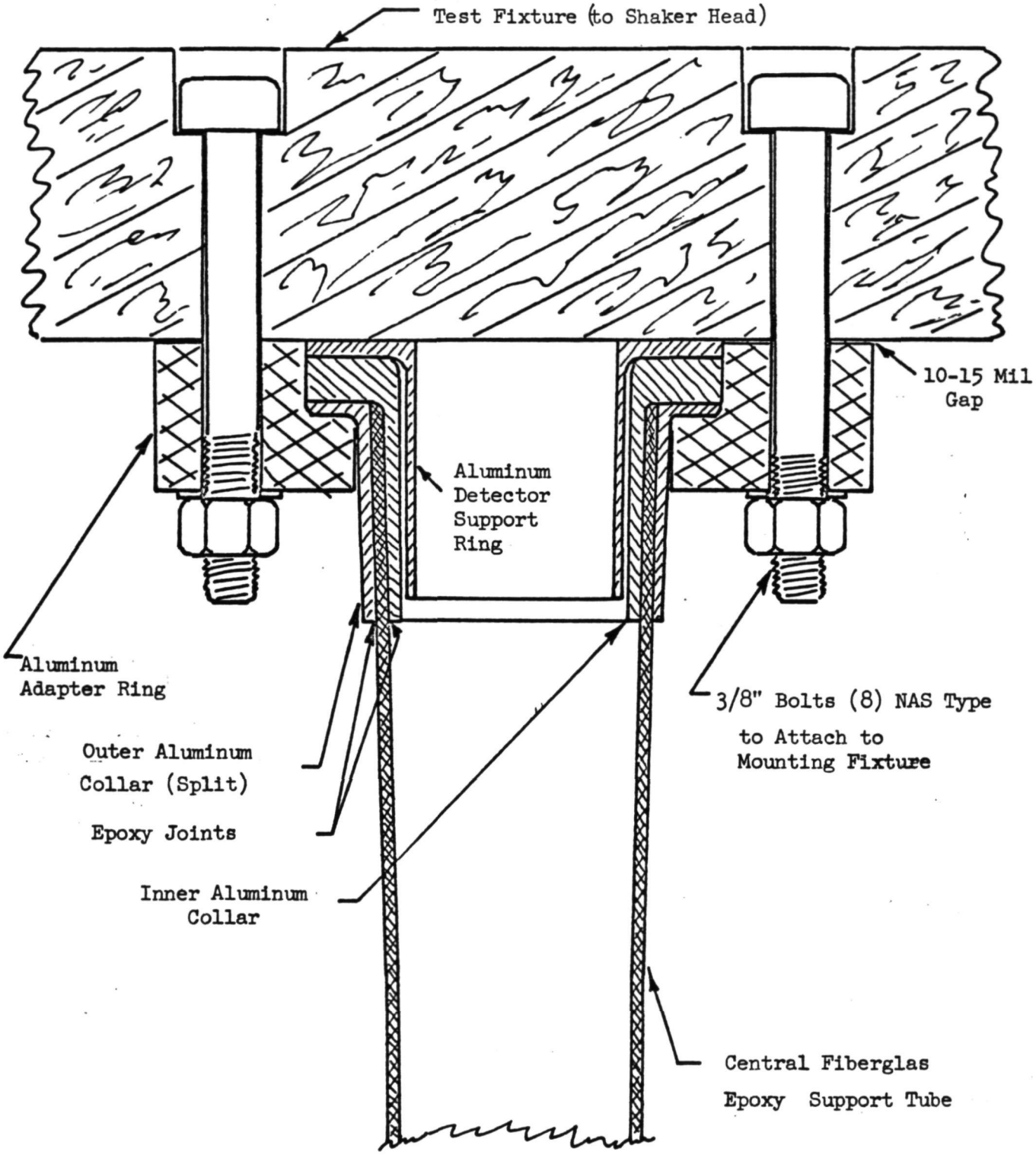

Figure 4-10 Modified Support Flange Configuration

Fig. 4-11 Structural Model Showing Argon Tank and Shroud Fairing

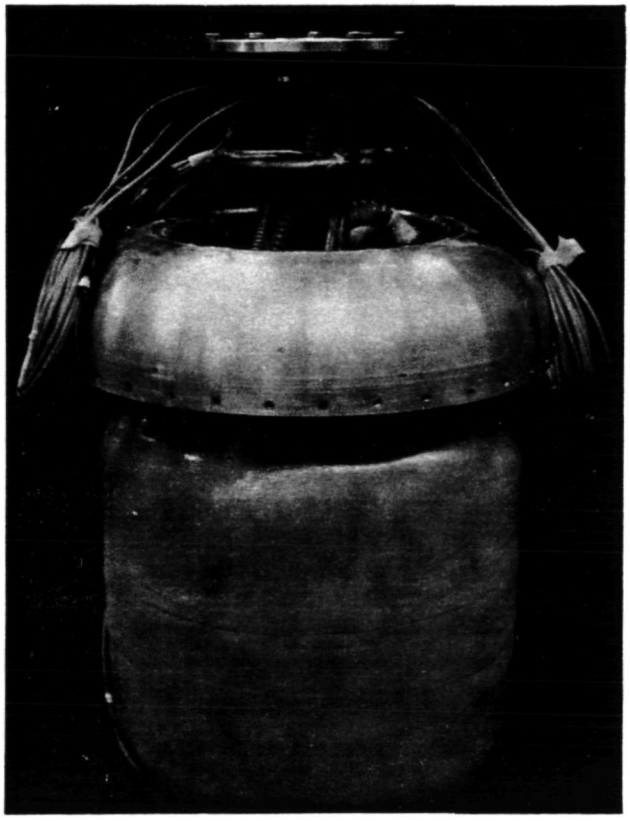

Fig. 4-12 Structural Model Showing Radiation Shield in Place

Fig. 4-13 Completed Structural Model After Multilayer Insulation

5.0 SOLID CRYOGEN REFRIGERATOR PERFORMANCE

5.1 Thermal Performance with Argon-Carbon Dioxide

a) Fill and Ground Hold Tests

The fill operation of the refrigerator was performed many times in a variety of ways, to determine the most favorable condition. The majority of the fill operations were performed with the vacuum chamber evacuated. Tests were also conducted with helium, argon and nitrogen gas present in the chamber during the fill operation. Although the heat which must be removed by the LN_2 coolant was greater with a gas filled insulation, only a small difference in fill rate was noted during the various fill conditions. The heat leak through the gas filled multilayer insulation was of the same order as the heat removal rate from the CO_2 solidification process, however, only a small additional heat input into the argon tank resulted due to the small temperature gradient between the argon and CO_2 tanks during fill. The LN_2 coolant heat capacity was more than sufficient to remove the heat input, for either the gas filled or evacuated condition.

The filling operation consisted of the following operations:

1) The condensible gases were removed from the vacuum chamber by pumping on the chamber for the evacuated chamber condition or by sequential pumping and backfilling for cases where the chamber was to be gas filled.

2) The cryogen tanks were evacuated and each filled with the fill gas at the room temperature conditions.(Three such cycles for each tank.)

3) The tanks were left filled with the fill gas and the supply lines were left opened to the tanks at a pressure near one atmosphere.

4) The LN_2 coolant flow was started through the system.

5) As the fill gas began to cryopump into the container, the throttling valves in the lines were adjusted to the desired flow rate.

The fill gas was bubbled through a water flask to saturate it with water, then passed through a precision wet test meter to meter the flow, then through columns of Ca CO_3 dessicant to dry the gas before entrance into the tank. This fill procedure resulted in direct formation of solid CO_2 from the gas and the formation of liquid argon from the gas. Subsequent formation of solid argon was obtained by further cooling of the argon with subcooled LN_2. The subcooled LN_2 was obtained by depressurizing the LN_2 supply, which is normally at approximately 20 psig, then repressurizing with helium gas. The resulting LN_2 temperature is sufficiently cold to freeze the argon.

The results of some preliminary fill tests on a cylindrical aluminum container are discussed in Section 3.1. The results of these tests indicated approximately a 3-1/2 hour CO_2 fill time for a tank the size of the thermal model. In addition, high CO_2 solid density was achieved.

Initial fill tests of the thermal model resulted in a complete fill of the CO_2 tank (2080 liters at NTP) in 3-1/2 hours with the chamber filled with argon gas at $\approx$ 20 torr pressure, and also a complete CO_2 fill test requiring 3-1/2 hours for an evacuated chamber. The solid CO_2 density inferred from the measured tank volume and the total mass of gas is 1.59 gm/cc $\pm$ 4% compared with the accepted maximum density of CO_2 at LN_2 temperature of 1.70 gm/cc. A complete fill of the argon tank was not made until the final qualification tests. During these tests the argon tank was filled to 5030 liters at NTP which is 80% of the total capacity of the tank. The resulting mass of argon was 18.4 lbs. compared with the design value of 19.8 lbs. Therefore, the fill resulted in 7% less mass than the design value. The time to fill the argon tank was 24 hours. During the qualification fill of the tanks, LN_2 at 20 psig was used. The saturation temperature corresponding to this pressure is 85.5°K which is above the triple point of argon (83.8°K). It is, therefore, likely that liquid argon was formed initially. Since the density of liquid argon is 1.40 gm/cc which is approximately 82% of the solid density, it appears that the container was filled with liquid argon initially. After the liquid argon fill had been completed, subcooled LN_2 was used to freeze the argon followed by unsuccessful attempts to fill more argon into the container. It appears that, after the

fill with liquid argon, subsequent freezing did not cause the resulting voids to be formed near the inlet, so that no further argon could be added. It is felt that an improved fill procedure would result if subcooled LN_2 were used, resulting in direct formation of the solid argon from the gas.

The results of the fill tests are summarized in Table 5-1. The results of these fill tests indicate that a flight system could utilize either an evacuated vacuum container or a purge bag purged with a non-condensible gas such as helium to exclude condensible gases. In the case where a purge bag was used the gas would bleed out during ascent of the vehicle.

Tests were also run which indicate that the refrigerator can be maintained in a non-vented condition for an indefinite time by circulating LN_2 through the heat exchanger. Once the LN_2 coolant is discontinued, the argon will begin to vent relatively soon depending on the temperature to which it is cooled with the LN_2, since the normal boiling point of the argon is relatively near the LN_2 coolant temperature. For a system in an evacuated container several days would be required before the CO_2 temperature increased to the point where the CO_2 vapor pressure is significant.

After filling of the refrigerator, pumping is commenced on the CO_2 and argon tanks until equilibrium conditions are obtained. In the qualification tests approximately three days were required for the argon to reach its equilibrium temperature and approximately 6 days were required for the CO_2 tank to reach its equilibrium condition. The detector holder requires approximately the same time to reach equilibrium as does the argon, since there is a small thermal lag down the copper link. Figure 5-1 shows the temperature response of the components during and after the qualification fill tests.

b) Lifetime Tests

Lifetime tests of the system were conducted with two loadings, the first approximately 20% full and the second at maximum capacity.

TABLE 5-1

SUMMARY OF FILL TESTS

Test	Cryogen	Fill Time Hours	Tank Capacity Liters at NTP	% Filled	Chamber Condition	Comments
Cylindrical Tank Fill Tests	CO_2	3.2	1860	98.6	Evacuated	Viewing ports show very clear, high density solid CO_2
Initial Tests on Thermal Model	CO_2	3.5	2180	99	20 Torr Argon Gas	
Qualification Tests on Thermal Model	CO_2	3.5	2180	84	0.2 Torr Helium	
Qualification Tests on Thermal Model	A	24	6330	80	0.2 Torr Helium	Tank filled with liquid initially then frozen with sub-cooled LN_2
Fill Tests on Previous Refrigerator Model. Developed under NAS 5-9549	A		3990	99.7	Evacuated	
	CO_2		2530	97.3	Evacuated	

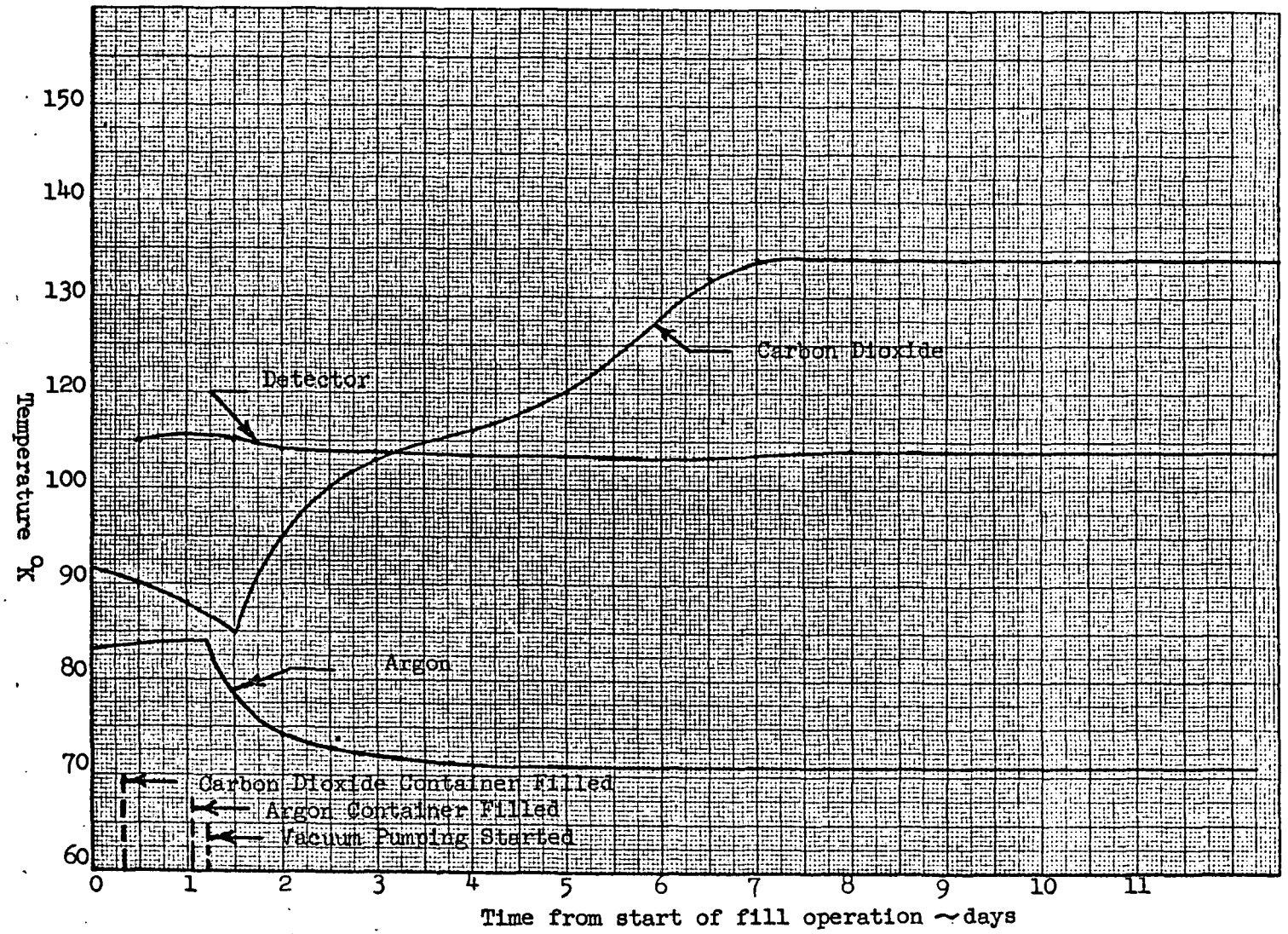

Fig. 5-1. Temperature Response of Refrigerator Components After Fill

In the maximum capacity test the refrigerator was filled with 1835 liters of CO_2 at NTP (7.40 lbs) and 5,030 liters of argon at NTP (18.4 lbs). These capacities represent 80% of the total argon tank capacity and 85% of the carbon dioxide capacity, and were the total amounts that the tanks would accept. Other fill tests have yielded greater percent fills as described in Section 5.1, part a. With this capacity the system lifetime was determined by metering the sublimation rate from the two tanks for a period of seventeen days, which was sufficient time for steady state conditions to be established.

For the maximum fill tests, the sublimation rates were measured with precision wet test meters. The resulting rates were 0.95 L/hr for the CO_2 tank and 2.2 L/hr for the argon, corresponding to heat rates of 292 mW and 204, respectively, to the two cryogens. The lifetime for the system using these vent rates and the total amount loaded into the tanks is 3.1 months for the argon and 2.7 months for the CO_2.

In a previous test the tanks were loaded with 420 liters of CO_2 and 1000 liters of argon which resulted in approximately a 20% loading. The resulting lifetime determined from these tests was 2.8 months for the argon and 8.6 months for the CO_2. The heat rates and resulting lifetime for the argon tank were approximately the same, however the CO_2 lifetime was approximately three times longer for the 20% fill test than for the maximum fill test. Only one explanation has been postulated for the difference in the CO_2 heat rates. It was noted by looking through the transparent window on the top of the vacuum container, that the CO_2 cooled aluminum tube surrounding the thermal link was off-center during the maximum capacity test. If sufficiently off-center to thermally short to the surrounding ambient temperature insulation, a large heat input would result. This is suspected as the cause of the different CO_2 lifetimes for the two tests. Confirmation would require removal of the insulation and CO_2 shroud and examination of the location of this tube, which was not possible within the time schedule. Table 5-2 summarizes these results.

These results were the culmination of an extensive thermal test program which consisted of numerous diagnostic tests for various configurations. These tests were run in an effort to reduce the heat leak in the argon tank to obtain the desired one year lifetime. The characteristics of the refrigerator and the

TABLE 5-2

MEASURED OPERATING PARAMETERS OF SOLID CRYOGEN REFRIGERATOR

With ≈ 20% Cryogen Load	
Detector Operating Temperature	105°K
Argon Temperature	61°K
CO_2 Temperature*	133°K
Net Heat Load to CO_2	92 mW
Total Heat Load to Argon	230 mW
Argon Lifetime	2.8 months
CO_2 Lifetime	8.6 months
With Maximum Cryogen Load	
Detector Operating Temperature	110°K
Argon Temperature	72°K
CO_2 Temperature*	134°K
Net Heat Load to CO_2	292 mW
Total Heat Load to Argon	204 mW
Argon Lifetime	3.1 months
CO_2 Lifetime	2.7 months

*Determined from Vapor Pressure Measurement of CO_2 in Tank

major reason for the excessive heat rate has become quite clear as a result of the test program.

The primary source of the high heat rates is believed to be due to the cryodeposition of water vapor on the detector mount and possibly portions of the thermal link and tank. This cryodeposition was visually observed during latter parts of the test program. This ice deposit could be clearly seen on the top region of the detector mount and also on the instrumentation and support wires which held the detector mount in place. This deposit was noted shortly after the fill was initiated and gradually built up with time. It is felt that the source of the water vapor which formed the cryodeposit is the multilayer insulation which outgasses water vapor as the major constituent. Investigations have been conducted regarding the outgassing of multilayer insulation and the results are described in Ref. 5. Data obtained from these tests are presented in Figures 5-2 and 5-3 for both Tissuglas and double-aluminized Mylar. In these tests it was determined that water vapor was the only significant offgassing constituent. The figures also show the effect of various pre-conditioning techniques which reduced the offgassing. These test data also showed that insulation outgassing was virtually eliminated at temperatures of 240°K and lower.

The free molecular flow paths for the water vapor which comes from the insulation and can enter the refrigerator interior is through a region of the top support flange which attaches the system to the vacuum chamber and down the interior of the number one support tube. As a result, the first cold surface which the water vapor contacts is the detector mount, and the major accumulation of ice is no doubt in this region, and diminishes as it moves down the link. The expected change in the heat rate accompanying this ice formation can be calculated as follows for the refrigerator configuration.

The surface area of the detector mount for the sides, bottom and top area excluding the aperture at the detector top is 4 cm^2. The absorbtivity of ice is 0.9 for thicknesses of 0.025 cm and greater for 300°K radiation (Ref. 6). The heat input assuming 300°K Hohlraum surroundings is 162 mW. The calculated heat

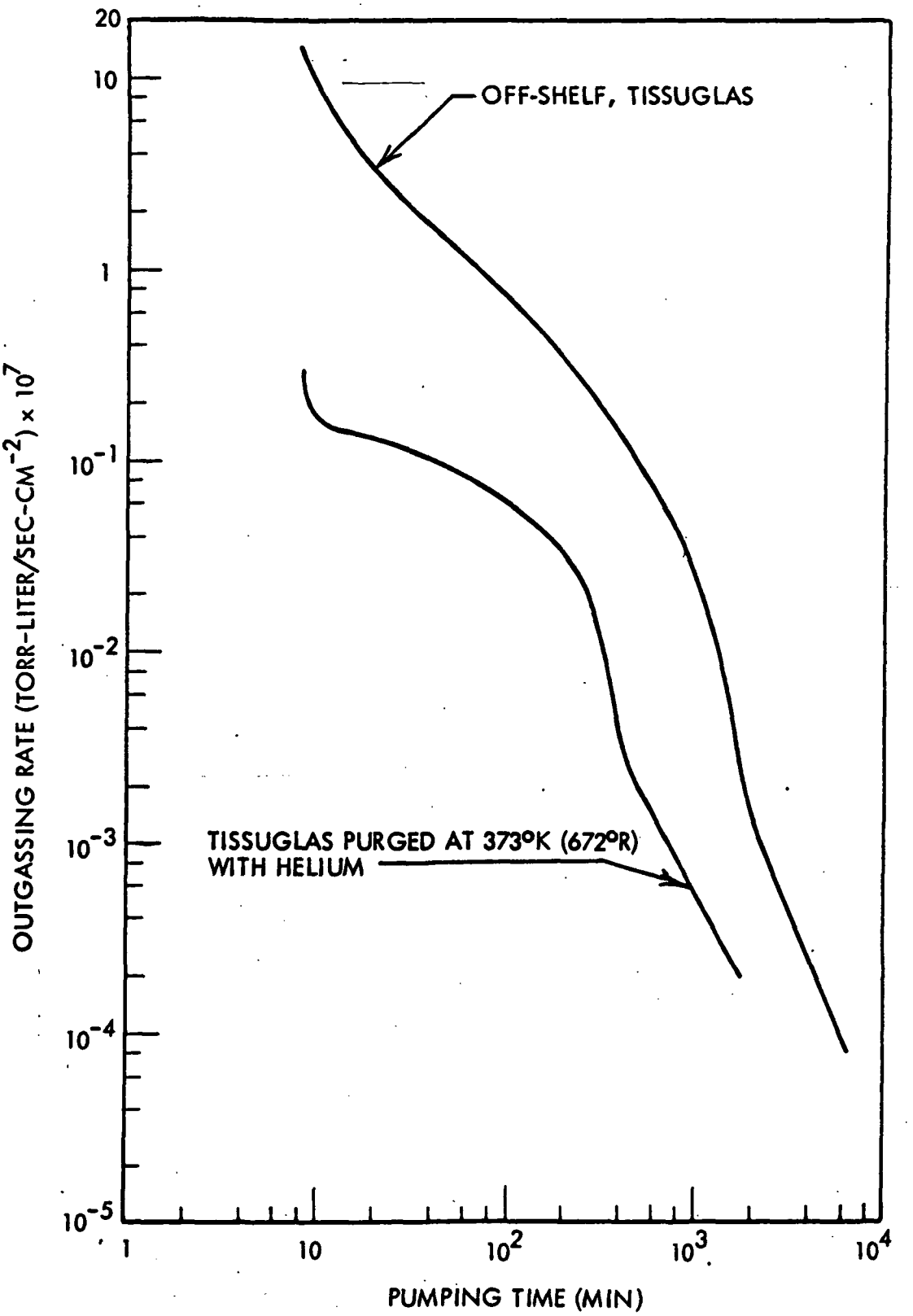

Fig. 5-2. Outgassing Rates for Tissuglas

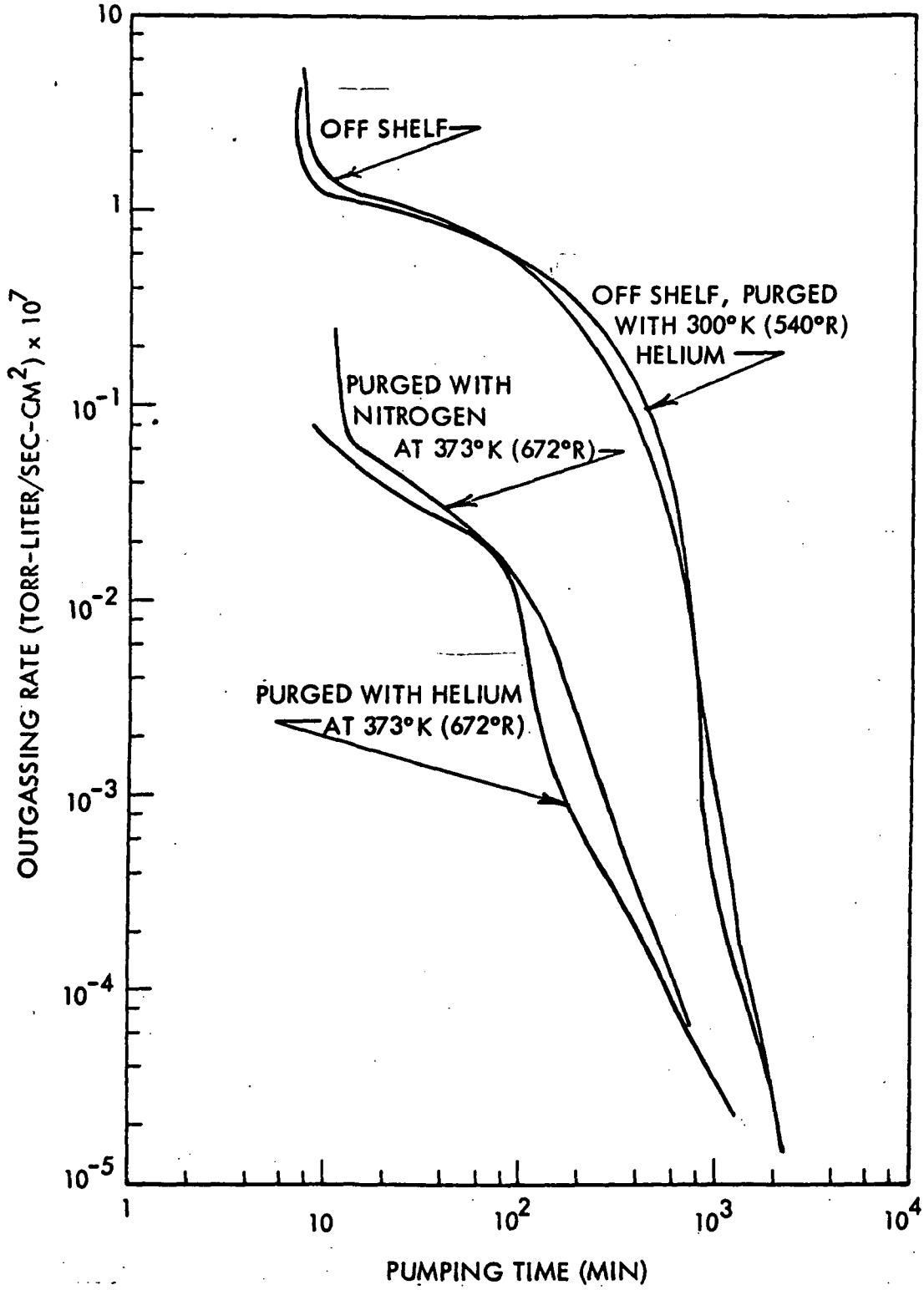

Fig. 5-3. Outgassing Rates for Double-Aluminized Mylar

rate corresponding to the same area, which is gold coated, without ice is 5.4 mW.

In addition, experimental measurements of the heat rate for a configuration which had the detector mount and the thermal link removed resulted in a reduction of the heat rate by 147 mW. If the difference in the actual heat rate for the link and detector assembly (147 mW) and the predicted heat input to the assembly (22 mW) is subtracted from the total heat input measured during the qualification tests (230 mW), then the total heat load would be 105 mW. With this heat rate the argon lifetime would be increased from 2.8 months to 6 months. Therefore, elimination of the cryodeposits would be expected to yield an argon lifetime of six months.

Another test of interest concerning the cryodeposits was one in which a configuration was tested which had only the thermal link with the detector mount removed. Removal of the detector mount resulted in a reduction of the heat rates by 120 mW. It is likely that the effects of the cryodeposition on the link and detector mount are not mutually independent since the detector mount would cryotrap water vapor and reduce the amount of water vapor which would collect on the link if the mount were not present. This consideration must be made when comparing the tests of the various configurations. In addition, some areas of the argon tank and/or radiation shield could be ice coated to a lesser degree, and some additional reduction in heat rates may take place if the H_2O vapor was eliminated from the system. Limited attempts were made to eliminate the cryodeposits. These consisted of pre-conditioning the insulation by simultaneous heating and vacuum pumping, and also by cryotrapping the water vapor with a LN_2 shroud near the refrigerator top.

The pre-conditioning was done by applying an electrical heater to the outside of the vacuum chamber and heating the empty refrigerator for a period of 9 days and simultaneously pumping on the system using the diffusion pump. This test did not eliminate the water vapor, and the resulting heat leak was only slightly reduced. The cryotrapping test was done by placing a LN_2 cooled copper disk at the top of the refrigerator. The "collar" covered almost the entire top of the refrigerator, and was external to the insulation. A comparison of the heat leak with and without this collar revealed a reduc-

cion of heat leak from 232 mW to 167 mW, as shown by comparing tests 5 and 6 in Table 5-3.

Solution of this problem will require further investigation to confirm that water vapor comes from the insulation and to determine what methods are required to eliminate this water vapor from the system. Possible solutions may require either a different type of insulation and/or a successful pre-conditioning technique. An alternate solution may be to provide for isolation of the cold detector from the water vapor.

During the thermal testing, various diagnostic tests were conducted which reveal the heat leak from various components. A summary of the more significant of these tests is presented in Table 5-3. These tests were conducted with a preliminary multilayer insulation wrap of one-half inch, which facilitated internal modifications to the refrigerator. For this reason the CO_2 heat rates are excessive and do not represent the condition realized with the full insulation wrap, which was added later. Comparison of the test results can only be made for consecutive tests since additional modifications were made between test series. The inferences made from these tests are that the heat leak to the argon tank from all sources except the thermal link is $\approx$ 83 mW and that the thermal link alone (i.e. no detector mount) increases the heat load by 44 mW. The heat leak contribution of the detector mount and link is 166 mW as previously discussed. The tests also show that the presence of the radiation shield reduces the argon heat leak from 111 mW to 84 mW (27 mW).

The effect of the LN_2 cooled collar at the top of the refrigerator in reducing the amount of cryopumped water vapor is also shown by comparison, and for the configuration tested resulted in a reduction of 65 mW.

c) Temperature Regulation Tests

During operation, the detector temperature should be relatively insensitive to changes in the environmental conditions. For example, it is desirable to minimize changes in detector operating temperature resulting from changing boundary temperature during orbital operation. The temperature regulation utilized here is completely passive, and the temperature regulation of the argon heat sink is accomplished by appropriate sizing of the argon vent line.

LOCKHEED PALO ALTO RESEARCH LABORATORY
LOCKHEED MISSILES & SPACE COMPANY
A GROUP DIVISION OF LOCKHEED AIRCRAFT CORPORATION

TABLE 5-3

SUMMARY OF THERMAL TESTS*

Configuration	Test No.	Argon		Carbon Dioxide		Temperature Dist. °K						Comments
		Temp °K	Heat Rate mW	Temp. °K	Heat Rate mW	Tube 1-2	Tube 3-4	Co_2 Shroud	Top	Middle	Bottom	
Thermal Link and Detector Removed	1	59	84	136	756	179	111.5	137	109	114	111.5	Test Comparison Shows a Reduction of 27 mW due to Radiation Shield
Same as above except radiation shield removed	2	59.7	111	137	805	170	108	-	-	-	-	
Same as Test No. 1 Configuration	3	59	82	137.5	684	175	111.5	138	114	115	113	Test comparison Shows an Increase of 164 mW due to installation of thermal link and detector mount.
Thermal Link and Detector Mount Installed	4	61.5	246	135.5	560	170	-	-	118.5	119.5	117	
Same as above	5	61	232	135	740	172	-	-	114	114.5	113	Test comparison Shows Effect of LN_2 Cooled Shield in Reducing Ice Accumulation on Detector Mount and Link
Same as above	6	77.5	167	134	526	170	-	-	117	118	117	

*These tests were conducted using ~ 1/2" thick preliminary insulation wrap.

The derivation of the control equations for both the argon and carbon dioxide refrigerants is described in Section 2.1. The resulting equations are:

For Carbon Dioxide

$$\frac{dT}{T} = 0.21 \frac{dQ}{Q} \qquad (\text{at } 134^{\circ}K)$$

and for Argon

$$\frac{dT}{T} = 0.039 \frac{dQ}{Q} \qquad (\text{at } 72^{\circ}K)$$

Therefore, changes in the heat rates of 100% should lead to changes of 2% and 4%, respectively, in the carbon dioxide and argon temperatures according to prediction.

In determining the change in the detector temperature subject to changing environmental conditions, the temperature drop down the thermal link between the detector and the argon tank must be superimposed on the argon temperature change.

In order to determine the sensitivity of the refrigerator to environmental changes and to test the validity of the derived equations, three types of tests were run. The first series of tests consisted of dissipating I^2R heat in the detector mount by means of a small resistor placed there. In addition to the lifetime test where there was no I^2R dissipation, two levels of heat dissipation were used: 50 mW and 100 mW. The results of these tests compared with the no heat dissipation condition are summarized in Table 5-4.

A comparison of the actual and predicted changes in the argon tank temperature is shown below for the full tank test.

Heat Dissipation mW	Argon Temp. °K	Measured $\Delta T \sim$ °K	Predicted $\Delta T \sim$ °K
0	72	0	0
50	73.5	1.5	0.64
100	74.5	2.5	1.19

TABLE 5-4

SUMMARY OF TEMPERATURE REGULATION TESTS

Test Conditions	Detector Temp °K	Argon Temp °K	CO_2 Temp °K	Argon Heat Rate mW	Comments
Nominal Condition, Full Tank	110	72	134	204	
Nominal Condition, approx. 10% cryogen	105	61	133	230	
50 mW heat dissipation in detector mount (Full Tank)	127.5	73.5	-	254*	Equilibrium temperatures not established for CO_2 in these tests.
100 mW heat dissipation in detector mount (Full Tank)	145	74.5	-	304*	
Outer boundary temperature increased to 105 - 145°R range (Full Tank)	125	73.5	-	249	

*These heat rates were determined by adding the detector dissipation to the argon heat rate determined from measured boiloff in the "nominal full tank test."

The actual temperature change as measured by the PRT at the bottom of the argon can was approximately twice the predicted value. It is felt that the difference between the predicted and measured values is due to the temperature gradient between the top and the bottom of the argon tank. Since the control equation utilized to predict the temperature is based on an isothermal tank assumption, it does not account for temperature gradients in the tank which would be a maximum for a full tank. During later tests the vapor pressure in the argon tank was measured with an alphatron gage and the temperature corresponding to this pressure was compared with the PRT measurement at the tank bottom. The temperature gradient from the top of the tank to the bottom determined in this manner was approximately 2.5°K for the condition of no detector heat dissipation and an 80% full tank. These measurements tend to support the contention that the difference between the measured temperature rise due to heat dissipation and the predicted rise is caused by temperature gradients in the tank.

The control equation for the detector temperature subject to heat dissipation was determined by a curve fit of the experimental results and yields a value of

$$\left\{ \frac{dT}{dQ} \right\} = 0.35 \ \frac{^{o}K}{mW} = \left\{ 0.32 \ \frac{^{o}K}{mW} \right\}_{link} + \left\{ 0.025 \ \frac{^{o}K}{mW} \right\}_{argon}$$

This value consists of both temperature changes due to the link and the argon as shown above. Approximately 90% of this change is due to the thermal resistance of the link itself. The thermal resistance of the link agrees with the predicted value; however, the temperature drop is greater than predicted due to the high, concentrated heat load at the top, resulting from the cryodeposition of ice.

A second test was conducted to determine the temperature regulation due to the variation in outer boundary temperature by applying heating blankets to the external surface of the vacuum chamber and measuring the change in heat rates, argon temperature and detector mount temperature. The resulting outer boundary

temperature distribution varied from 110° to 115°F on the top and from 105 to 145°F on the sides. The heat rates and the temperature resulting from this condition are included in Table 5-4. The steady state heat rate and temperature of the carbon dioxide container were not attained in the duration of this test, which was six days. This was due to the very slow transient response of the 2.05" thick insulation blanket when subjected to temperature changes. The argon heat rate increased from 204 to 249 mW and the detector temperature increased from 110°K to 125°K during this period and this was a result of the increased radiation load on the detector holder. These changes were a result of an increase in the radiation load on the detector holder due to a variation of the external boundary temperature from 294°K to an average of 318°K or 8%. The relatively large increase in the detector temperature can be attributed to the high thermal absorbtivity of the ice covered detector mount and the corresponding high heat rates.

The third test which was conducted to determine the temperature regulation characteristics was one in which the tank was filled to approximately 20% of its capacity. The results of this test were quite surprising inasmuch as the argon temperature at the tank bottom was 61°K. This value was 11°K lower than measured for the full tank condition. The difference in temperature for the two tank loading conditions can be explained only in part by the presence of a temperature gradient through the tank from top to bottom as previously described. The only other possibility which might explain this result is that there was a partial constriction in the argon vent line which would cause the argon to reach a higher equilibrium temperature condition.

In summary, the test results did not yield the desired value of 75°K for the detector holder, due primarily to the large temperature gradient in the link caused by the excessive heat loads at the top. For the present model, the argon vent tube could be enlarged without a singificant increase in heat leak to allow an argon temperature of approximately 50°K. Superimposing the 38°K temperature drop of the link would reduce the detector temperature to 88°K. The detector temperature could be further reduced by increasing the diameter of the thermal link, however, this would lead to an increase in the heat leak to the thermal link.

5.2 Thermal Performance with Methane-Ethylene

The use of methane and ethylene respectively as the primary and secondary cryogens in place of argon and carbon dioxide would lead to a substantial reduction in system weight, or conversely an increased life-time. Consideration of system advantages must weigh the flammability of both methane and ethylene and the handling required, against thermal gains. The thermal gain of the system is due to the higher heats of sublimation and the reduced guard temperature which the ethylene provides, as shown in the table below:

Cryogen	Solid Temp. Range* °K	Latent Heat of Sublimation J/cm³	J/gm	Density g/cm³
Argon	47.8 - 83.9	344	202	1.7
Methane	59.8 - 90.7	308	615	0.5
CO_2	125 - 217.5	1060	607	1.7
Ethylene	95 - 104	515	708	0.73

* Minimum temperature taken at 0.1 torr vapor pressure.

Tests of the refrigeration system were conducted with methane and ethylene substituted for the argon and carbon dioxide. The tests were made without the thermal link or detector mount installed during diagnostic thermal tests. The results of these tests as compared to the results with argon and carbon dioxide are summarized in Table 5-5. The temperature for ethylene shown in the table was a result of throttling the vent line outlet to achieve these temperatures for comparative purposes with other tests. The minimum temperature obtained with the ethylene as the secondary was 104°K for the vent line configuration used. A comparison of the primary cryogen heat rates shows a reduction of 38 mW or approximately 50% without the thermal link. This reduction is due to the lower ethylene guard temperature which reduces the radiant and conductive heat rates from this source.

TABLE 5-5

COMPARISON OF THERMAL PERFORMANCE TESTS
FOR TWO DUAL CRYOGEN SYSTEMS

Configuration	A/CH_4		CO_2/C_2H_4		Temperature Dist ~ °K						Comments
	Temp °K	Heat Rate mW	Temp °K	Heat Rate mW	Tube 1-2	Tube 3-4	CO_2/C_2H_4 Shroud	Radiation Shield Top	Radiation Shield Middle	Radiation Shield Bottom	
Argon and CO_2 used; no thermal link (#23)	60	73	136.5	771	166	104	137	114	115	111.5	
Methane and Ethylene used; no thermal link (#25)	84	35	120	800	169	101	121	107	108	106.5	38 mW reduction in primary cryogen heat rate

*Preliminary 1/2 inch insulation wrap was used in both of these tests.

These tests with methane-ethylene indicated there were no unusual servicing problems associated with the formation of either solid methane or solid ethylene in the respective tanks. A vent stack was installed to vent the ethylene and methane to the outside.

Since the latent heats of methane and argon are approximately the same per unit volume, but methane is only 30 percent as dense as argon, the use of methane in place of argon represents a 70% primary cryogen weight savings or similarly a large gain in lifetime for the same weight. The comparative lifetime gain for the same weight, although substantial, is more difficult to assess since a redesign of the primary cryogen container is necessary to contain the less dense methane.

Since the latent heat of sublimation/unit volume of ethylene is approximately one-half that for carbon dioxide, substitution of ethylene for CO_2 would decrease the secondary cryogen lifetime to one-half with the existing tank configuration. However, since the per unit mass heat of sublimation for ethylene is approximately 15 percent greater than for CO_2 a redesign of the secondary cryogen system for ethylene would result in approximately the same secondary cryogen system weight (cryogen, tank etc.) yet would present the advantage of providing the lower boundary temperature for the primary cryogen.

Unfortunately, complete systems tests (thermal link and detector mount installed plus full insulation wrap) were not performed with methane-ethylene due to time limitations; however, the tests that were performed did show the superiority of this combination of cryogen over argon - CO_2 in terms of thermal performance-system weight considerations.

5.3 Structural Performance

5.3.1 Introduction

The contract originally called for only a low level resonant survey test of a structural model of the refrigerator. However, under a contract modi-

fication extensive acceleration and vibration testing of the structural model was conducted. These tests were conducted at the equivalent of the acceleration and vibration specifications outlined in "GSFC Specification TIROS M/ Improved TOS", January 31, 1967.

The structural tests were conducted with the model at room temperature, and with the cryogen tanks loaded with sealing wax to simulate the respective cryogen masses. Since the fiberglas-epoxy material used in the construction of the folded support tube configuration exhibits an increased ultimate strength of approximately 20% in the cold condition, and the support tubes are designed for the cold condition, the "qualification level" g loadings were accordingly scaled down by 20% to represent "equivalent" test conditions. In the "acceptance level" tests the g loadings were not scaled down, however. Table 5-6 summarizes the details of the acceleration and vibration tests conducted on the structural model. They correspond to the specifications outlined in "GSFC Specification TIROS M/ Improved TOS," January 31, 1967, with a 20% reduction in the g loadings for the "qualification level" tests.

Three accelerometers were mounted at each of three locations on the model: bottom of argon tank, on CO_2 tank and lower end of main support tube. In each set one was oriented axially and the other two were oriented laterally and orthogonal to each other.

The acceleration tests were performed on a 60K capacity centrifruge, and the vibration tests were performed on a 7.5 K capacity shaker system.

5.3.2 Test Results

The test plan consisted of performing the specific tests in the sequence given in Table 5-6 i.e. starting with the tests considered least severe and progressing through the more severe tests. The vibration tests were considered to be more severe because of the system resonant frequencies. The goal was to maximize the amount of information which could be gained prior to a possible structural failure of the system. The test results are summarized below:

TABLE 5-6

ACCELERATION & VIBRATION TEST SUMMARY

A. Acceleration Tests:	1.	10 g (accept. level), 3 axes, 5 min. each
	2.	17.6 g (qual. level), 3 axes, 5 min. each
B. Vibration Tests: (Resonant Survey)	3.	Low Level Resonant Survey (sinusoidal) in each of three perpendicular planes
(Acceptance Level)	4.	Sinusoidal (acceptance level) 5 to 2000 cps at 5 g zero to peak at 4 oct./min. and 0.17 inch displacement* single amplitude below 17 cps; in each of 3 perpendicular planes.
	5.	Random (acceptance level) 20 to 2000 cps with sharp roll-off above 2000 cps and at 10 g rms at 0.05 g^2/cps for 2 min. in each of 3 perpendicular planes
(Qualification Level)	6.	Sinusoidal (qualification level) 5 to 2000 cps at 8 g zero to peak at 2 oct./min., and 0.25 inch displacement** single amplitude below 18 cps; in each of 3 perpendicular planes.
	7.	Random (qualification level) 20 to 2000 cps with sharp roll-off above 2000 cps and at 16 g rms at 0.13 g^2/cps for 4 min. in each of 3 perpendicular planes.

Notes:

*The TIROS specifications allow for a 0.17 in. minimum single amplitude displacement; thus, this displacement is used below 17 cps.

**The 0.25 in. single amplitude displacement below 18 cps due to equipment limiatations corresponds to the minimum allowed in the TIROS specifications.

- The system satisfactorily survived the acceptance level acceleration tests in three axes: axial compression, axial tension and lateral. (The lateral test is considerably more severe).

- The system survived the qualification level acceleration test in axial tension; however, in the lateral orientation a few seconds after the centrifuge had levelled out at 17.6 g's, the support flange failed, resulting in complete destruction of the structural model and all accelerometers. Following analysis of the flange area it was concluded that the failure was precipitated by the supporting bolts, however, additional reinforcement of the flange area itself was also felt warranted.

- A second structural model was fabricated with the flange area modified accordingly. (Similar to Figure 2-6) Two additional layers (4 and 3 inches long) of glass-epoxy were added to the top and one additional layer (2-1/2 inches long) was added at the bottom of the main support tube. In addition, an aluminum collar 3/4 inch long was epoxy bonded to the outside of the main support tube at the support end to transmit the restoring moment from the flange to the support tube by shear. An aluminum adapter ring and eight 3/8 inch NAS bolts in place of the original six 1/4 inch standard steel bolts were used to mount the flange to the test fixture.

- With the revised model, low level ($\sim$ 1 g) resonant survey (sinusoidal) tests were conducted in three axes: axial, and two orthogonal transverse axes. There was no significant difference in the two transverse surveys. Specific resonant frequencies were observed in these tests.

- Acceptance level sinusoidal and random vibration tests were satisfactorily conducted in both the axial and lateral orientations.

- Qualification level sinusoidal and random vibration tests were satisfactorily conducted in the axial orientation.

- During the qualification level random vibration test in the lateral orientation, a failure occurred in the support flange. This failure which resulted in no other damage to the model, indicated there was insufficient shear area between the aluminum collar and glass-epoxy tube. This was substantiated by subsequent analysis using possible loadings present in the vibration tests.

- The support flange area was further modified by epoxy bonding aluminum collars (each 1-1/2 inches long) to both the inside and outside of the main support tube (see Figure 2-6) to essentially quadruple the shear area. All subsequent tests were conducted with this configuration.

- Qualification level acceleration tests were satisfactorily conducted in both the axial (compression) and lateral orientations.

- Qualification level sinusoidal and random vibration tests in the lateral orientation were conducted with the basic structural configuration satisfactorily surviving these environments

- Following these tests examination of the system revealed some abrasion of, though no apparent structural damage to, the main support tube adjacent to the top of second tube, indicating sufficient displacement of the support tubes to cause contact at this location. This is consistent with the analysis of the deformation of the support system under 30 g's lateral loading. No evidence of contact was apparaent at any other location.

- On completion of the vibration testing the taut wire support system for the detector mount had failed. At what point in the vibration tests the failure occurrred was undetermined. This is felt to be a result of the wire supports being subjected to excessive stress from the thermal link assembly. This cannot be fully substantiated; and further effort is required in this area.

- As a general conclusion, the basic structural design of the support system was found to satisfactorily withstand all required acceleration environments.

Figure 5-4 shows the control (input) acceleration for the axially oriented resonant survey test. There was significant feedback near 120 Hz which results in the behavior observed near that frequency. Figures 5-5, 5-6 and 5-7 show the axial response accelerations for the argon and CO_2 tanks and support tube, respectively. At all three locations an amplification is observed near 120 cps. Based on an input acceleration of $\approx$ 1.35 g (Figure 5-4) the q factors for the argon, CO_2 and tube are 16, 12 and 7, respectively. It is noted that the amplification factors attenuate toward (along the distributed spring) the support. Although these q factors are high, the resultant stresses are purely axial, and the support tubes as well as the brackets, tanks and epoxy joints were designed to withstand the resultant stresses in the axial qualification level tests. There is also observed to be a second, though less important resonance near 350 cps which is distinct except in the case of the argon tank. Analysis confirms the presence of these two resonant frequencies. The lower frequency corresponds to the combined argon and CO_2 masses simply oscillating axially in phase on the first two support tubes in a one-degree-of-freedom fashion. The higher frequency is due to the CO_2 mass oscillating axially on two springs between the support and argon mass, with the argon mass essentially fixed at this frequency (note the small amplification of the argon at 350 cps). Although not observed for the CO_2 or argon tanks, the support tube exhibits significant amplification (Fig. 5-7) at higher frequencies. This is apparently a result of some asymmetry in the model which induces lateral vibrations, of the support tube with axial input. These accelerations are relatively unimportant in terms of resultant stresses because of the small mass of the support tubes.

Two lateral resonance survey runs (orthogonal to each other) were made; however, there was no significant difference in the results, which indicates the model was essentially axisymmetric. Thus, only one of these (designated simply as lateral orientation) is discussed. The control acceleration for

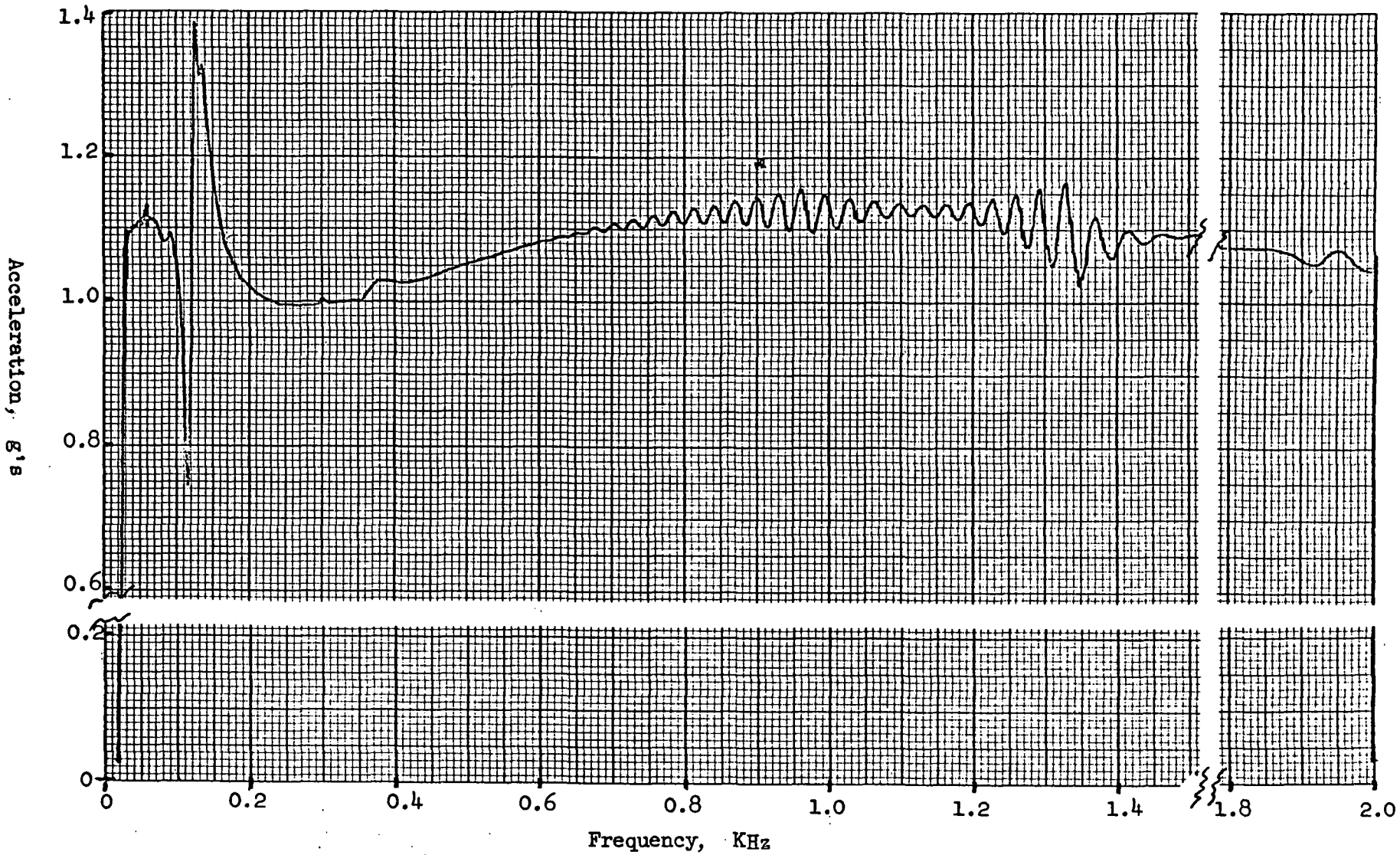

Figure 5-4. Control (Input) for Axially Excited Resonance Search

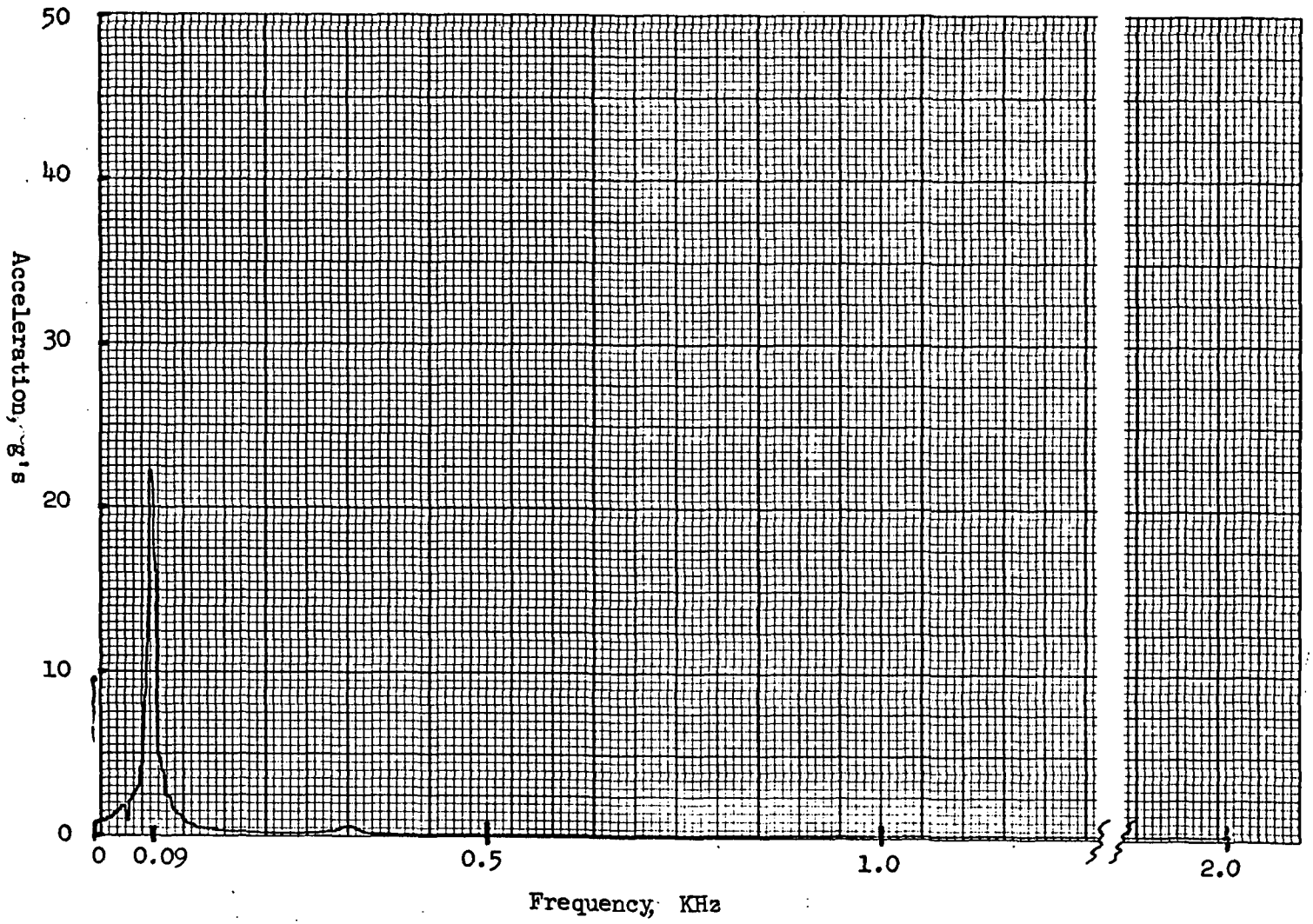

Figure 5-5 Argon Axial Response for Axially Excited Resonance Search

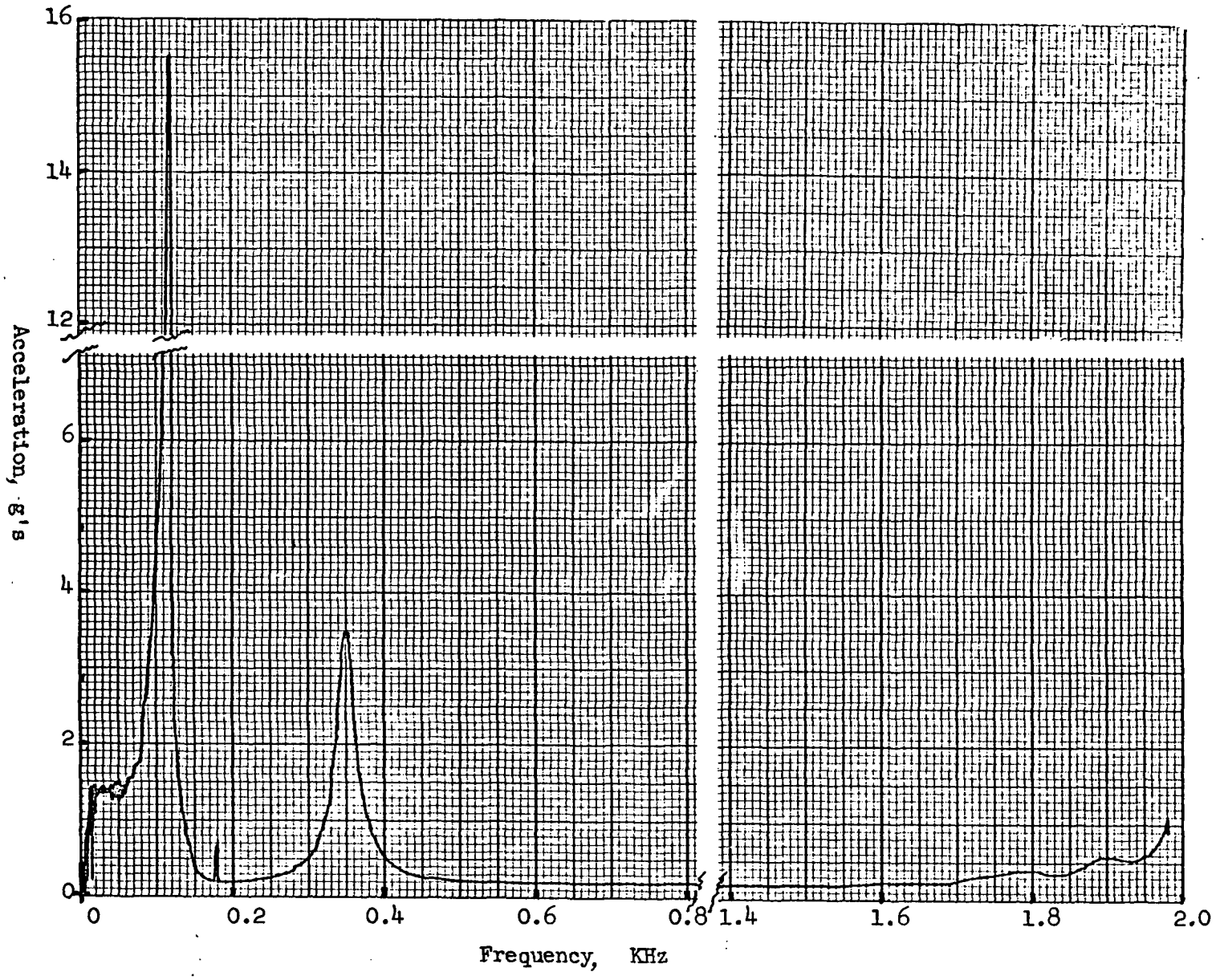

Figure 5-6. CO_2 Axial Response for Axially Excited Resonance Search

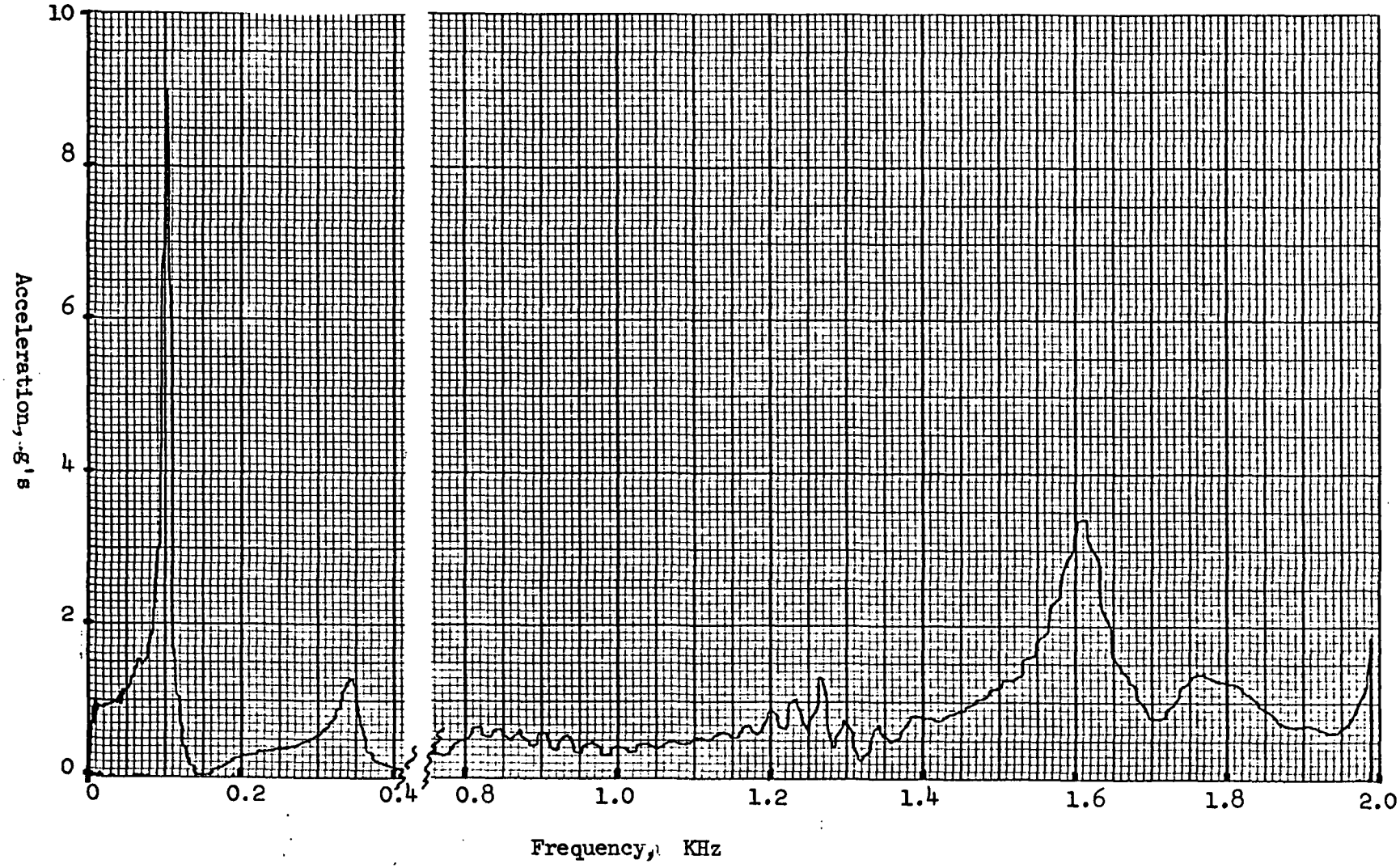

Figure 5-7 Tube Axial Response for Axially Excited Resonance Search

this run (not shown) was held at 1.05 ($\pm$ 10%) g. Figures 5-8, 5-9 and 5-10 show the responses of the argon, CO_2 and tube, respectively. The significant lateral resonances of the two major masses (CO_2 and argon) were found to occur at approximately 13 and 20 cps. At the lower frequency the resultant magnification factors were 6 for the argon and 8 for the CO_2 (Figures 5-8 and 5-9). For the higher frequency, the magnification factors are 3 for the argon and 4 for the CO_2. The two observed frequencies are predicted very well by a two degree-of-freedom dynamic model which consists of the argon mass being essentially rigidly connected to the CO_2 mass with the combined mass free to translate and rotate as a rigid body attached to the first two folded support tubes which act as a spring. Based on this dynamic model, the computed maximum stresses for the qualification and acceptance level inputs were considered to be within the allowables. However, for these higher input acceleration levels the actual response of the CO_2 mass and attached argon mass would be limited by the interference of the upper end of the second support tube and the main support tube. Although this interference creates high local stresses estimates of these local stresses showed them to remain within the allowables.

The above observations and considerations were verified by the results of the qualification and acceptance level sinusoidal and random vibration tests which were conducted in both the axial and lateral orientations. The basic structure of the model, after the modification to the flange area described above, satisfactorily survived all of these tests. Figure 5-11 shows the control (input) acceleration for the acceptance level, axial, sinusoidal vibration test. Figures 5-12 and 5-13 show the responses of the argon, and CO_2 tanks respectively for this test. As for the resonance survey test the system exhibits resonances near 350 cps and in the region 80 to 100 cps. The amplification factors near 100 cps for the argon and CO_2 tanks are approximately 5 and 3, respectively (compared to 16 and 12 for the similar resonance survey test). Thus, there was considerably greater damping for the higher input test. The amplification factor near 350 cps is only significant for the CO_2 tank where it is 6, which is approximately twice as high as it was for the resonance survey test.

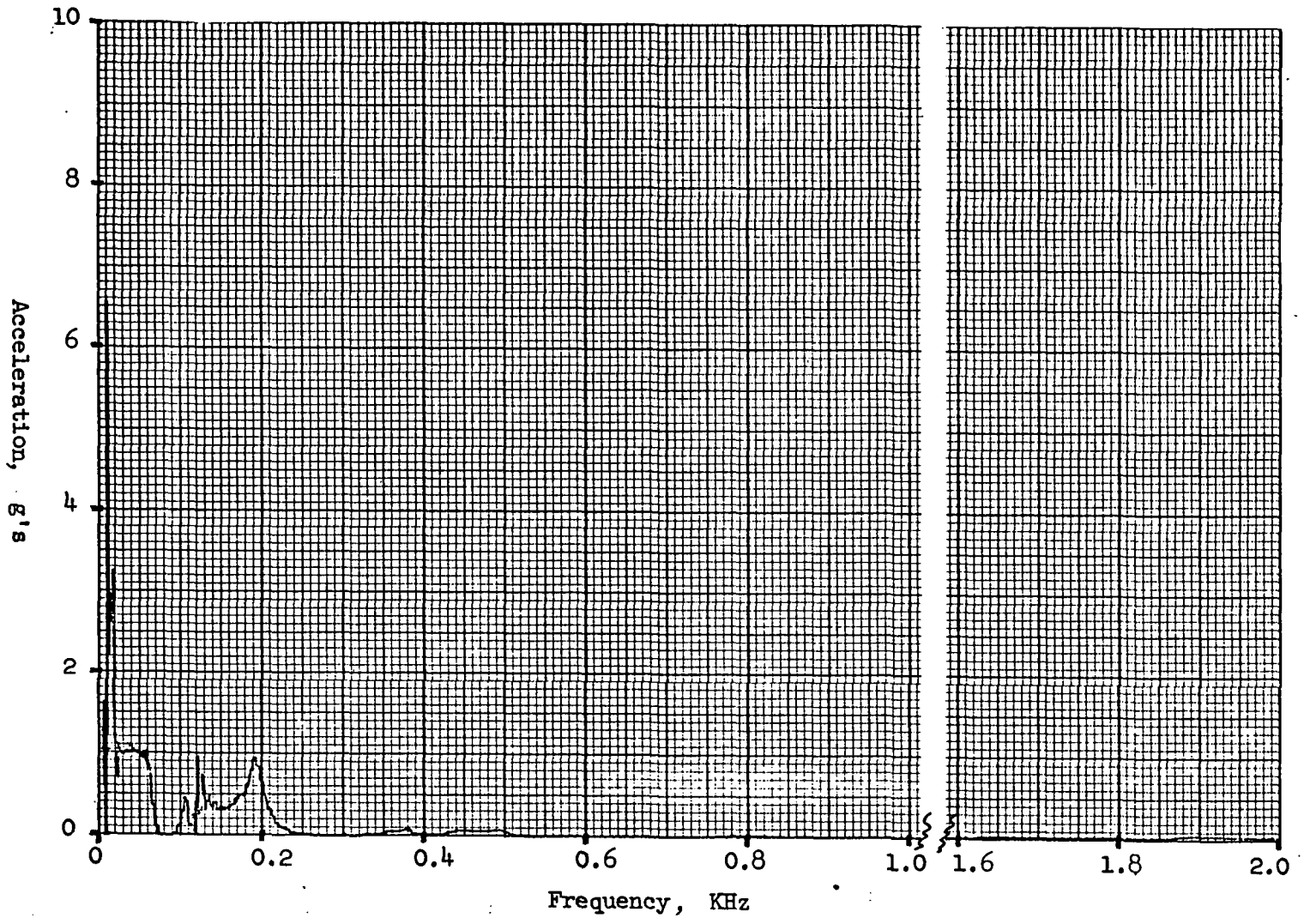

Figure 5-8. Argon Lateral Response for Laterally Excited Resonance Search

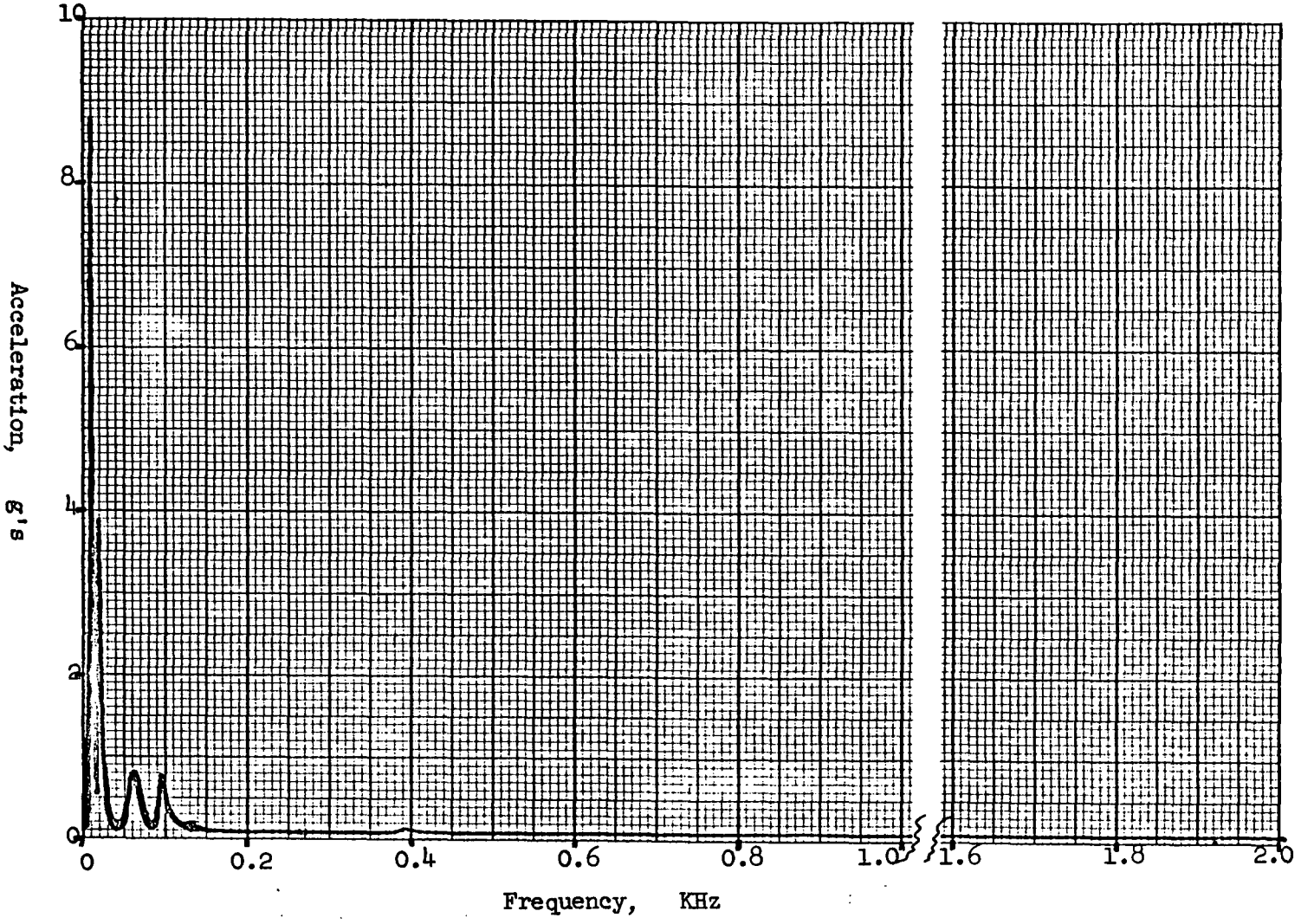

Figure 5-9 CO_2 Lateral Response for Laterally Excited Resonance Search

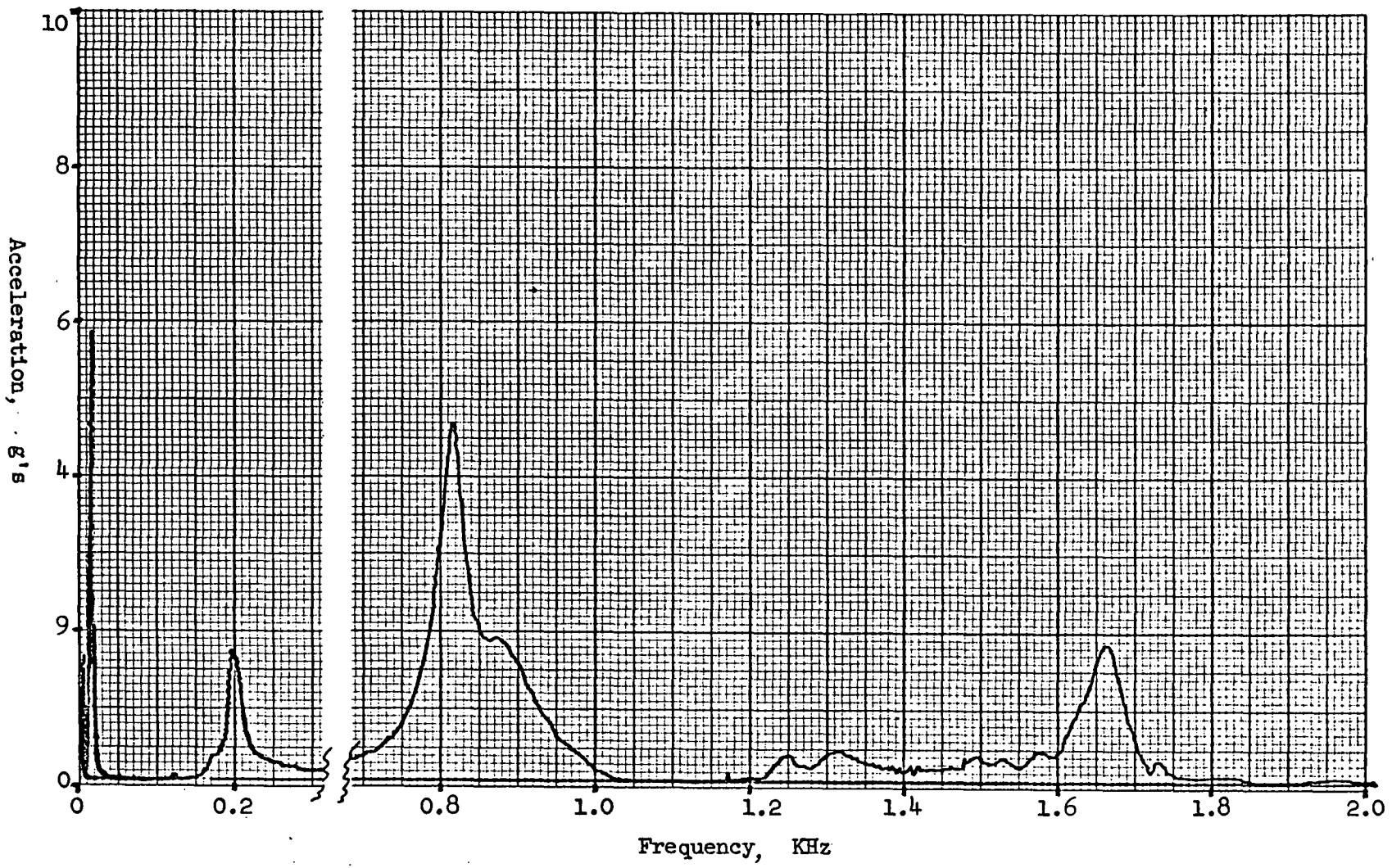

Figure 5-10. Tube Lateral Response for Laterally Excited Resonance Search

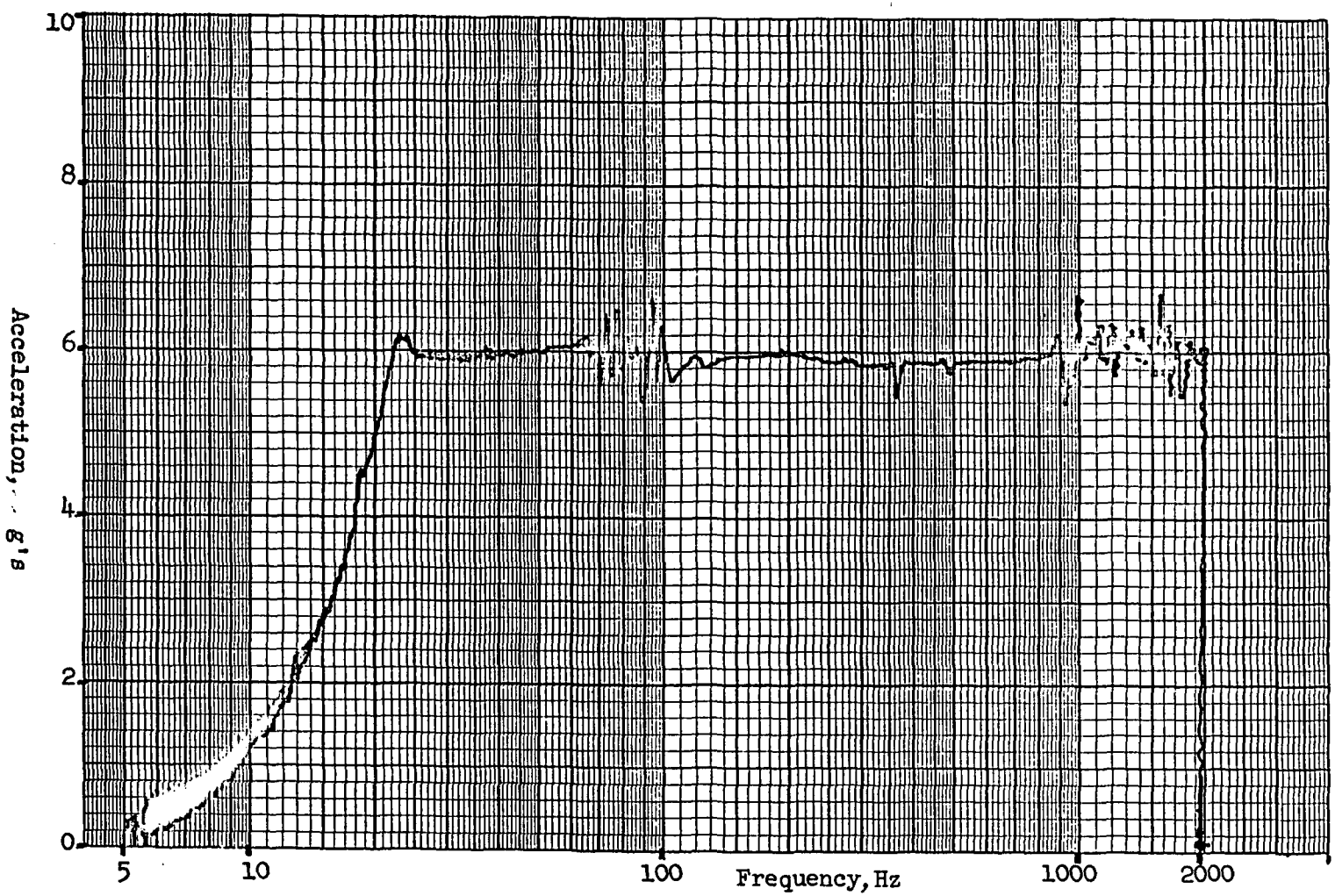

Figure 5-11. Control (Input) for Axially Excited Acceptance Level Sinusoidal Test

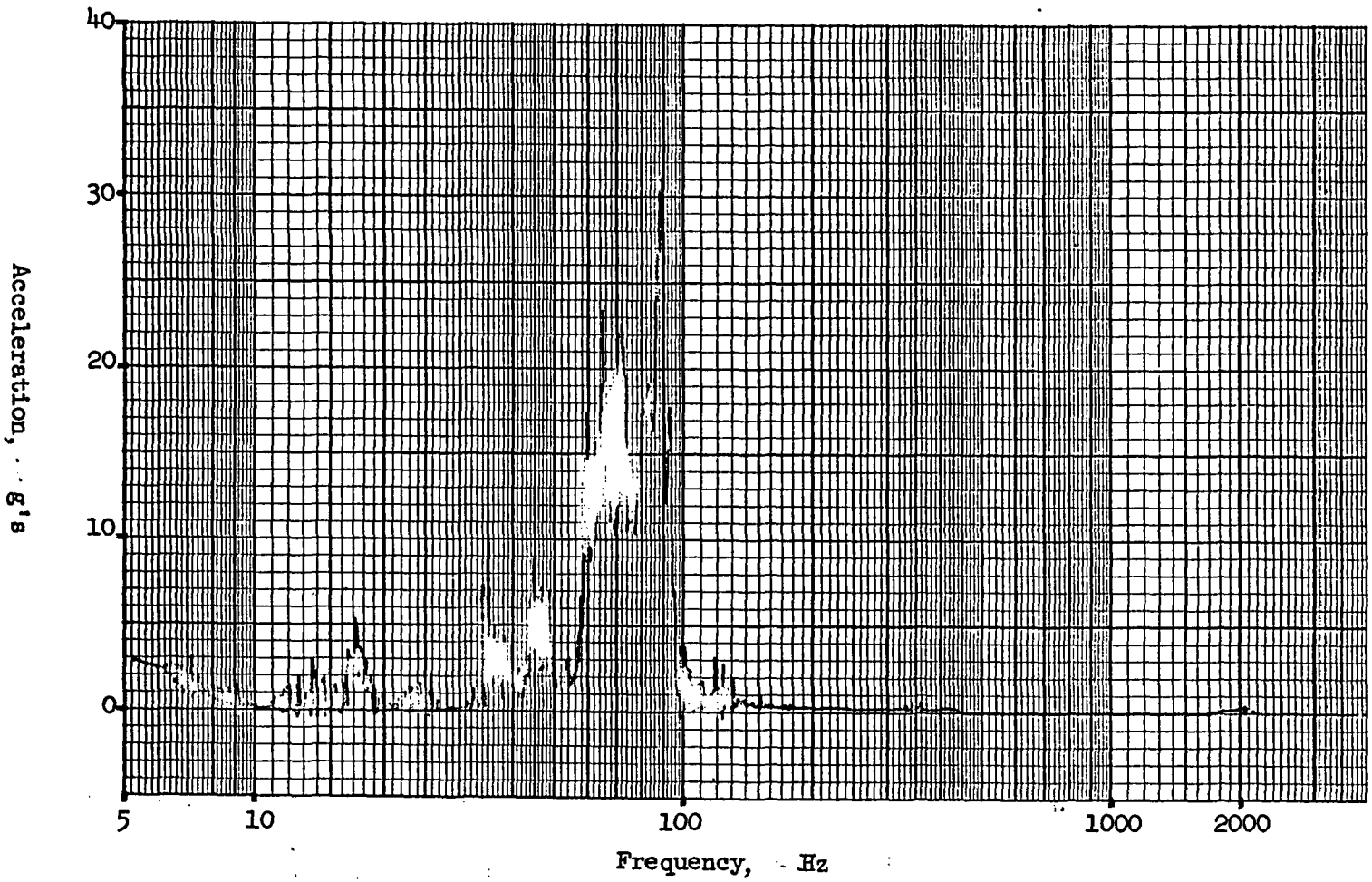

Figure 5-12 Argon Axial Response for Axially Excited Acceptance Level Sinusoidal Test

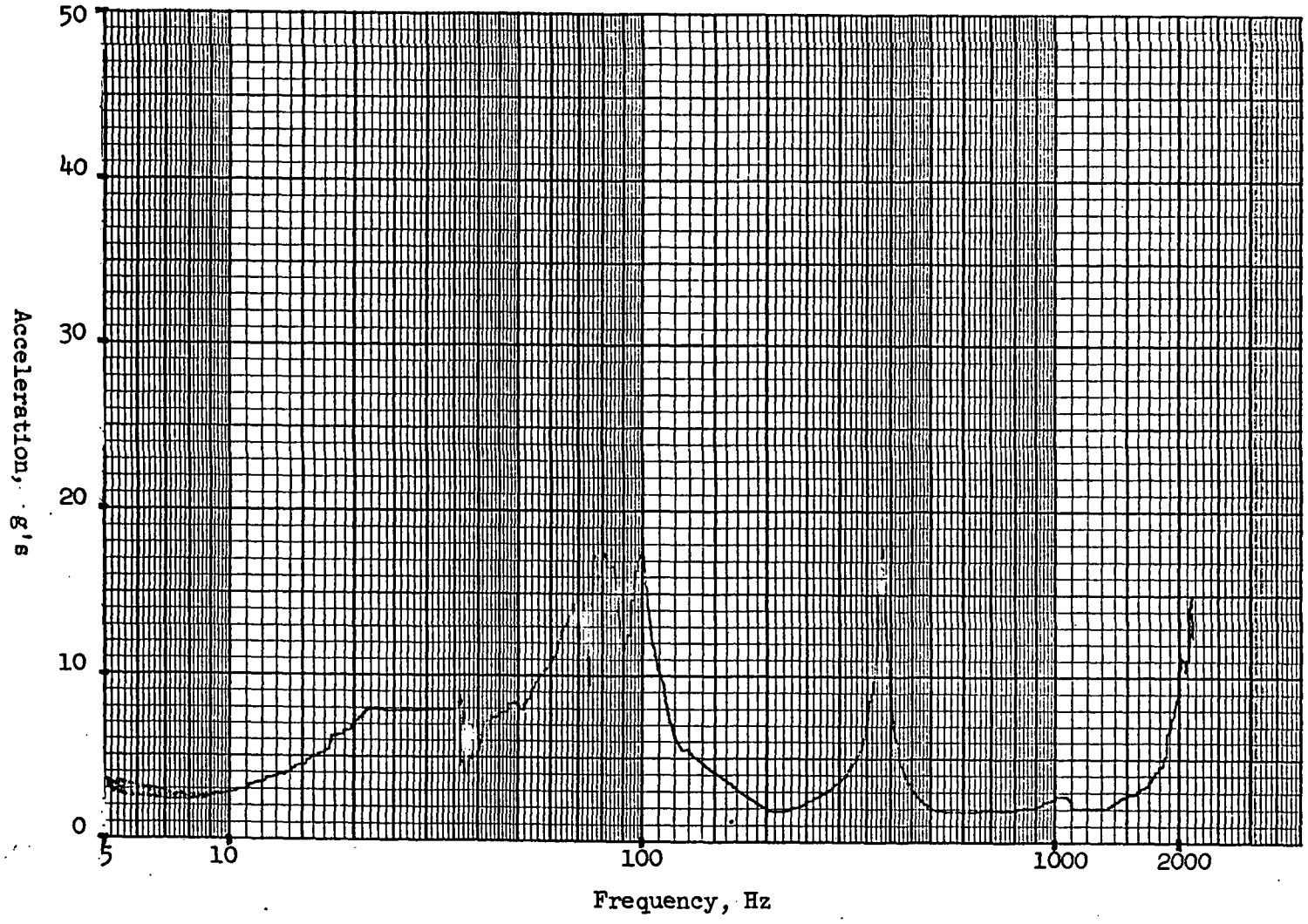

Figure 5-13. CO_2 Axial Response for Axially Excited Acceptance Level Sinusoidal Test

Figure 5-14 shows the input acceleration for the acceptance level, lateral, sinusoidal vibration test. The response accelerations for the argon and CO_2 tanks are shown in Figures 5-15 and 5-16 for this test. Again, the two resonant frequencies 13 and 20 cps, are similar to the resonant survey test. At the higher resonant frequency ($\sim$20 cps) the magnification factors are 3.2 and 4.4 for the argon and CO_2, respectively (compared to 3 and 4 respectively for the resonant survey test), while for the lower resonance ($\sim$13 cps) the magnification factors are 9.2 and 4.5 for the argon and CO_2, respectively (compared to 6 and 8, respectively for the resonant survey test). At the lower resonant frequency the limitation of the amplitude of the CO_2 container due to contact with the main support tube reduces the CO_2 amplification factor; however, this has also resulted in a greater amplification factor for the argon mass.

Similar results were obtained for the qualification level sinusoidal tests. Figures 5-17 and 5-18 show the response for the argon and CO_2 for axial excitation. The input acceleration was approx. 8.5 g's. At the lower resonant frequency ($\sim$ 100 cps) the amplification factors were 5.1 and 2.7 for the argon and CO_2, respectively, while at the higher frequency (350 cps) the CO_2 amplification factor was 2.7. Output data for the qualification level, lateral, sinusoidal test are not available. A summary of the sinusoidal vibration data, including the resonant survey tests, is presented in Table 5-7.

TABLE 5-7 SINUSOIDAL VIBRATION TESTS

Test	Freq.(cps)	Orientation: Axial 70 - 100 cps	Axial 350 cps	Lateral 13 cps	Lateral 20 cps
Resonant Survey	Argon	16	(neg)	6	3
	CO_2	12	2.7	8	4
Acceptance Level	Argon	5	(neg)	9.2	3.2
	CO_2	3	6	4.5	4.4
Qualification Level	Argon	5.1	(neg)	-	-
	CO_2	2.7	2.7	-	-

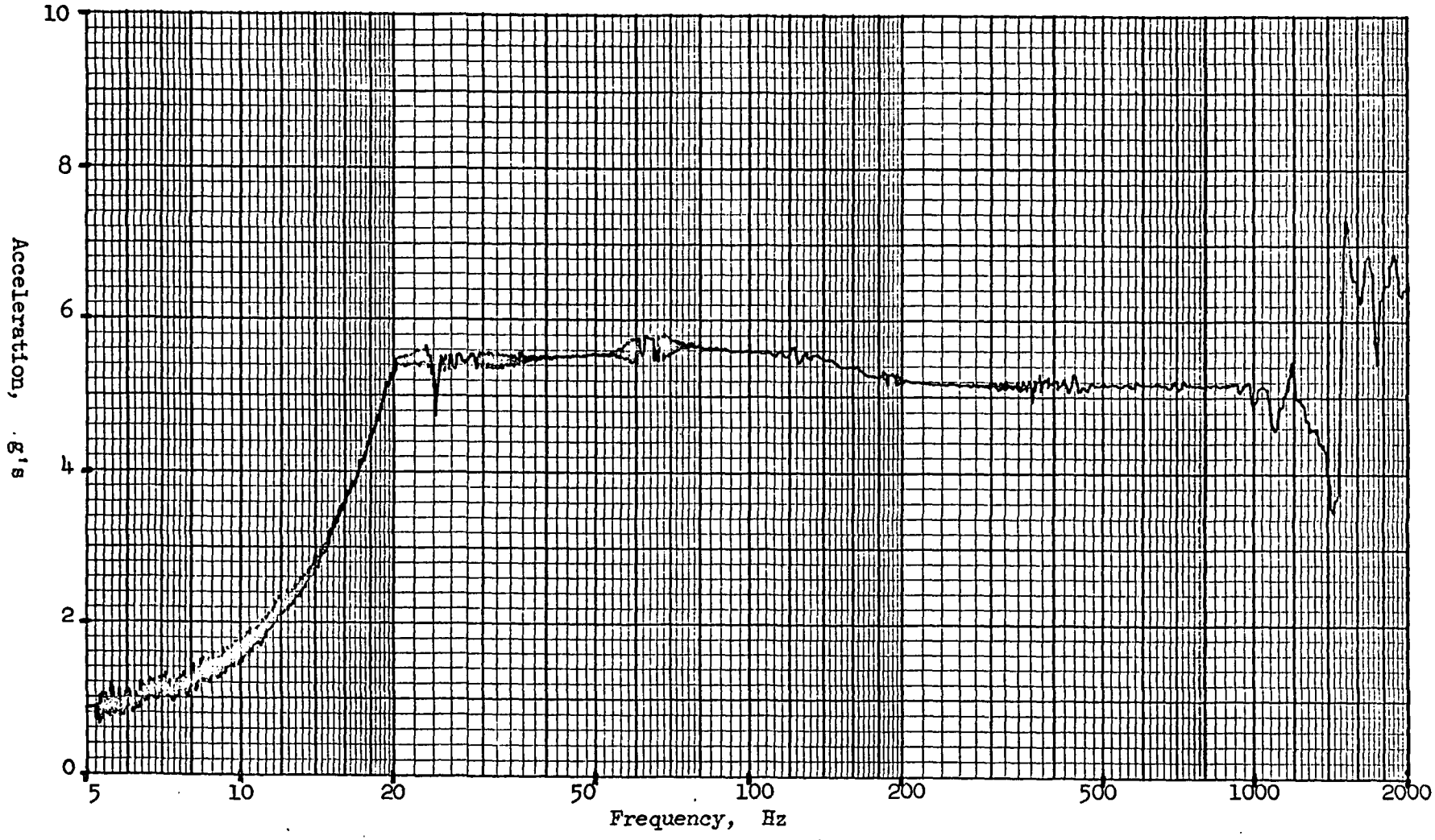

Figure 5-14. Control (Input) for Laterally Excited Acceptance Level Sinusoidal Test

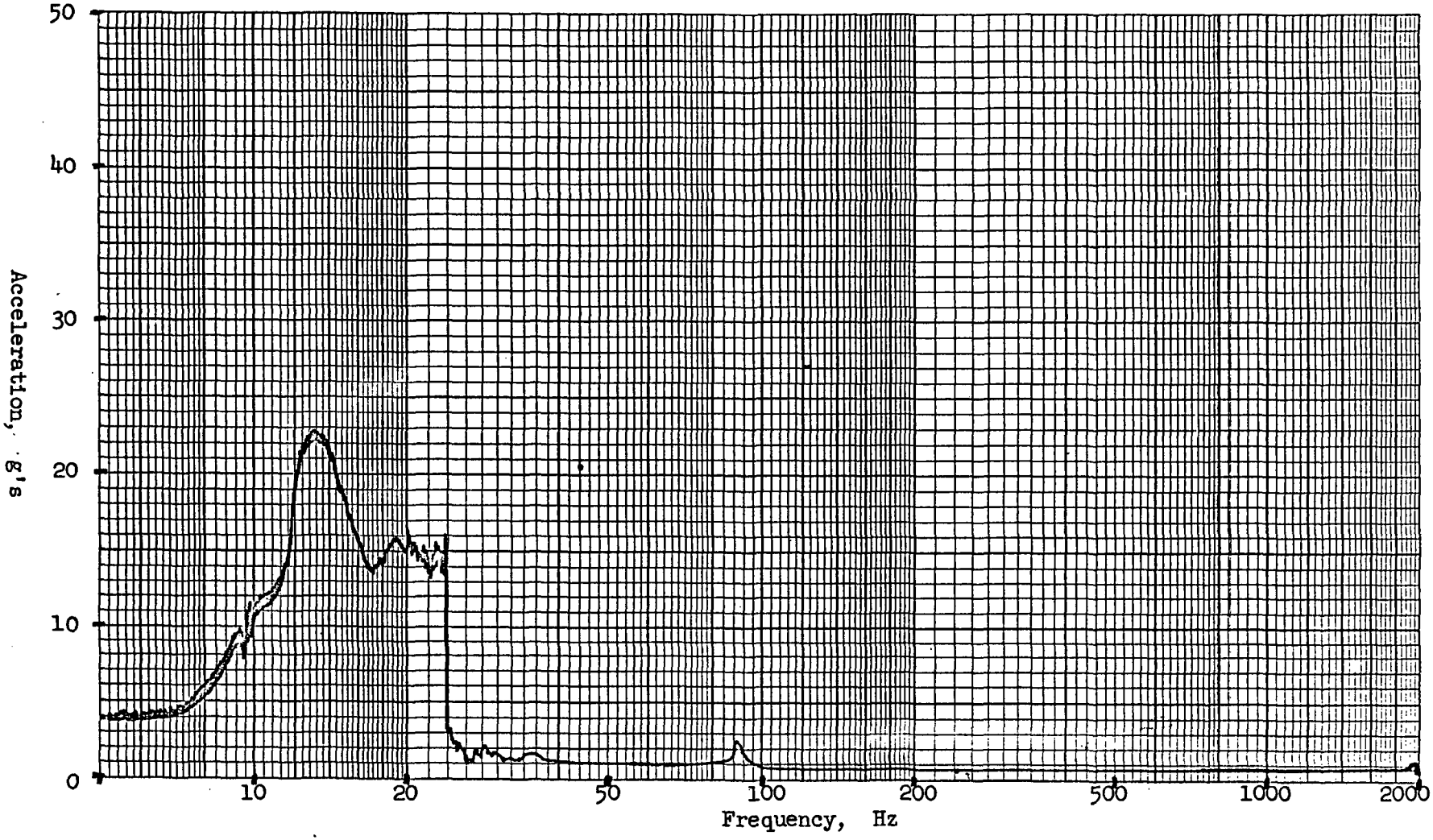

Figure 5-15. Argon Lateral Response for Laterally Excited Acceptance Level Sinusoidal Test

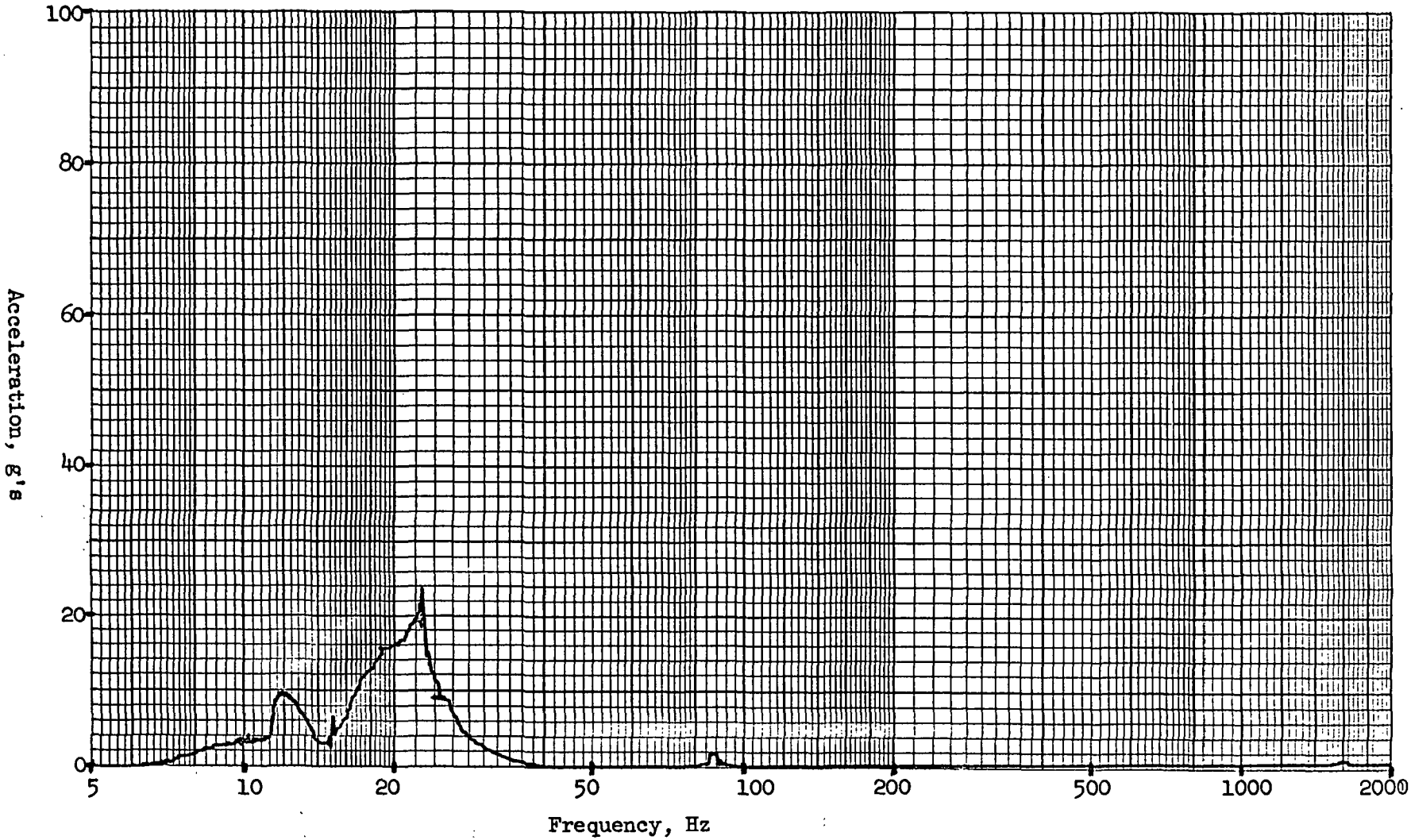

Figure 5-16 CO_2 Lateral Response for Laterally Excited Acceptance Level Sinusoidal Test

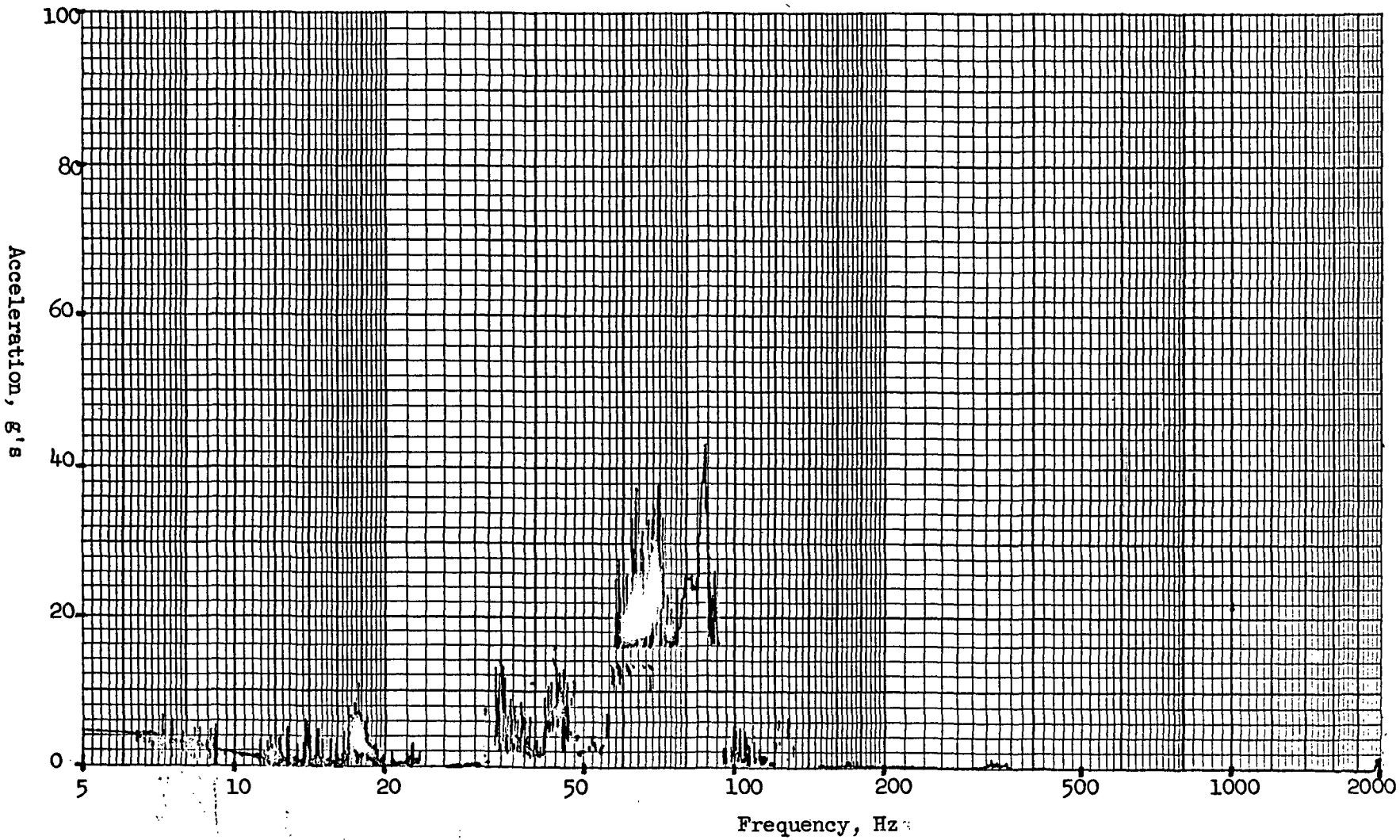

Figure 5-17. Argon Axial Response for Axially Excited Qualification Level Sinusoidal Test

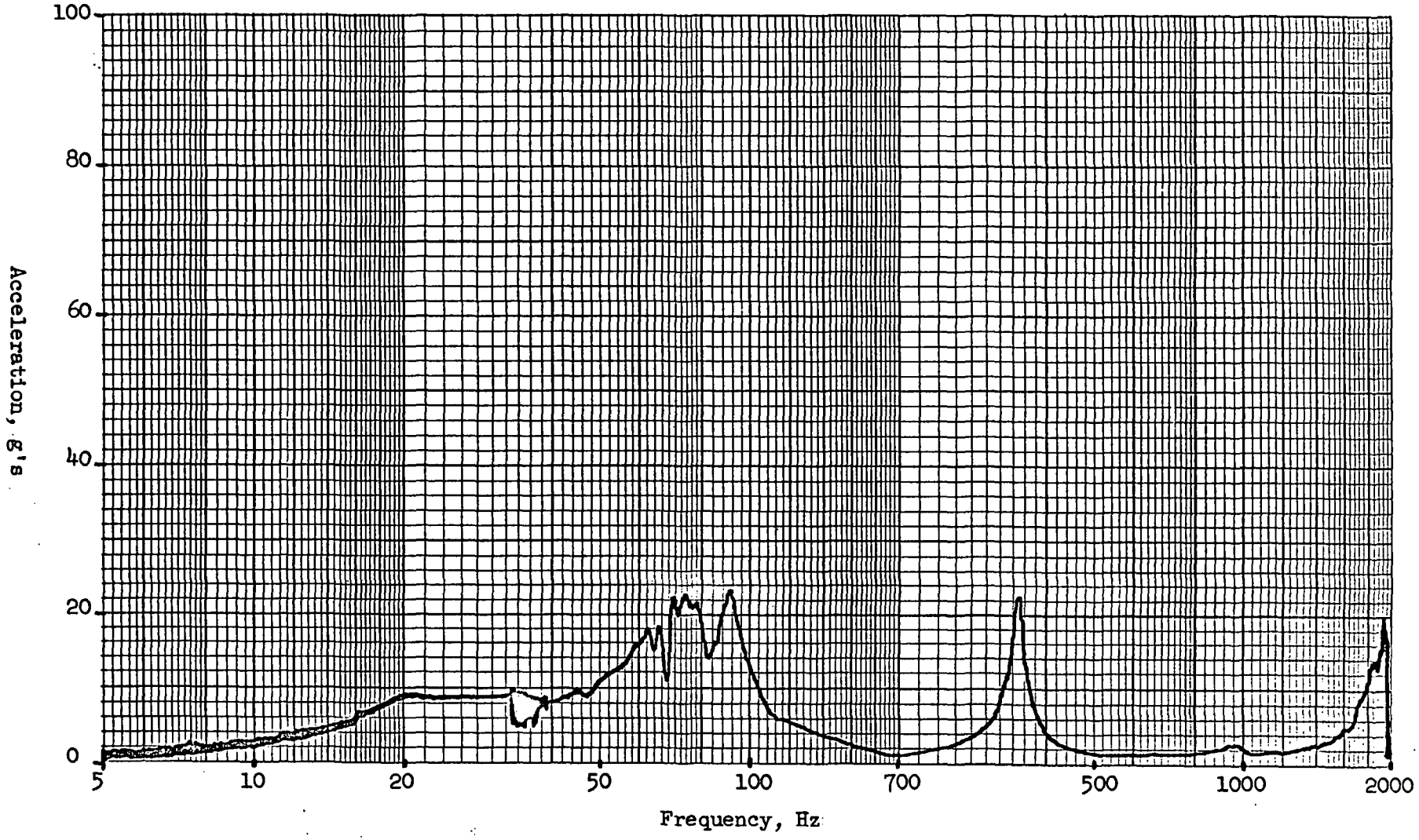

Figure 5-18. CO_2 Axial Response for Axially Excited Qualification Level Sinusoidal Test

The structural model also satisfactorily withstood the random vibration tests (Table 5-6) except that the tests were conducted in only two axes, axial and one lateral, due to time constraints. The accelerometer output data for these tests was poor and thus is not presented.

The one portion of the system which did not satisfactorily survive the structural testing was the detector mount and its taut wire support. After the conclusion of the random vibration tests three of the taut wires on the mount were broken. Since the detector mount was not examined until the conclusion of the vibration testing, it was undetermined as to when the failures occurred. It is suspected that the failure was a result of excessive stresses imposed on the wires due to vibrations of the thermal link; however, this cannot be fully substantiated and further effort will be required to determine the mode of failure and to make the necessary modifications to the detector mount.

6.0 SUMMARY, CONCLUSIONS AND RECOMMENDATIONS

The ground rules for the design of the solid argon-carbon dioxide subliming refrigerator were one year lifetime, a system weight of 35 lb (exclusive of vacuum container) detector dissipation of 10 mW and detector operating temperature of 75 to 80°K, when exposed to a 300°K space vacuum environment. In addition, the refrigerator was to withstand the acceleration and vibration environment of a TIROS launch. The thermal mechanical design of the refrigerator resulted in a design which would meet the above requirements except for the weight limitation, the design weight being approximately 38 lb. The selected refrigerator configuration consisted of toroidal aluminum containers for the argon and carbon dioxide, with the support system being a central fiberglas epoxy tubular structure. The system was insulated with a multilayer insulation and the insulation load was borne by the CO_2 since a CO_2 cooled shroud, on which the insulation was laid, surrounded the argon and thus provided a low temperature environment for the argon. In addition, there was one radiation shield between the CO_2 and argon and all internal surfaces were gold coated to reduce radiative exchange. The detector holder was supported on a taut wire system and connected to the argon through a gold link passing down the central support tube. The argon and CO_2 containers each had a single plumbing line used both for fill and vent. A liquid nitrogen coolant line routed first through the argon container and then along the CO_2 container was used to form the solid cryogens from their respective vapors.

Separate models of the refrigerator were constructed for the thermal and mechanical tests. The thermal model was constructed to meet both thermal and structural requirements. In the construction of the structural test model certain features, which were considered essential only for (unique to) thermal performance, were eliminated, i.e. gold coatings, etc. In the course of the testing of the thermal model, it was rebuilt twice as a result of damage due to overpressurization caused by vent line blockage. In the course of the structural testing, the model was rebuilt once as a result of a structural failure during the centrifuge tests, and a further modification of the support flange was later required to withstand stresses resulting from vibration tests.

LOCKHEED PALO ALTO RESEARCH LABORATORY
LOCKHEED MISSILES & SPACE COMPANY
A GROUP DIVISION OF LOCKHEED AIRCRAFT CORPORATION

The refrigerator thermal performance was substantially below the design goal and numerous diagnostic tests were conducted in an attempt to determine the source of the abnormally high thermal loads. Lifetime tests were conducted both under partially loaded (~20 percent) and fully loaded conditions, and both with and without the thermal link and detector mount installed. The thermal lifetime was determined to be different for the two cryogens: for the fully loaded condition the lifetimes for the argon and CO_2 were 3.1 and 2.7 months, respectively, whereas for the partially loaded tests conducted earlier the argon and CO_2 lifetimes were 2.8 and 8.6 months, respectively.

The discrepancy between the CO_2 lifetimes measured for the fully loaded and partially loaded tests is felt to be a result of a thermal short which developed between the times these two tests were conducted, and was not unique to the fraction of loading; however, this was not fully resolved because of contract time limiations. Considering the 8.6 month measured CO_2 lifetime, this can be largely explained by the 2 inch thickness of insulation used rather than the 3 inch design value. In addition, the support tube heat leak is larger than originally computed in the design study.

Of particular importance is the reason for the poor argon performance. The design thermal load on the argon was computed to be 44 mW whereas the thermal load determined by boiloff measurements was 230 mW, resulting in approximately a 2.8 month lifetime. Tests run with and without the thermal link and detector assembly indicated that approximately 147 mW was load on the link assembly and the remainder (83 mW) was radiative and conductive load on the argon tank itself. Observation of the detector holder during the test indicated a significant ice film, which from computation and published emittance values for ice films explains the abnormally high load on this link. This water vapor is believed to come from outgassing of adsorbed water vapor in the insulation and this icing problem was not significantly improved by "conditioning" the insulation. The interior cold regions of the refrigerator may possibly also have been contaminated by condensed water vapor, thus explaining the larger than expected thermal load on the argon container itself. It

would be expected that this contamination would be significantly less severe than on the detector holder and link which are directly exposed to the water vapor in the vacuum chamber and also because the detector is exposed to a 300°K environment. It was of particular consternation to us that the thermal performance of the current refrigerator was below that of the refrigerator developed under Contract NAS 5-9549. However, in discussing the tests and configuration with personnel associated with that contract, it was discovered that during their thermal lifetime tests, an aluminized mylar cover was placed across the support flange above the thermal link. It is agreed that this fortuituous choice of geometry unintentionally provided a barrier to water vapor in the chamber from migrating to the cold thermal link area. In our configuration the IRTRAN window is located above the detector on the flange of the vacuum chamber. If this were to be located on the top of the support flange, it would provide a similar vapor barrier to the geometry in NAS 5-9549, and would not otherwise affect the optical qualities of the system. Unfortunately, this was not done during the contract because the "icing" problem was not detected until late in the program,and further comparative tests and corrective steps as described above were not possible within the time permitted. However, such tests would be desirable and it is suspected that they would result in significant performance improvement.

As a result of the large thermal load on the link and detector holder the detector operating temperature was approximately 105°K rather than the 75-80°K design goal. This would be corrected by elimination of the water condensation problem. Temperature regulation tests gave results quite consistent with predicted values.

The refrigerator was filled both with and without the chamber evacuated, the evacuated fill requiring approximately 24 and 3-1/2 hours for the argon and CO_2, respectively, and was somewhat faster than the purged fill condition. However, the tests demonstrated that the purged fill test is entirely feasible.

Specific warmup tests including measurement of the emptying times and time to reach room temperature were not conducted; however, several warmups of the

system were conducted. One of the problems experienced was blockage of the fill lines. In one case this was caused by the LN_2 coolant line being too near the fill line resulting in freezing of the cryogen at that point in the line resulting in temporary blockage. This was subsequently corrected. On other occasions it was suspected that there was gradual accumulation of ice in the fill line due to minute quantitites of water vapor passing through the drying columns. This was corrected by cycling warm GHe several times into the vent line until it unblocked.

In addition to the argon-CO_2 tests, fill and lifetime tests with methane-ethylene were conducted. No unusual problems were experienced with these flammable gases during the fill operation and no problems were experienced with their solidification. The lifetime tests indicated that a substantial improvement of lifetime (or reduction in system weight) would result from use of these cryogens. This is a result of the methane being only 30% as dense as the argon yet having a sublimation heat/unit volume similar to that of argon. In addition the ethylene provides a lower boundary temperature for the primary cryogen than does CO_2, and though its volumetric heat of sublimation is only 40% of that of CO_2, its sublimation heat/unit mass is slightly superior to CO_2. The methane-ethylene is therefore superior to the argon-CO_2 system based on thermal lifetime or overall system weight.

The structural tests were conducted with the model warm and loaded with a tooling compound to simulate the cryogen masses. Acceleration, as well as both sinusoidal and random vibration tests, were conducted at both qualification and acceptance levels (TIROS launch), and with the refrigerator in both the axial and lateral orientation. Low level resonant survey tests in both orientations were also conducted. The taut wire support system for the detector mount was found to be broken on inspection following the final tests. This is suspected to be a result of excessive stresses placed on the mount by the thermal link, and further work is required on this part of the model. The basic structural portions of the system (flange mount, support tubes, tank brackets and cryogen tanks) passed all the structural tests satisfactorily and can be considered essentially qualified for a launch environment.

It is recommended that further testing, both thermal and structural be conducted to improve and further qualify this refrigerator model.

In particular, an attempt should be made to eliminate condensation of water vapor on the exposed detector holder as it significantly degrades the thermal performance and also would probably result in the detector being inoperable. Ways of eliminating this problem include: use of an insulation system which does not include a spacer material (the primary source of outgassing), and placement of the IRTRAN window immediately above the detector holder to have it form part of a barrier to the migration of water vapor to the exposed, cold detector holder. The latter step in particular seems advisable. Elimination of the spacer material or thorough conditioning of the insulation, would further reduce the migration of water vapor into the inner region of the refrigerator, where condensation also degrades the system thermal performance.

Further structural testing should also be conducted, even though the basic structure satisfactorily survived all structural tests. These tests should include qualification of the taut wire detector support concept, and complete structural tests of the refrigerator thermal model loaded with solid cryogens. The detector support tests should be preceded with additional analysis of the dynamic coupling between the thermal link, the flexible link and the detector holder before further structural tests are conducted. The basic structural design has survived the required launch environment; however, ultimate qualification of the system must include structural tests of the thermal model loaded with solid cryogens, followed by thermal performance tests to validate that the thermal performance is not seriously affected by the launch environment.

7.0 NEW TECHNOLOGY

The design, fabrication and testing of the argon-carbon dioxide subliming refrigerator resulted in the development of some specific items which are considered to be reportable under the contract's "New Technology Clause."

A. Item A

1. Title

Concentric Support Tube - Cryogenic Tank Design

2. Abstract

The basic configuration for the refrigerator consists of separate toroidal CO_2 and argon containers supported on a tubular support structure consisting of four fiberglas-epoxy concentric tubes arranged in a folded manner. The fiberglas-epoxy material is ideal for cryogenic supports because of its high strength and low thermal conductivity and the concentric configuration is advantageous for a dynamic system and permits ease of assembly. This configuration satisfactorily underwent acceleration and vibration tests typical of qualification for a TIROS launch and was also used in the refrigerator thermal model.

3. Detailed Description

a. General Purpose - The configuration was used in the refrigerator system to provide a structurally reliable, low heat leak support system for efficient storage of cryogenic refrigerants.

b. Improvements and Advantages - During the refrigerator design this concept was chosen over several other concepts evaluated. This concept represents a significant improvement over a support configuration used for a similar requirement under Contract NAS 5-9549 in that it was qualified during extensive structural testing during the current contract and that it greatly facilitates the refrigerator assembly.

c. Principle of Operation and Construction - The configuration is shown in Figure 1-1. The cryogen containers were constructed from spun sections of 6061-T6 aluminum and welded together at the seams. Mounting brackets attached to each tank and made of the same material were epoxy bonded to the support tube structure at the two mounting locations. The four glass-epoxy tubes were custom fabricated from S glass-1581 cloth/E-787 epoxy (U.S. Polomeric, Inc.). Each tube was fabricated by spiral wrapping the required number of layers ($\sim$ 10 mil/layer) to produce the required tube thickness. The tube thicknesses were partially tailored to meet the local stresses. The outer two support tubes were of uniform diameter, whereas the central tube was tapered at the top due to stress considerations, and the second tube was tapered throughout its length to simplify construction and assembly. The tubes were assembled in a "folded" configuration, the joining technique utilized epoxy adhesive with an area sufficient to limit shear stresses below allowables. The tubes were designed to withstand stresses resulting from axial and transverse loading. Ultimate shear, ultimate compressive and critical local buckling stresses were used as the criteria.

The design, construction and testing, both thermal and structural, are given in greater detail in the body of this report.

d. New Features - It is believed that this basic configuration is new in its application to the storage of cryogenic fluids under a severe vibration environment.

e. Additional Information - N/A

4. Applications

This basic configuration would find possible application in systems requiring support structures which exhibit efficient thermal insulation (hot or cold) and high strength.

5. Possible Extension

The basic configuration would be applicable to a system requiring support of one or several masses at different temperature levels. The support tubes could be tailored both in thickness and diameter for optimum performance. Furthermore, since local buckling becomes critical for the larger diameter - thinner wall tubes, these tubes could be given additional strength with little effect on thermal performance by spacing circumferential stiffening ring along the tube.

6. Degree of Development

Development is completed and prototype thermal and structural models have been constructed. Each model has been tested: the thermal model for a thermal lifetime test and the structural model has satisfactorily undergone acceleration and vibration tests equivalent to qualification tests for a TIROS launch.

7. Technological Significance

This "new technology item" is considered to be a substantial design improvement.

8. Innovators' Names

T. C. Nast, G. C. Vliet and G. B. Cline

9. Previous Publication or Disclosure

There has been no previous specific disclosure of this item. However, the item was very briefly described in the context of a paper by G. C. Vliet and D. O. Murray dealing with solid cryogen refrigerators which was published in the 1968 Proceedings of the Infrared Information Symposium (IRIS).

10. Technical Supervisor of Innovators

Not identified.

B. Item B.

1. Title

Taut Wire Infrared Detector Support

2. Abstract

The taut wire infrared detector support concept consists of the suspension of the detector mount on a series of symmetrically arranged wires placed in tension. This configuration provides a low heat leak support and because of the symmetrical arrangement minimizes detector misalignment due to thermal effects.

3. Detailed Description

a. General Purpose - The taut wire support concept was used in the subliming refrigerator to support and accurately position the cold infrared detector with respect to the ambient temperature surroundings.

b. Improvements and Advantages - The taut wire support has advantages over the pedestal type of support in that it passively maintains detector position (alignment) relative to its surroundings in the presence of temperature differences between detector and surroundings.

c. Principle of Operation and Construction. The taut wire support concept consists of supporting the cold detector on a number (six) of symmetrically arranged wires placed in tension. The configuration shown in Figure 1-1 is that used in the refrigerator developed under NAS 5-10457, and consists of the minimum number of support wires which will provide reasonable axial, lateral and torsional stability to the supported mass (detector). Three pairs of wires 120 degrees apart, with each pair themselves at right angles provide the necessary support. Each wire is oriented 45 degrees to the axis to optimize both the axial and lateral stiffness. The upper set and lower set of wires are located so that their force vectors do not intersect the centerline at the same location, thus providing torsional stability about axes perpendicular to the centerline. The wires are designed such that their combined spring con-

stant and the supported mass (detector) will not resonate within the anticipated range of exciting frequencies experienced by the system. They are attached at the ends by epoxy-adhesive and are placed in tension. The selection of wire material is based primarily on maximizing strength/thermal conductivity. The candidate material used was Ti: 6 Al, 4V. The system was designed for a TIROS launch environment and for a resonant frequency well above 200 Hz.

Further details of the taut wire support system are included in the body of this report.

d. New Features - It is believed that this is the first attempt at using the taut wire support concept to provide a low heat leak support for a cryogenically cooled infrared detector sensing element.

e. Additional Information - N/A

4. Application

This basic configuration would find use in systems requiring simultaneous thermal isolation and structural support, primarily where alignment is critical.

5. Possible Extension

The taut wire support system can be applied when as few as two wires are used. However, the two wire system provides stiffness only in the line of direction of the wires. To provide stiffness in three orthogonal axes a minimum of four wires are required. The four wire system does not provide much torsional stiffness since all four wires have the same point of action. The six wire system described above provides stiffness in all axes except torsional about the centerline. A further improvement would be to use an eight wire system such that the upper and lower sets do not act through the same point (similar to 6 wire system) but also such that opposing wires in the same set do not have the same point of action. Such an eight wire system would provide transverse stiff-

ness in three orthogonal axes as well as torsional stiffness in three orthogonal axes.

6. Degree of Development

Development is partially completed. The taut wire system was used in both the thermal refrigerator model and also the structural model. In the structural model some of the taut wires were found to have failed at the conclusion of the vibration tests; however, this is attributed to rosult from insufficient support of the thermal link which was connected to the detector mount. The thermal link and its flexible connection to the detector mount require further improvement followed by additional testing of the taut wire supported detector mount connected to a thermal link of improved design.

7. Technological Significance

This item is considered to be a design improvement.

8. Innovators' Names

G. C, Vliet, T. C. Nast, and G. Bell.

9. Previous Publication or Disclosures

There has been no previous specific disclosure of this item. However, the item was briefly described in the context of a paper by G. C. Vliet and D. O. Murray dealing with solid cryogen refrigerators which was published in the 1968 Proceedings of the Infrared Information Symposium.

10. Technical Supervisor of Innovators.

Not identified.

8.0 BIBLIOGRAPHY

1. Toth, L. W., et al, "Program for the Evaluation of Structural Reinforced Plastic Materials at Cryogenic Temperatures," Goodyear Aerospace Corp., Akron, Ohio, Rept. No. GER-12792. NASA N67 12051, Aug. 1966.

2. Goetzel, et al, "Space Materials Handbook", Addison and Wesley, 1965.

3. Levy, D. J., et al, "Spray Deposition of Low Emittance Gold Thermal Control Coatings," SAMPE Journale, April/May 1969.

4. Cunnington, G. R., et al, "Total Emittance Measurements of Thin Metallic Films at Cryogenic Temperatures," to be presented at AIAA Conference, Jan. 1970.

5. "High Performance Thermal Protection Systems," LMSC A96494, December 31, 1969, Vol. I.

6. Caren, R. P., et al, "Thermal Absorptances of Cryodeposits for Solar and 290°K Blackbody Sources," in Advances in Cryogenic Engineering, Vol. 9, Plenum Press, New York (1963) p. 457.